Imaging

Transmission electron microscopy

- TEM is an analytical tool that allows detailed investigation of the morphology, structure, and local chemistry of metals, ceramics, polymers, biological materials and minerals. It also enables the investigation of crystal structures, crystallographic orientations through electron diffraction, as well as second phase, precipitates and contaminants distribution by x-ray and electron-energy analysis.

- Magnifications of up to 500,000x and detail resolution below 0.2 nm are achieved routinely. Quantitative and qualitative elemental analysis can be provided from features smaller than 10 nm. For crystals with interplanar spacing greater than 0.2 nm, crystal structure, symmetry and orientation can be determined.

Remember: Abbe's principle of imaging

Unlike with visible light, due to the small λ, electrons can be coherently scattered by crystalline samples so the diffraction pattern at the back focal plane of the object corresponds to the sample reciprocal lattice.

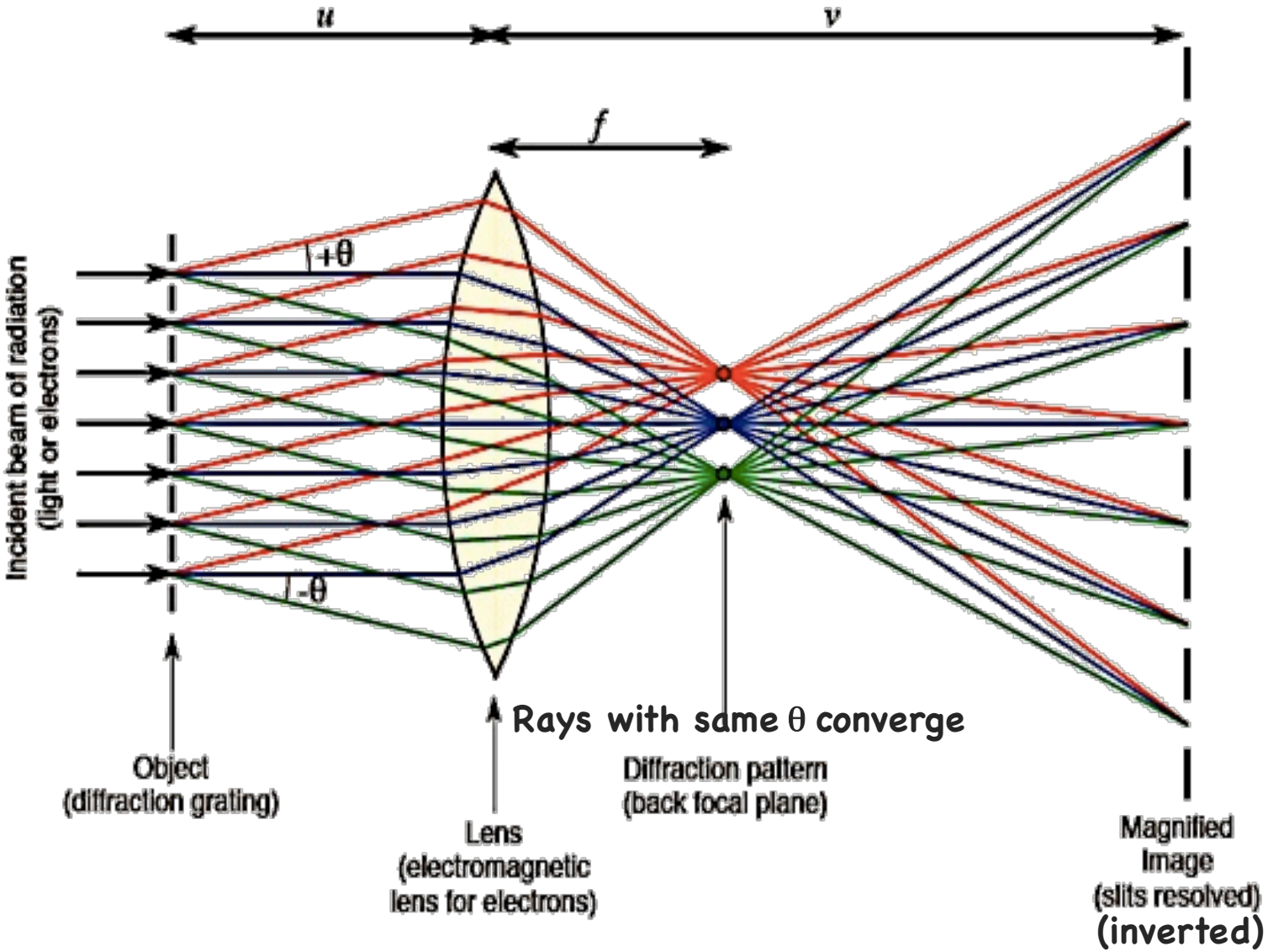

Remember: Abbe's principle of imaging

A diffraction pattern is always formed at the back focal plane of the objective (even in OM). To view this diffraction pattern one has to change the excitation of the intermediate lens. A higher strength projects the specimen image on the screen, a lower strength project the DP.

The optical system of the TEM: The objective lens simultaneously generates the diffraction pattern and the first intermediate image. Note that the ray paths are identical until the intermediate lens, where the field strengths are changed, depending on the desired operation mode. A higher field strength (shorter focal length) is used for imaging, whereas a weaker field strength (longer focal length) is used for diffraction.

Contrast enhancement requires mastering the TEM both in diffraction and imaging modes...

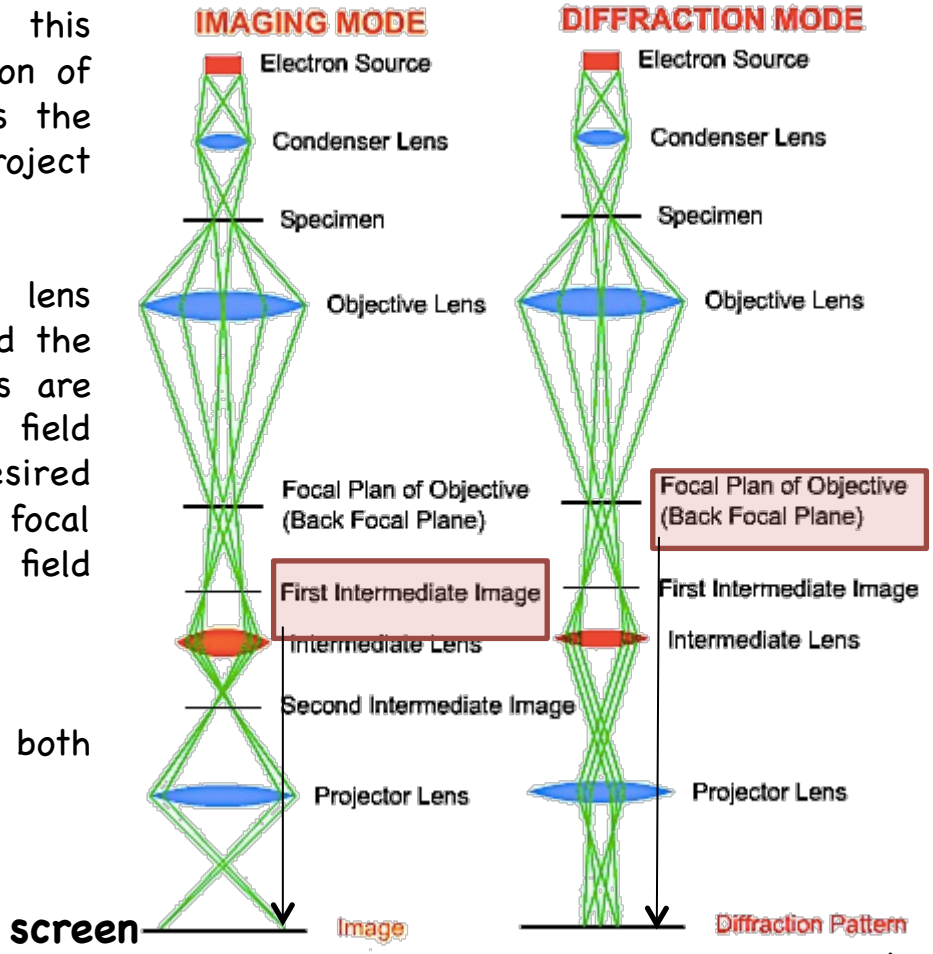

Basic imaging mode: Bright field

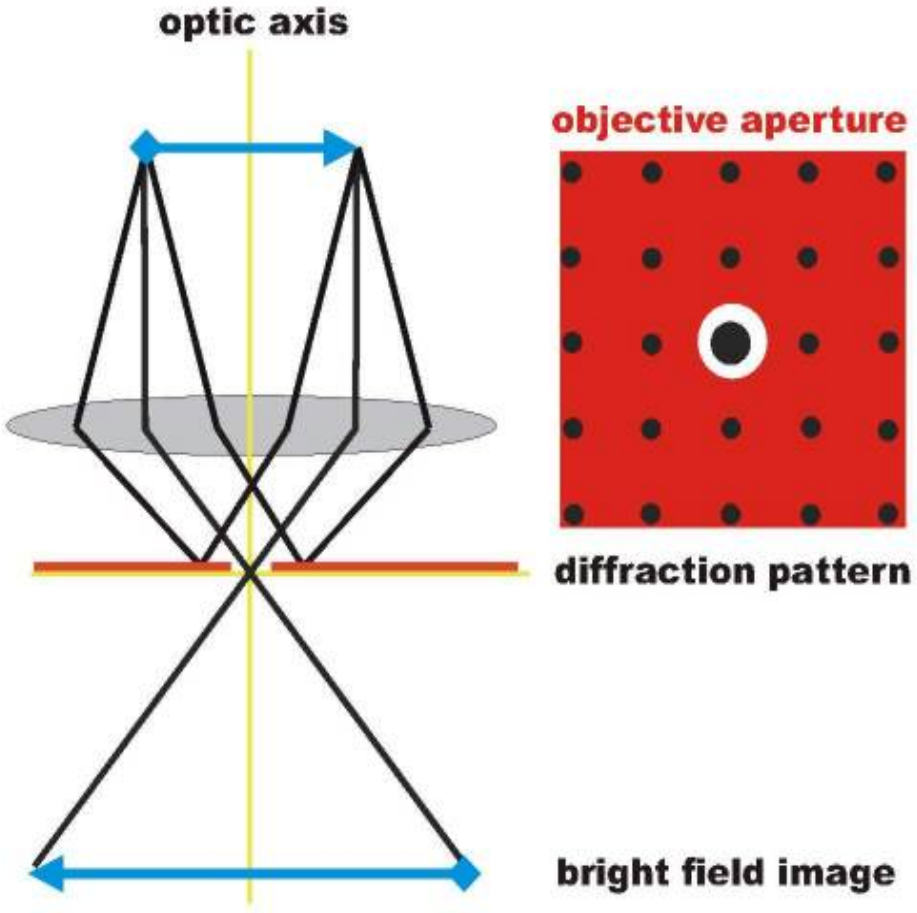

In the bright field (BF) mode of the TEM, an aperture is inserted into the back focal plane of the objective lens, the same plane at which the diffraction pattern is formed.

The aperture allows only the direct beam to pass. The scattered electrons are blocked. Dark regions are strongly dispersing the light. This is the most common imaging technique.

Basic imaging mode: Dark field

(used usually only for crystalline materials)

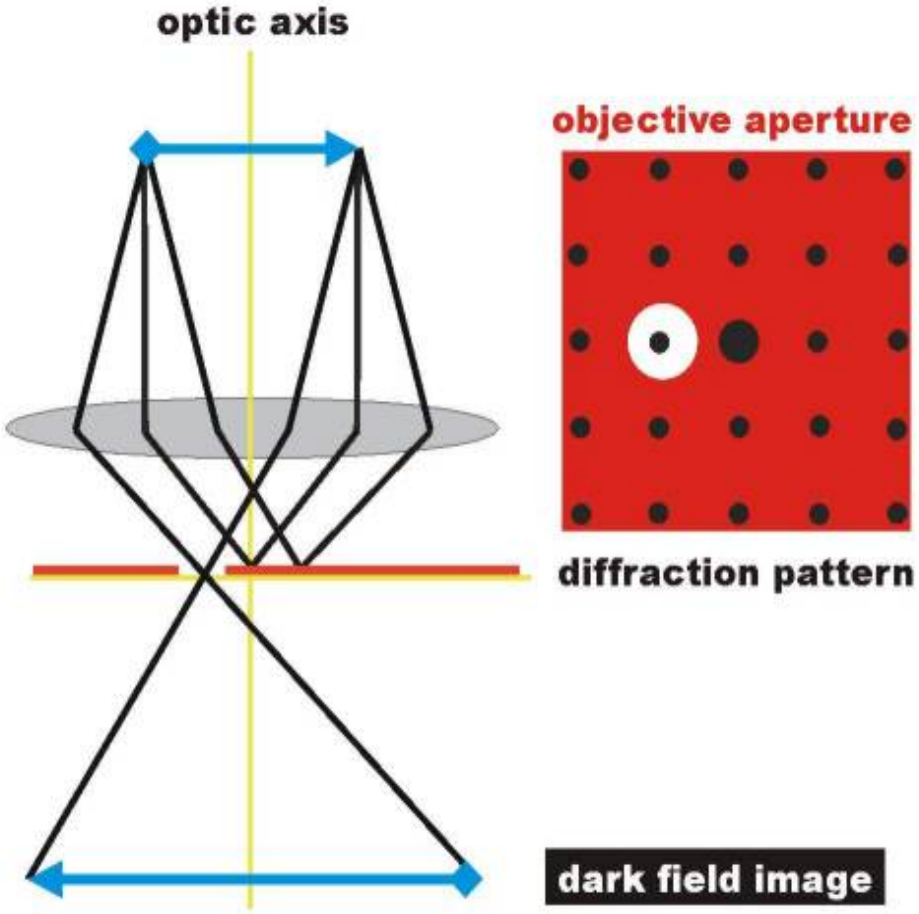

In dark field (DF) images, the direct beam is blocked by the aperture while one or more diffracted beams are allowed to pass trough the objective aperture. Since diffracted beams have strongly interacted with the specimen, very useful information is present in DF images, e.g., about planar defects, stacking faults or particle size.

Contrast mechanisms

The image contrast originates from:

Amplitude contrast

- Mass - The only mechanism that generates contrast for amorphous materials: Polymers and biological materials

- Diffraction - Only exists with crystalline materials: metals and ceramics

Phase (produces images with atomic resolution)

Only useful for THIN crystalline materials (diffraction with NO change in wave amplitude): Thin metals and ceramics

Mass contrast

- Mass contrast: Variation in mass, thickness or both

- Bright Field (BF): The basic way of forming mass-contrast images
- No coherent scattering

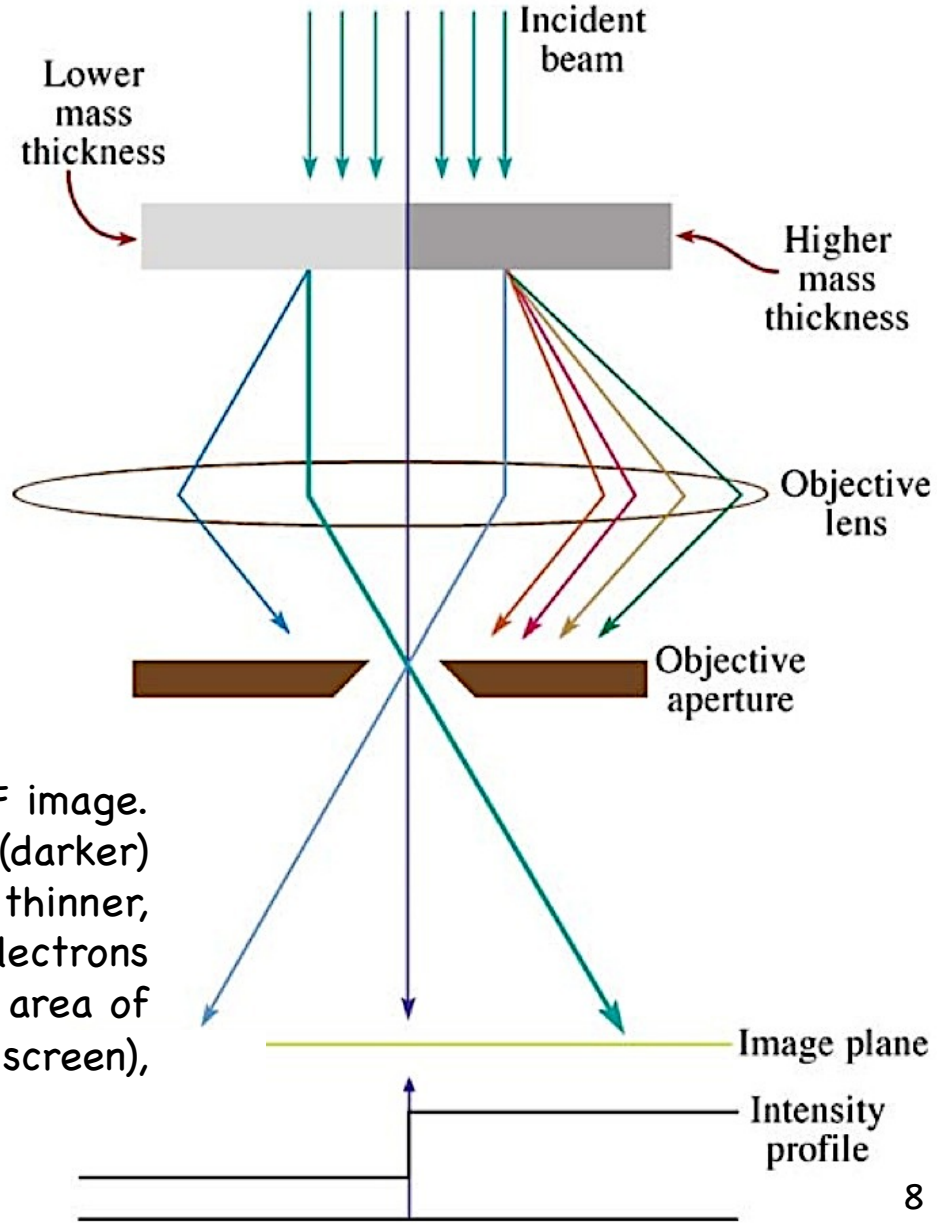

Mechanism of mass-thickness contrast in a BF image. Thicker or higher-Z areas of the specimen (darker) will scatter more electrons off axis than thinner, lower mass (lighter) areas. Thus fewer electrons from the darker region fall on the equivalent area of the image plane (and subsequently the screen), which therefore appears darker in BF images.

Mass contrast

- Heavy atoms scatter more intensely and at higher angles than light ones.

- Strongly scattered electrons are prevented from forming part of the final image by the objective aperture.

- Regions in the specimen rich in heavy atoms are dark in the image.

- The smaller the aperture size, the higher the contrast.

- Fewer electrons are scattered at high electron accelerating voltages, since they have less time to interact with atomic nuclei in the specimen: **High voltage TEM result in lower contrast and also damage polymeric and biological samples**

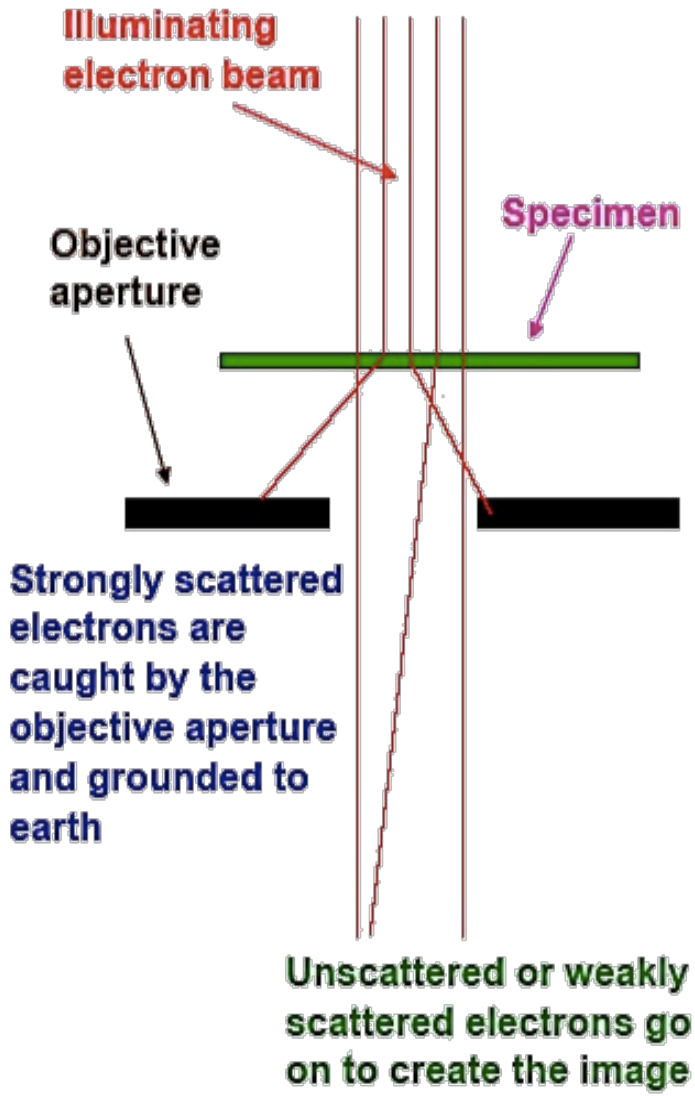

Mass contrast

Bright field images

(J.S.J. Vastenhout, Microsc Microanal 8 Suppl. 2, 2002)

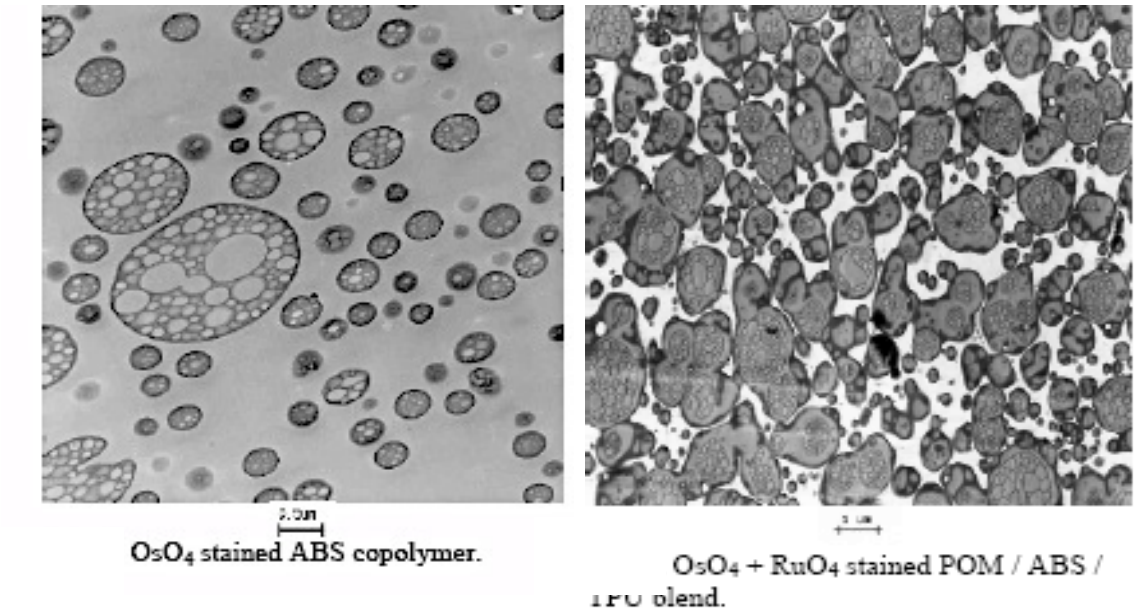

OsO_4 stained ABS copolymer.

OsO_4 + RuO_4 stained POM / ABS / TPU blend.

Stained with OsO_4 and RuO_4 vapors
Os and Ru are heavy metals...

In the case of polymeric and biological samples, i.e., with low atomic number and similar electron densities, staining helps to increase the imaging contrast and mitigates the radiation damage.

The staining agents work by selective absorption in one of the phases and tend to stain unsaturated C-C bonds. Since they contain heavy elements with a high scattering power, the stained regions appear dark in bright field.

Mass contrast

Bright field: Typical image of a stained biological material

faculty.une.edu

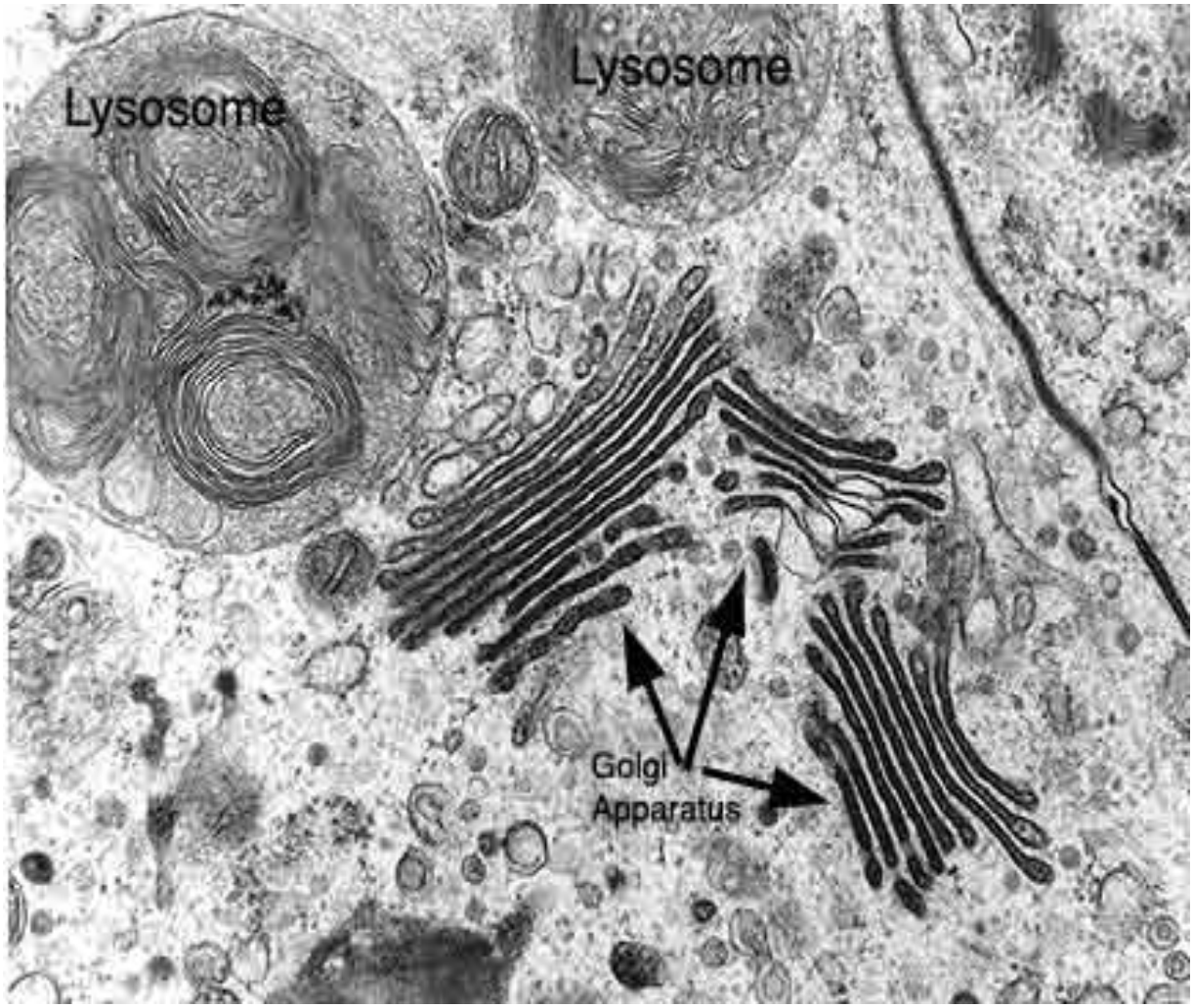

Diffraction contrast

Bright field

If the sample has crystalline areas, many electrons are strongly scattered by Bragg diffraction (especially if the crystal is oriented along a zone axis with low indices), and this area appears with dark contrast in the BF image. The scattered electron beams are deflected away from the optical axis and blocked by the objective aperture, and thus the corresponding areas appear dark in the BF-image

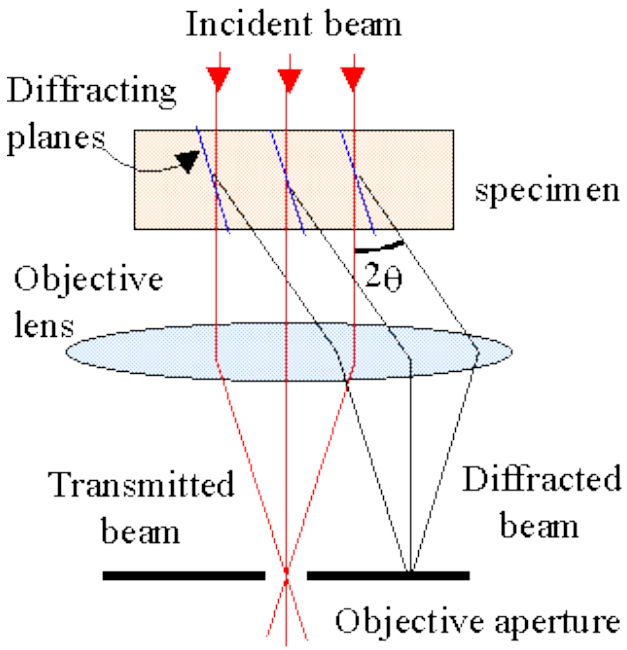

Bright Field Imaging

Diffraction contrast

Dark field

Dark-field images occur when the objective aperture is positioned off-axis from the transmitted beam in order to allow only a diffracted beam to pass. In order to minimize the effects of lens aberrations, the diffracted beam is deflected from the optic axis,

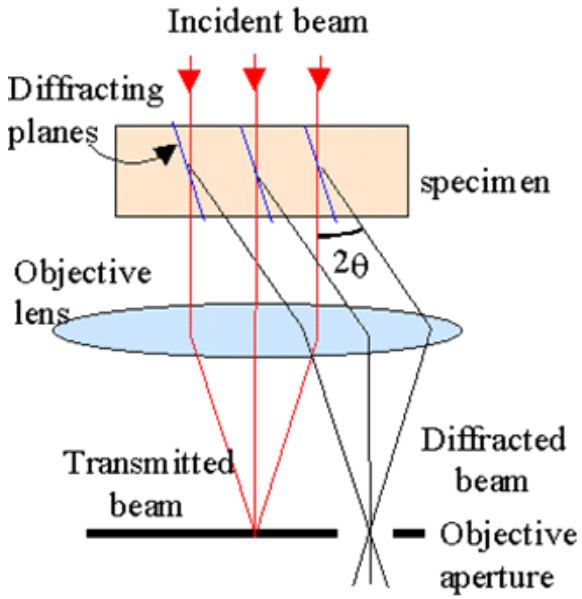

Off-axis Dark Field

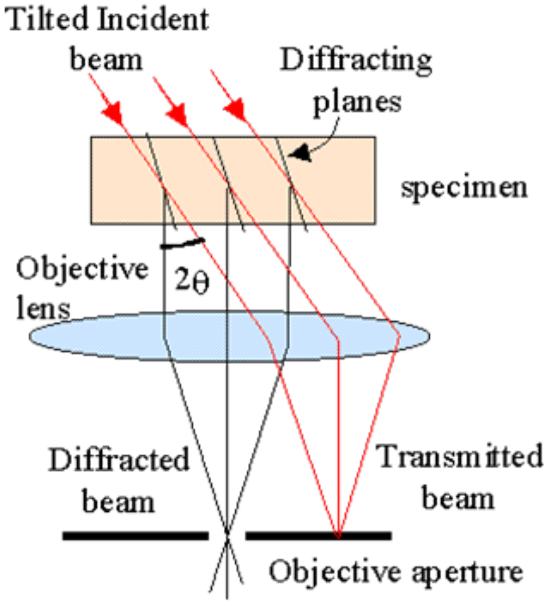

On-axis Dark Field

One diffracted beam is used to form the image. This is done with the same aperture which is displaced. However, as these electrons are not on the optical axis of the instrument, they will suffer from severe aberrations that will lower the resolution. If an inclined beam is used, the diffracted beam will be at the optical axis, i.e., aberration are minimized. This is not required is aberration corrected instruments.

Remember: two-beam conditions

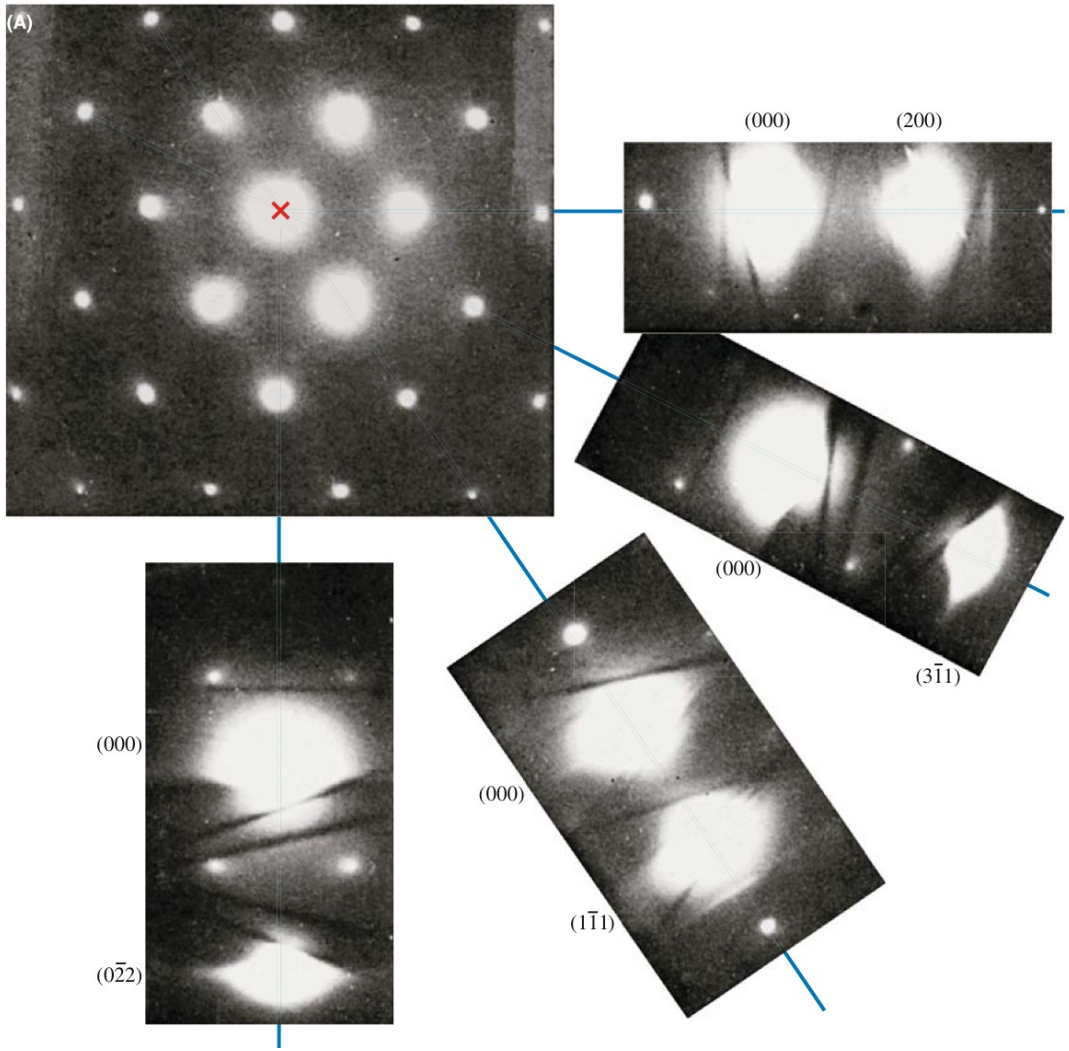

The [011] zone-axis diffraction pattern has many planes diffracting with equal strength. In the smaller patterns the specimen is tilted so there are only two strong beams, the direct 000 on-axis beam and a different one of the hkl off-axis diffracted beams.

Diffraction contrast

Bright field images (two beam condition)

When an electron beam strikes a sample, some of the electrons pass directly through while others may undergo slight inelastic scattering from the transmitted beam. Contrast in an image is created by differences in scattering. By inserting an aperture in the back focal plane, an image can be produced with these transmitted electrons. The resulting image is known as a bright field image. Bright field images are commonly used to examine micro-structural related features.

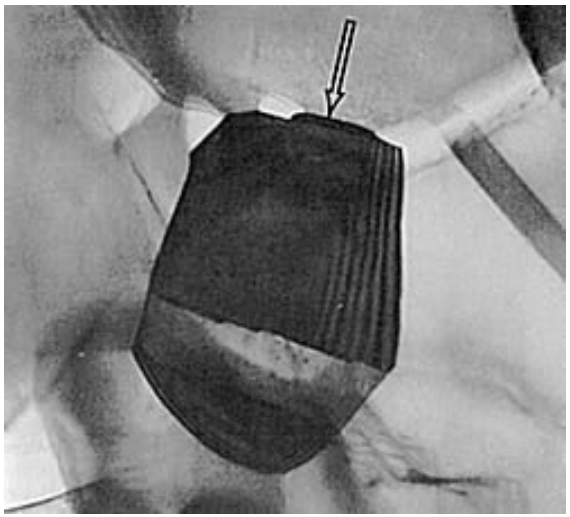

Two-beam BF image of a twinned crystal in strong contrast.

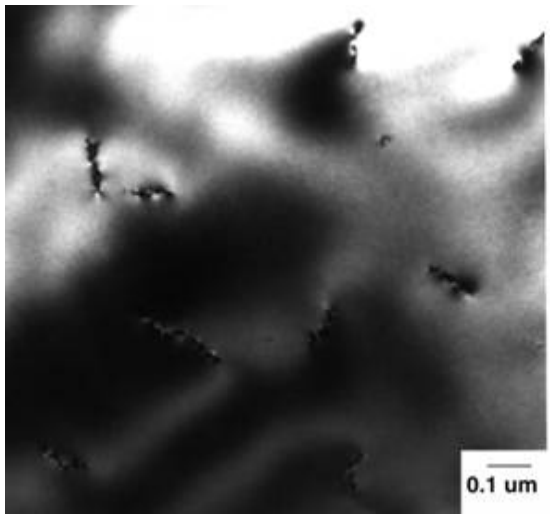

Crystalline defects shown in a two-beam BF image

Diffraction contrast

Dark field images (two beam condition)

If a sample is crystalline, many of the electrons will undergo elastic scattering from the various (hkl) planes. This scattering produces many diffracted beams. If any of these diffracted beams is allowed to pass through the objective aperture a dark field image is obtained. In order to reduce spherical aberration and astigmatism and to improve overall image resolution, the diffracted beam will be deflected such that it lies parallel the optic axis of the microscope. This type of image is said to be a centered dark field image. Dark field images are particularly useful in examining micro-structural detail in a single crystalline phases.

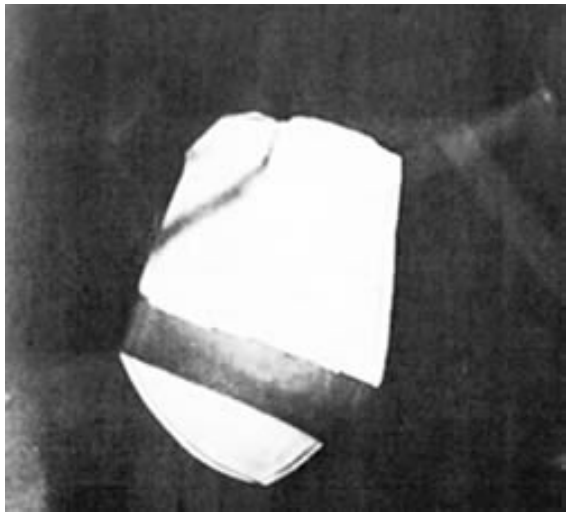

Two-beam DF image of a twinned crystal in strong contrast.

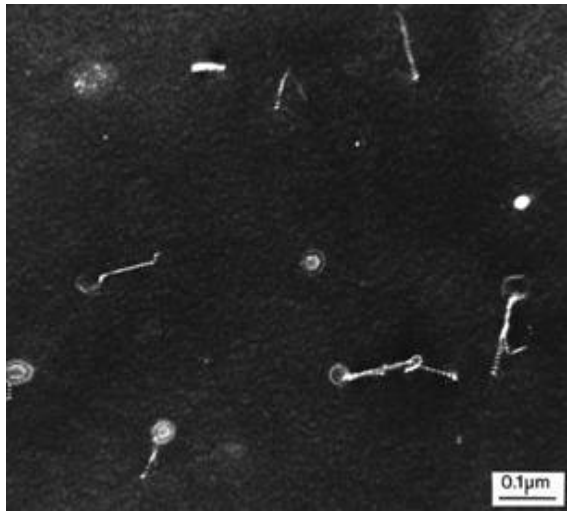

Crystalline defects shown in a two-beam DF image

Remember: the excitation error or deviation parameter

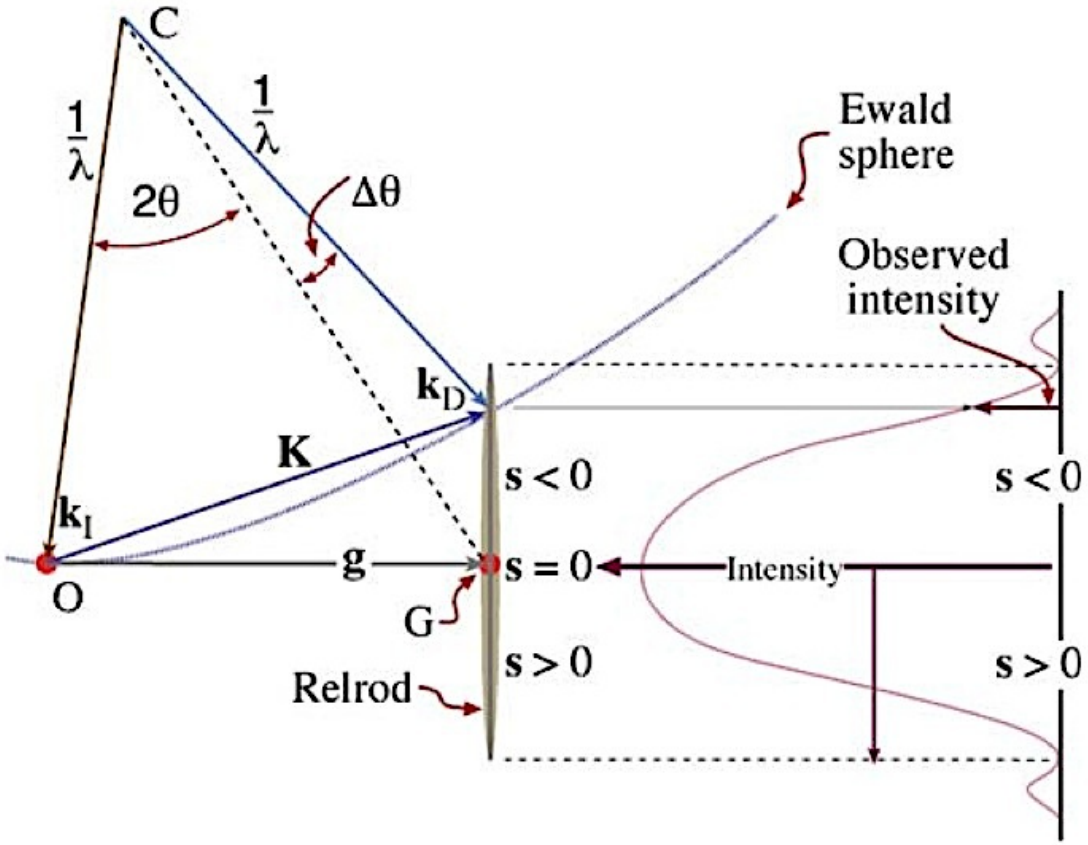

Other notation (Williams and Carter):
$\mathbf{K}=\mathbf{k}_D-\mathbf{k}_I=\mathbf{g}+\mathbf{s}$

The relrod at g_{hkl} when the beam is $\Delta\theta$ away from the exact Bragg condition. The Ewald sphere intercepts the relrod at a negative value of **s** which defines the vector **K** = **g** + **s**. The intensity of the diffracted beam as a function of where the Ewald sphere cuts the relrod is shown on the right of the diagram. In this case the intensity has fallen to almost zero.

Remember: Kikuchi lines

Useful to determine s...

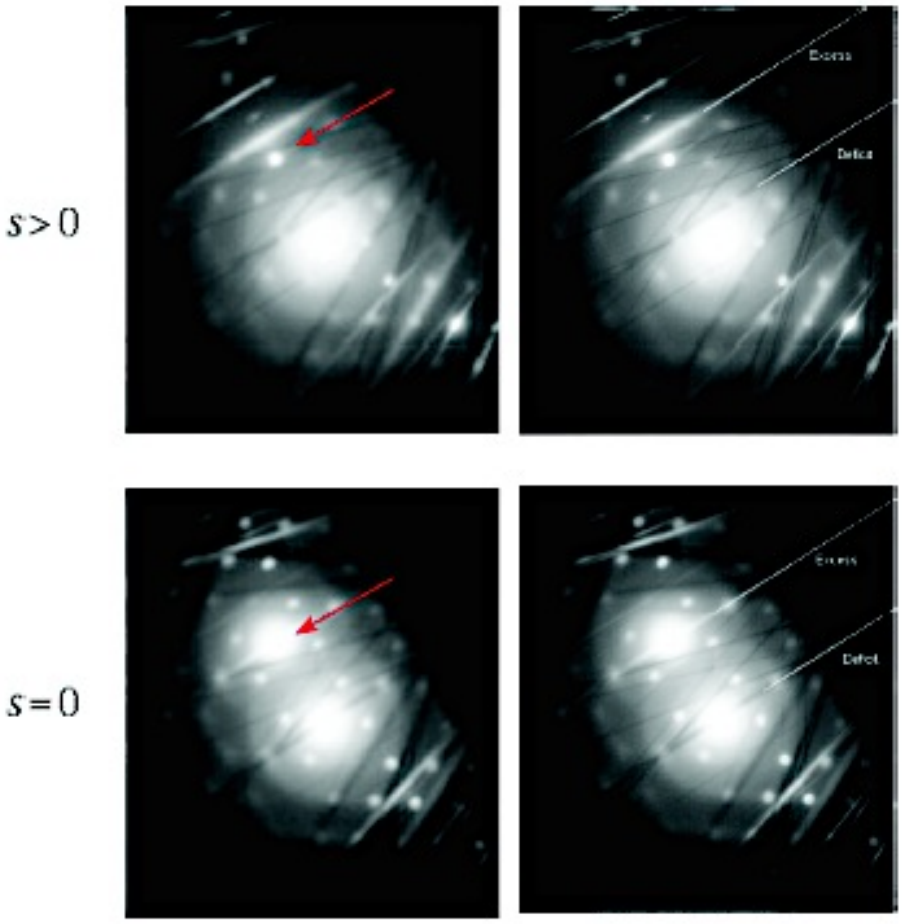

Excess Kikuchi line on G spot
Deficient line in transmitted spot

Diffraction contrast

As **s** increases the defect images become narrower but the contrast is reduced:

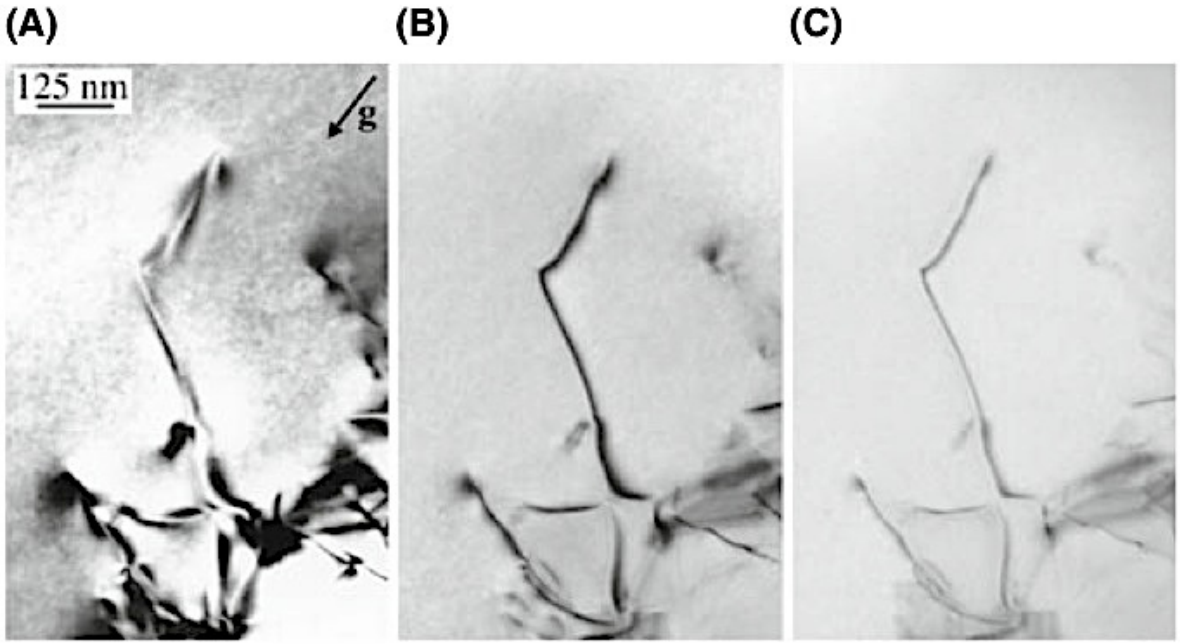

Variation in the diffraction contrast when s is varied from (A) zero to (B) small and positive and (C) larger and positive.

Bright field two-beam images of defects should be obtained with s small and positive.

Phase contrast

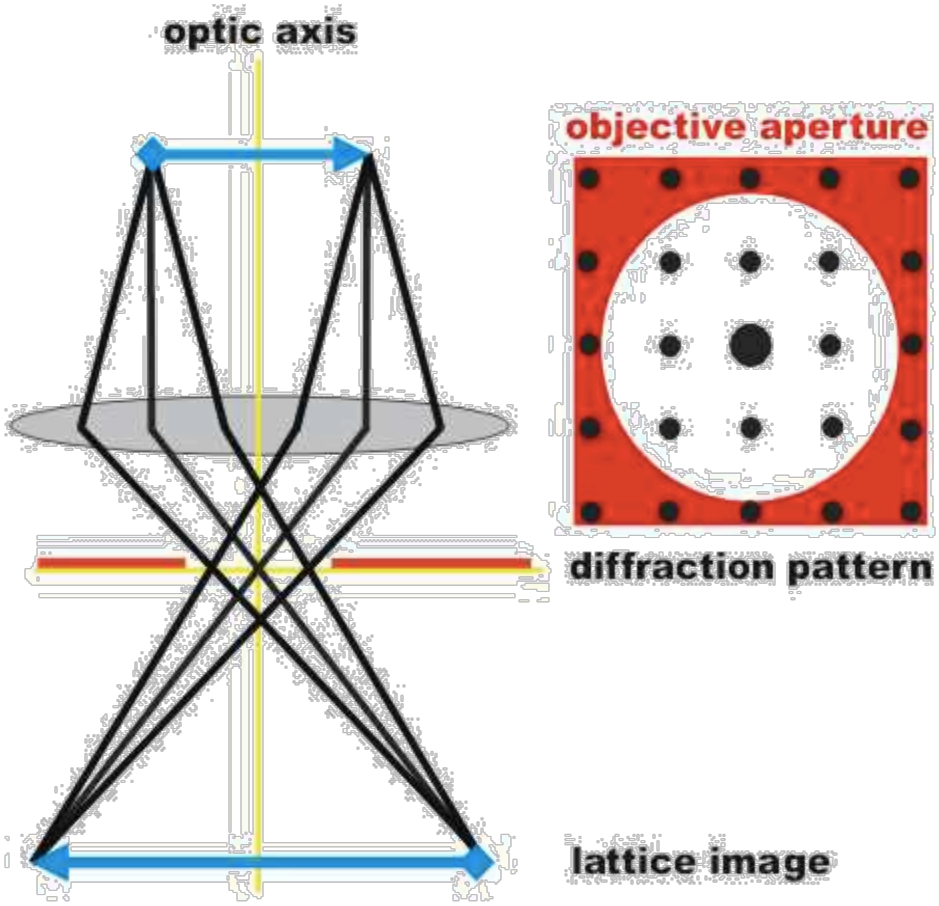

Contrast in TEM images can arise due to the differences in the phase of the electron waves scattered through a **thin specimen**.

Many beams are allowed to pass through the objective aperture (as opposed to bright and dark field where only one beam pases at the time).

To obtain lattice images, a large objective aperture has to be selected that allows many beams to pass including the direct beam.

The image is formed by the interference of the diffracted beams with the direct beam (phase contrast). If the point resolution of the microscope is sufficiently high and a suitable crystalline sample is oriented along a low-index zone axis, then high-resolution TEM (HRTEM) images are obtained.

In many cases, the atomic structure of a specimen can directly be investigated by HRTEM

Phase contrast

Generally speaking, there exists within the field of electron microscopy of materials a distinction between *amplitude contrast* methods (bright and dark field imaging) and *phase contrast* methods ('lattice' imaging):

- If only a single scattered beam is accepted by the objective aperture of the microscope, no interference in the image plane occurs between the different beams and amplitude contrast is generated by the interception of specific electrons scattered by the aperture. This method offers real space information at a resolution of the order of a nanometer, which can be combined with diffraction data from specific small volumes, enabling the analysis of crystal defects by what is known as *Conventional Transmission Electron Microscopy* (CTEM).

- If the objective aperture accepts a number of beams, their interference, resulting from phase shifts induced by the interaction with the specimen, produces intensity fringes generating what is called phase contrast. Since this mechanism can reveal structural details at a scale of less than 1 nm, it can be used to produce 'lattice' images. Phase contrast represents the essence of *High-Resolution Transmission Electron Microscopy* (HRTEM) and allows, under appropriate conditions, to examine the atomic detail of bulk structures, defects and interfaces.

Phase contrast

An atomic resolution image is formed by the "phase contrast" technique, which exploits the differences in phase among the various electron beams scattered by the **THIN** sample in order to produce contrast. A large objective lens aperture allows the transmitted beam and at least four diffracted beams to form an image.

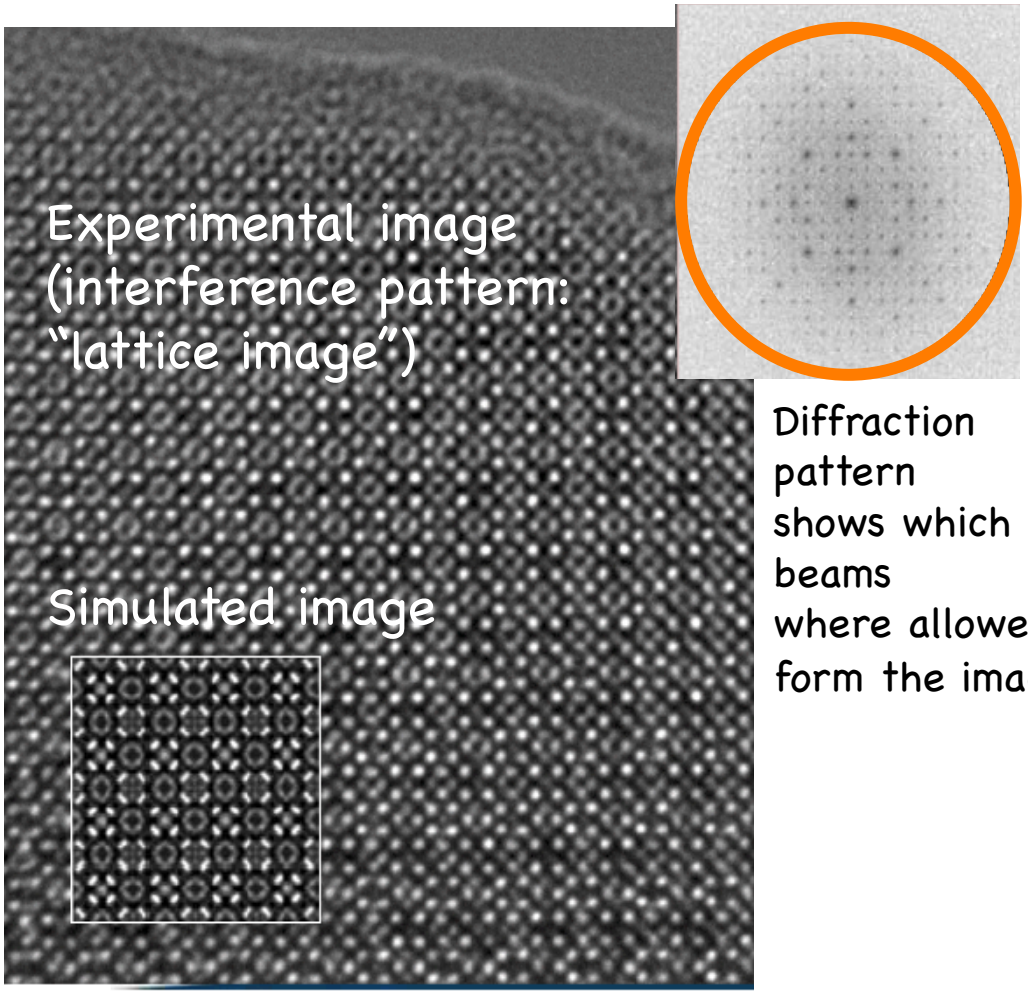

Diffraction pattern shows which beams where allowed to form the image

Phase contrast

- However, the location of a fringe does not necessarily correspond to the location of a lattice plane.
- So lattice fringes are not direct images of the structure, but just give information on lattice spacing and orientation.
- Image simulation is therefore required.

Remember: stacking faults

Stacking faults

For FCC metals an error in ABCABC packing sequence

- Ex: ABCABABC: the local arrangement is hcp
- Stacking faults by themselves are simple two-dimensional defects. They carry a certain stacking fault energy g~100 mJ/m^2

Perfect sequence
<110> projection of
fcc lattice

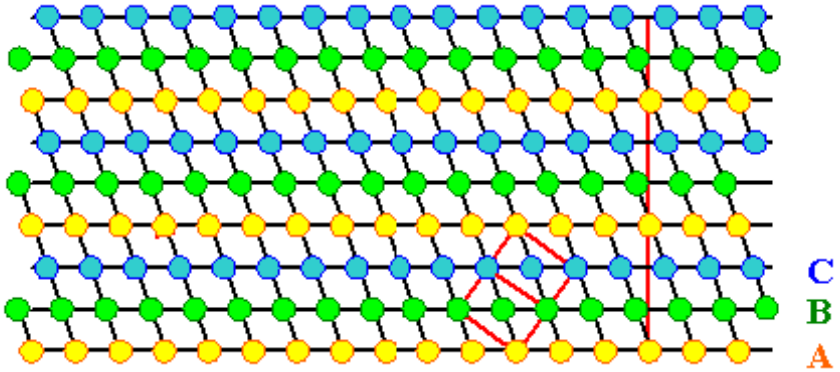

collapse of vacancies disk

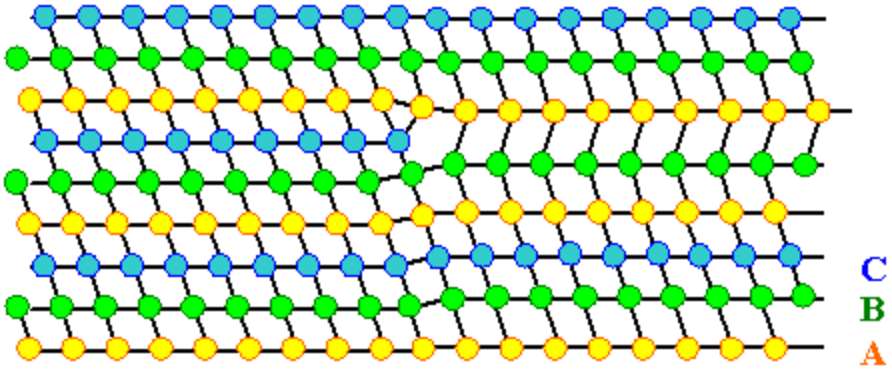

condensation of interstitials disk

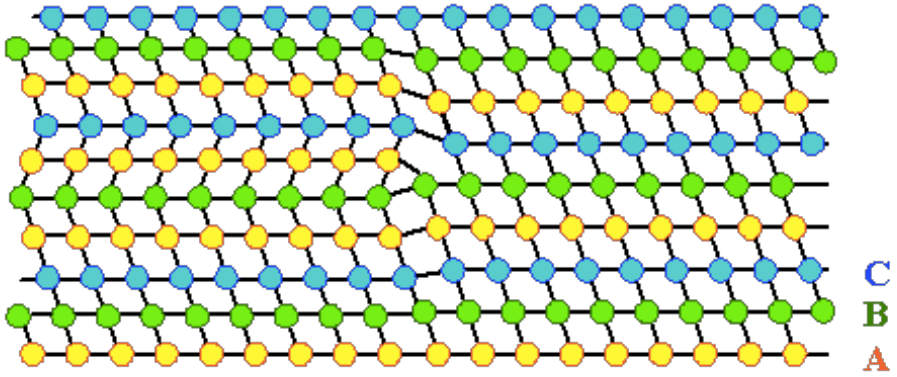

Phase contrast

Example of easily interpretable information: Stacking faults viewed edge on

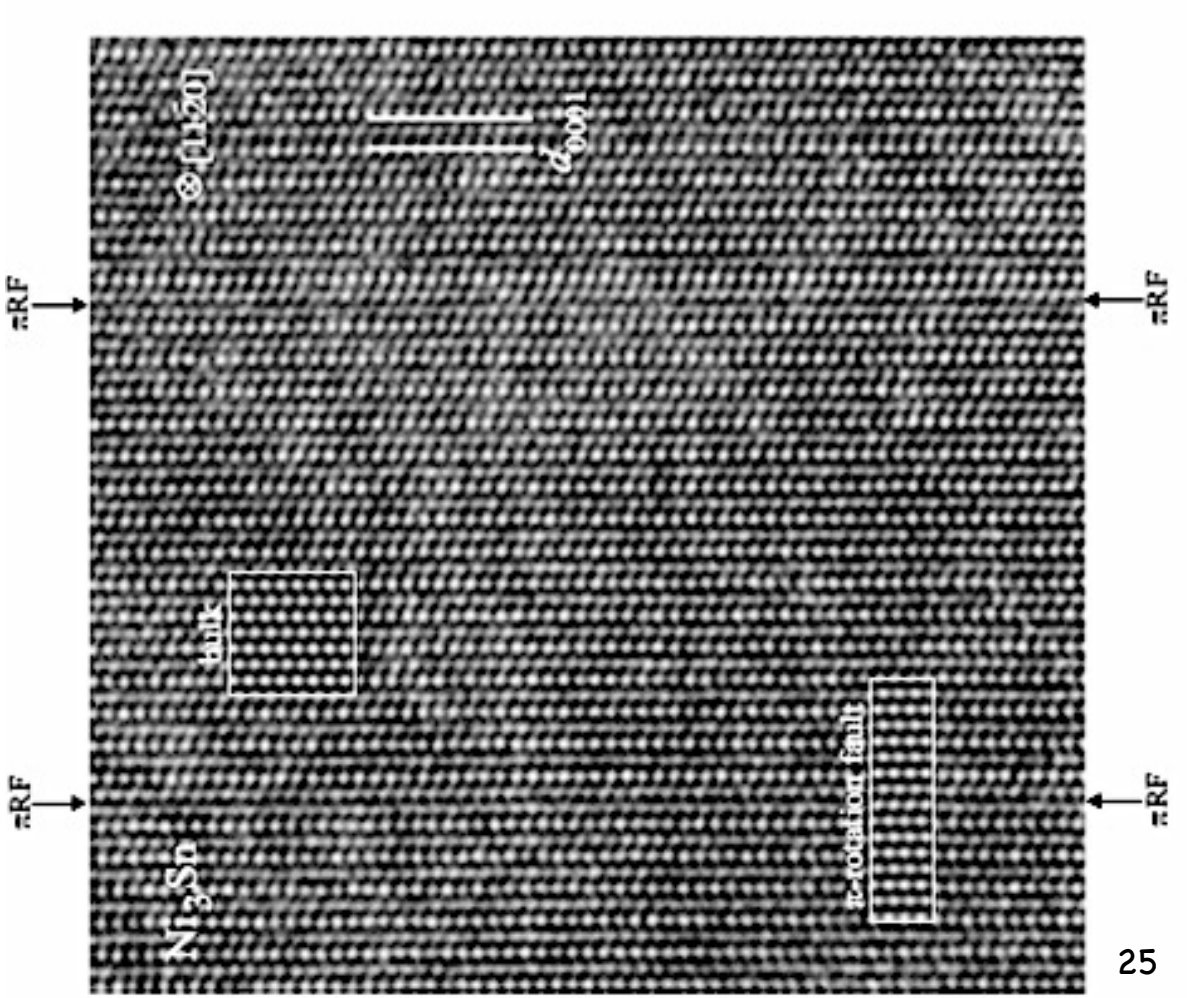

Stacking faults are relative displacements of blocks in relation to the perfect crystal

Phase contrast

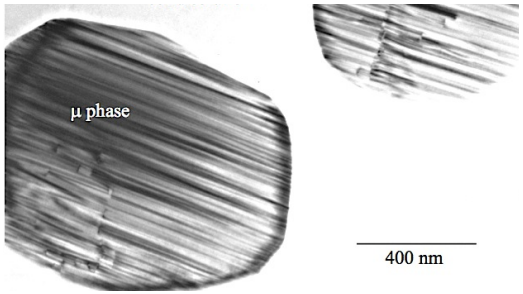

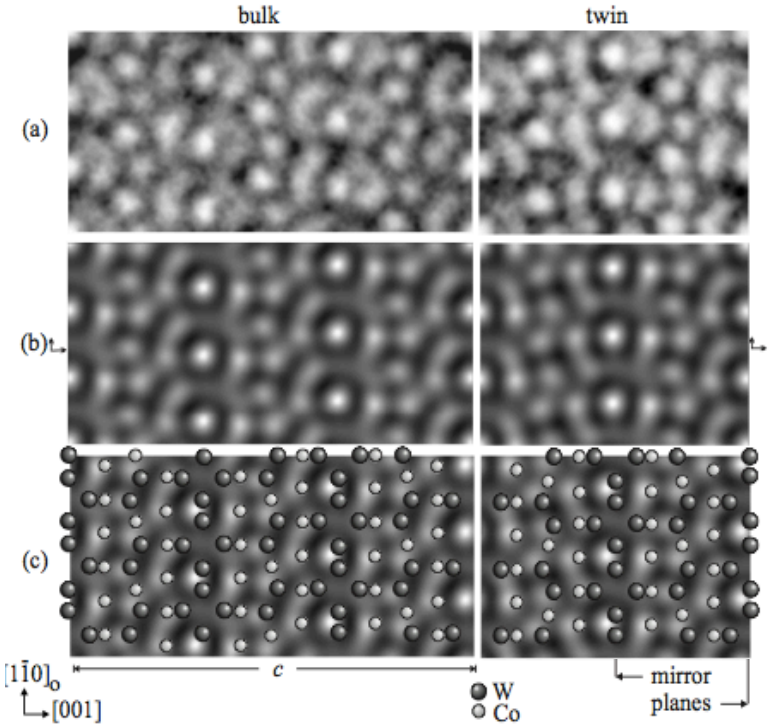

Compare the relative position of the atoms and intensity maxima!

Example of easily interpretable information:
Polysynthetic twins viewed edge on

Co_7W_6

$R\bar{3}m$

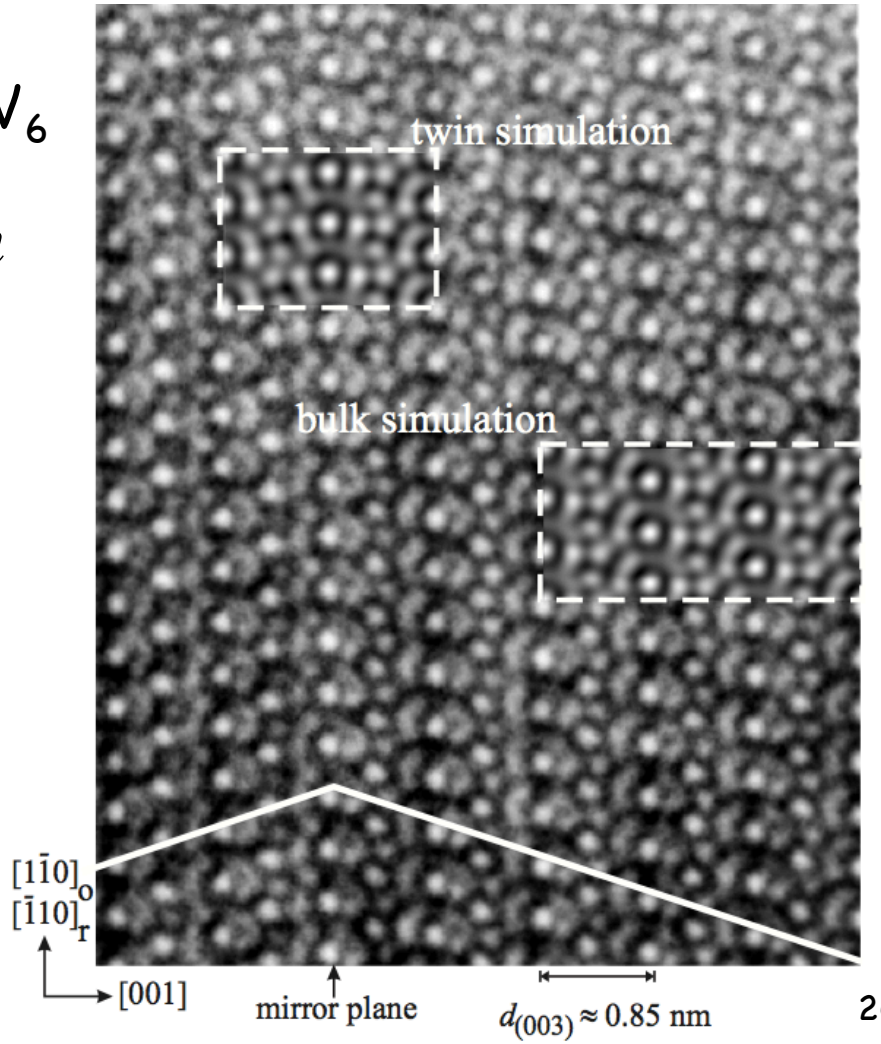

Phase contrast

Example of easily interpretable information:
The spinel/olivine interface viewed edge on

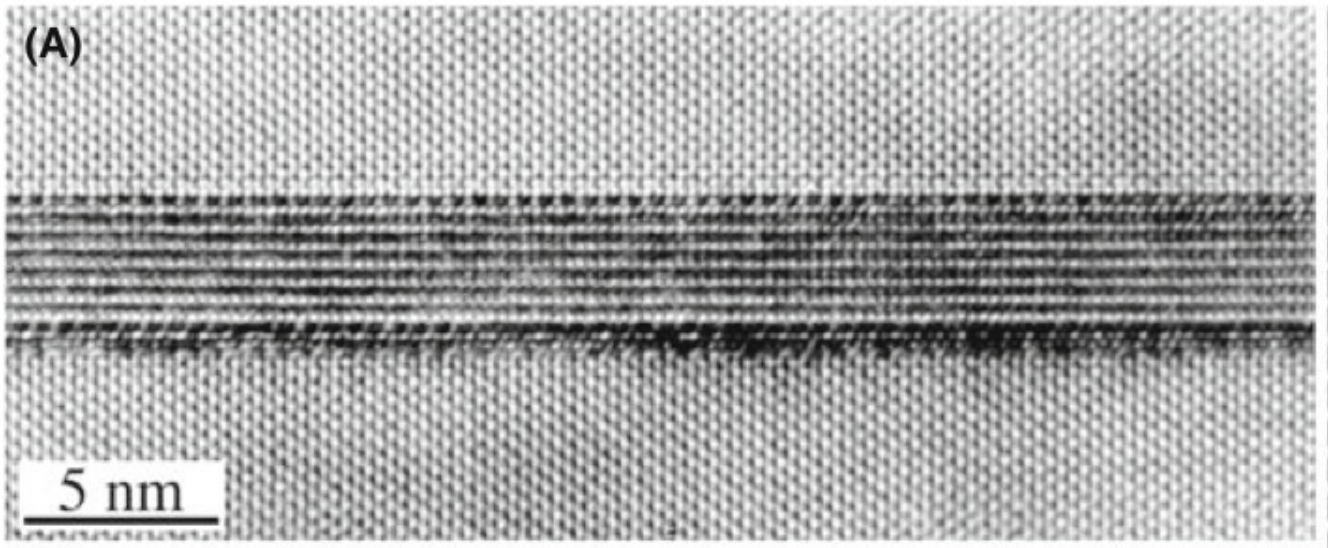

Williams and Carter book

Phase contrast

Example of easily interpretable information:
Faceting at atomic level at a Ge grain boundary

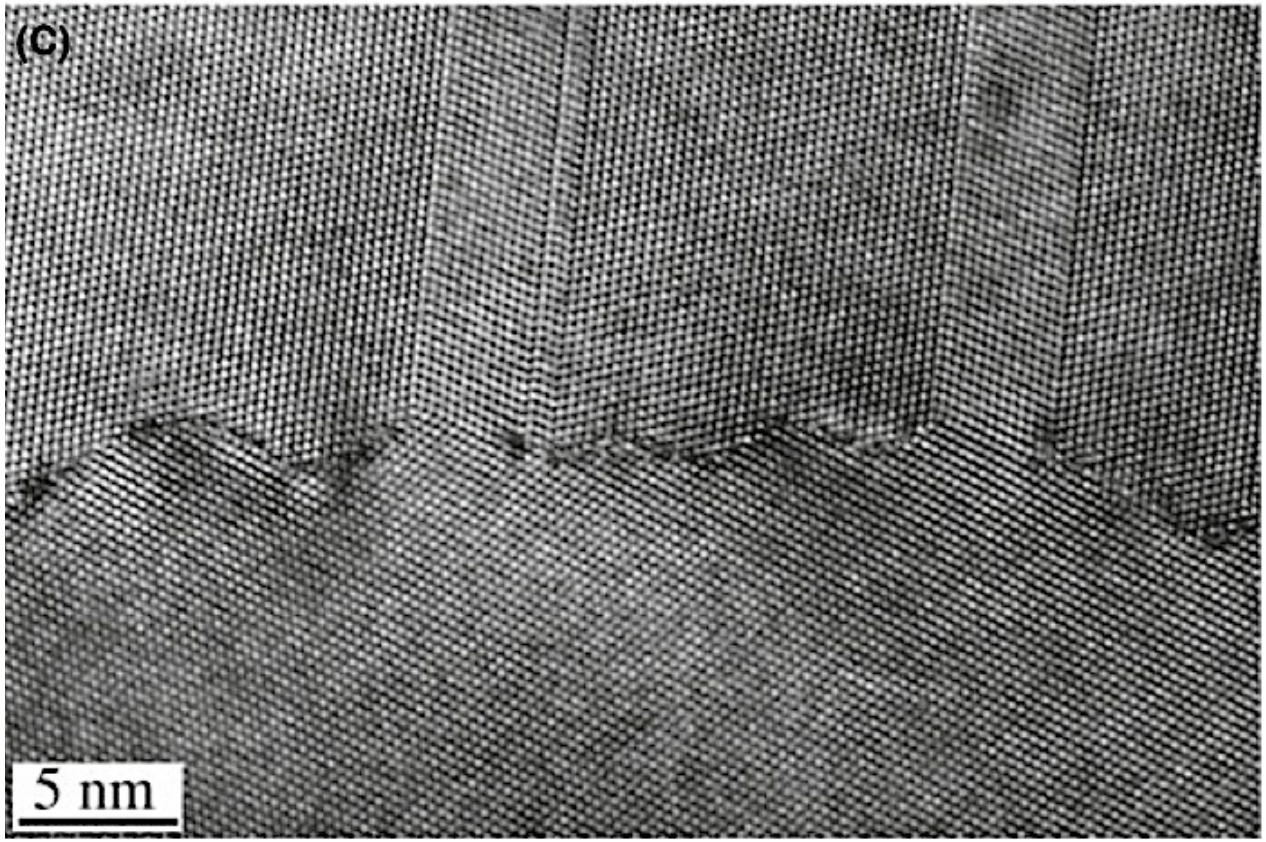

Williams and Carter book

Phase contrast

Example of easily interpretable information:
misfit dislocations viewed end on at a heterojunction between InAsSb and InAs

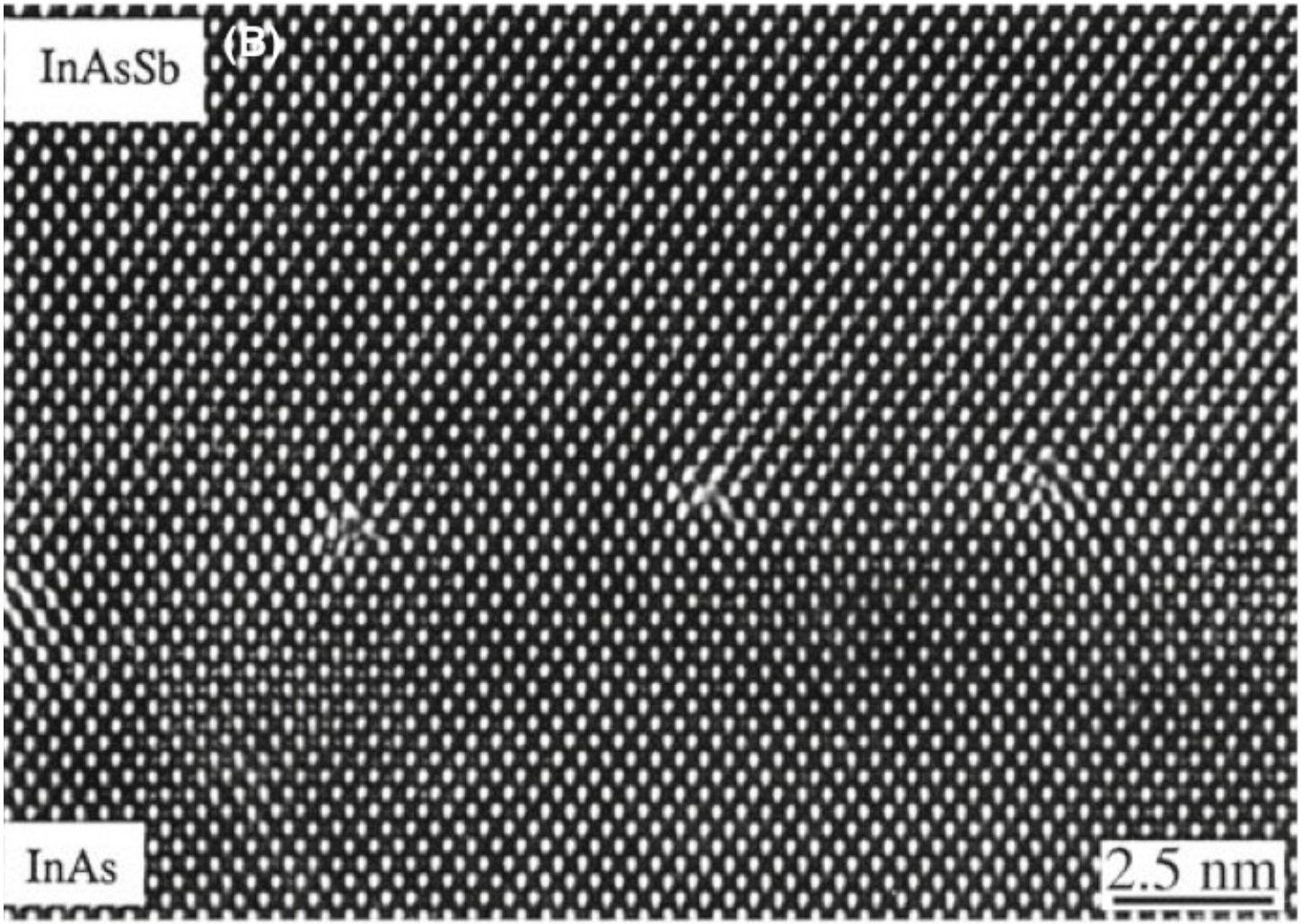

Williams and
Carter book

Remember: dislocations

Edge dislocation:

- extra half-plane of atoms inserted in a crystal structure
- **b** ⊥ to dislocation line

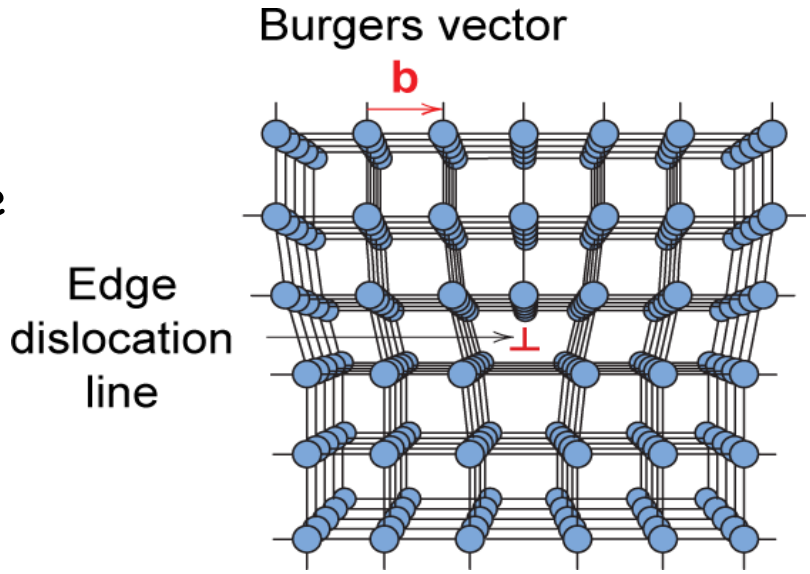

Dislocation movement: slip

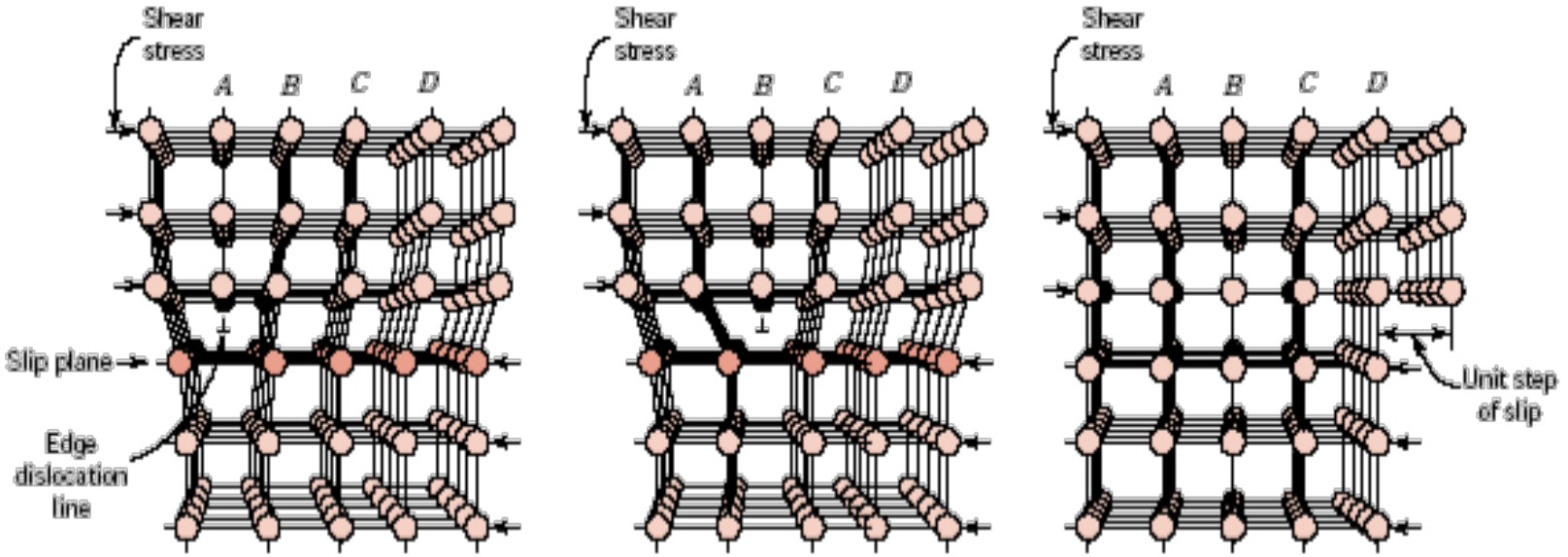

Remember: dislocations

Burgers circuit
Definition of the Burgers vector, **b**, relative to an edge dislocation.
(a) In the perfect crystal, an m × n atomic step loop closes at the starting point.
(b) In the region of a dislocation, the same loop does not close, and the closure vector **(b)** represents the magnitude of the structural defect.

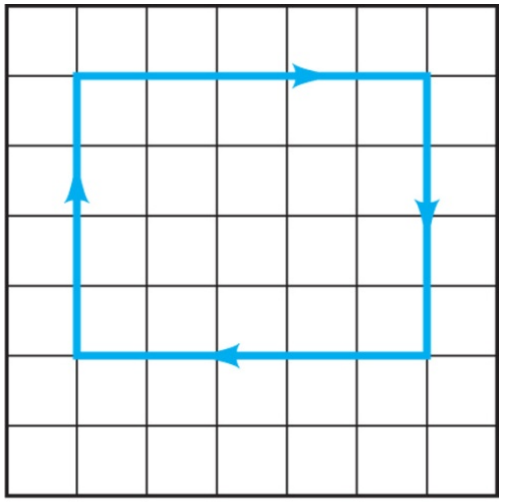

(a)

In an edge dislocation the Burgers vector is perpendicular to the dislocation line.

The Burgers vector is an invariant property of a dislocation (the line may be very entangled but **b** is always the same along the dislocation)

The Burgers vector represents the step formed by the dislocation when it slips to the surface.

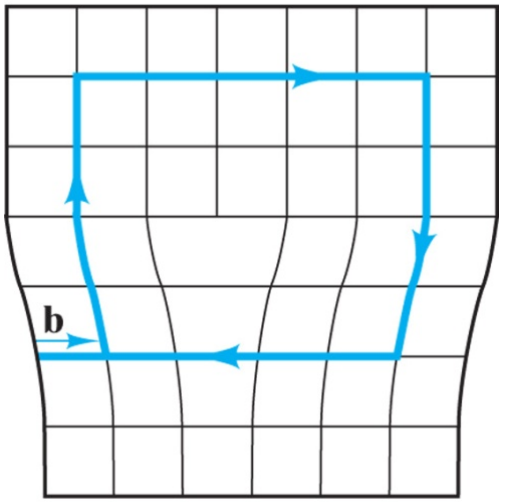

(b)

Phase contrast

Example of easily interpretable information:
misfit dislocations viewed end on at a heterojunction between InAsSb and InAs

Direct use of the Burgers circuit:
Burgers vector of the dislocation

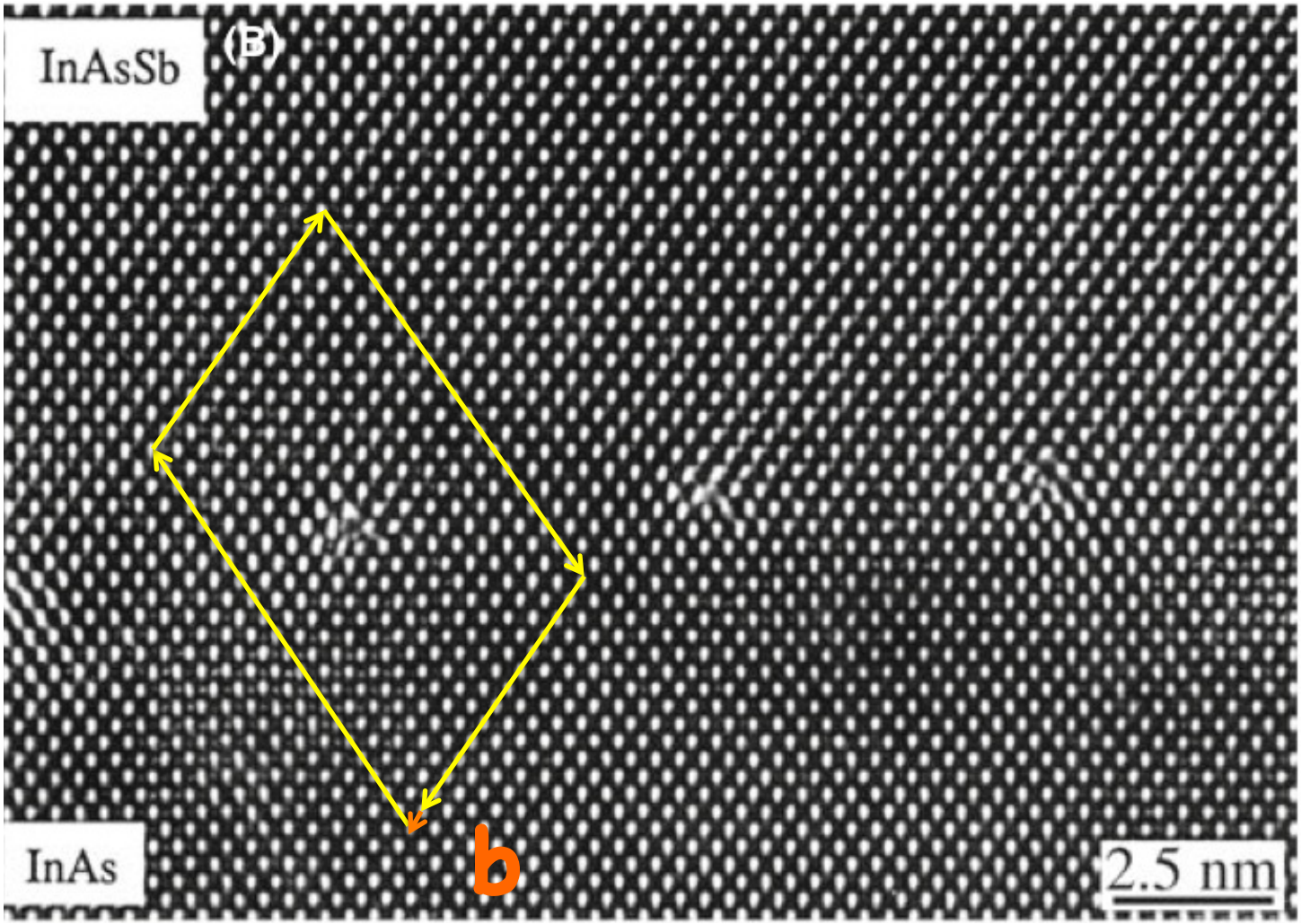

Williams and Carter book

More on planar defects

Remember: dynamical scattering for 2-beam conditions

$$\frac{d\Psi_0}{dz} = \frac{i\pi}{\xi_0}\Psi_0 + \frac{i\pi}{\xi_g}\Psi_g \exp\left(2\pi i s_g z\right)$$

$$\frac{d\Psi_g}{dz} = \frac{i\pi}{\xi_0}\Psi_g + \frac{i\pi}{\xi_g}\Psi_0 \exp\left(-2\pi i s_g z\right)$$

$$I_g = \Psi_g \Psi_g^* = \frac{\pi^2}{\xi_g^2}\frac{\sin^2 \pi t s_g}{(\pi s_g)^2}$$

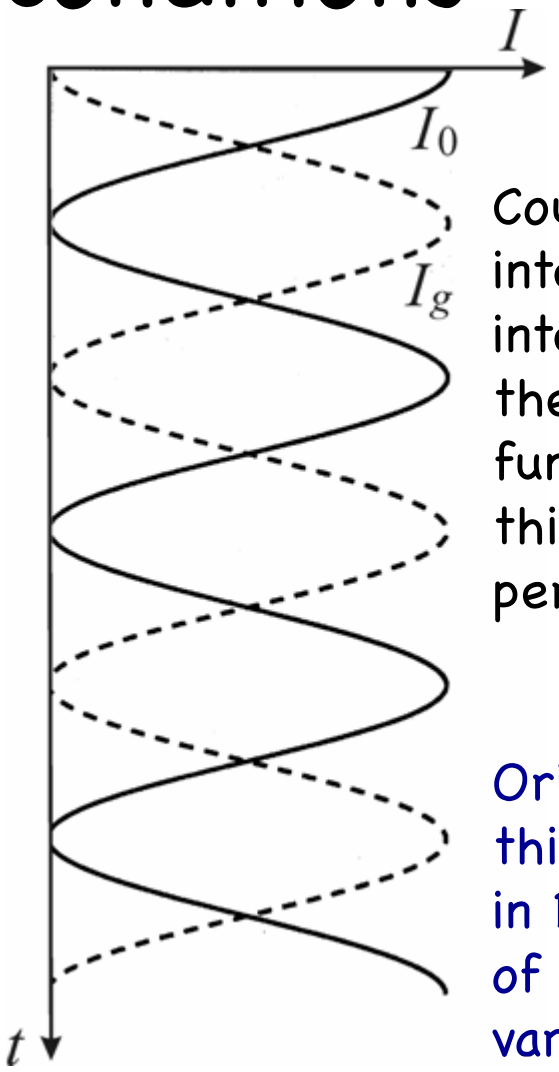

Coupling: interchange of intensity between the two beams as a function of thickness *t* for a perfect crystal

Originates thickness fringes, in BF or DF images of a crystal of varying *t*

Remember: dynamical scattering for 2-beam conditions

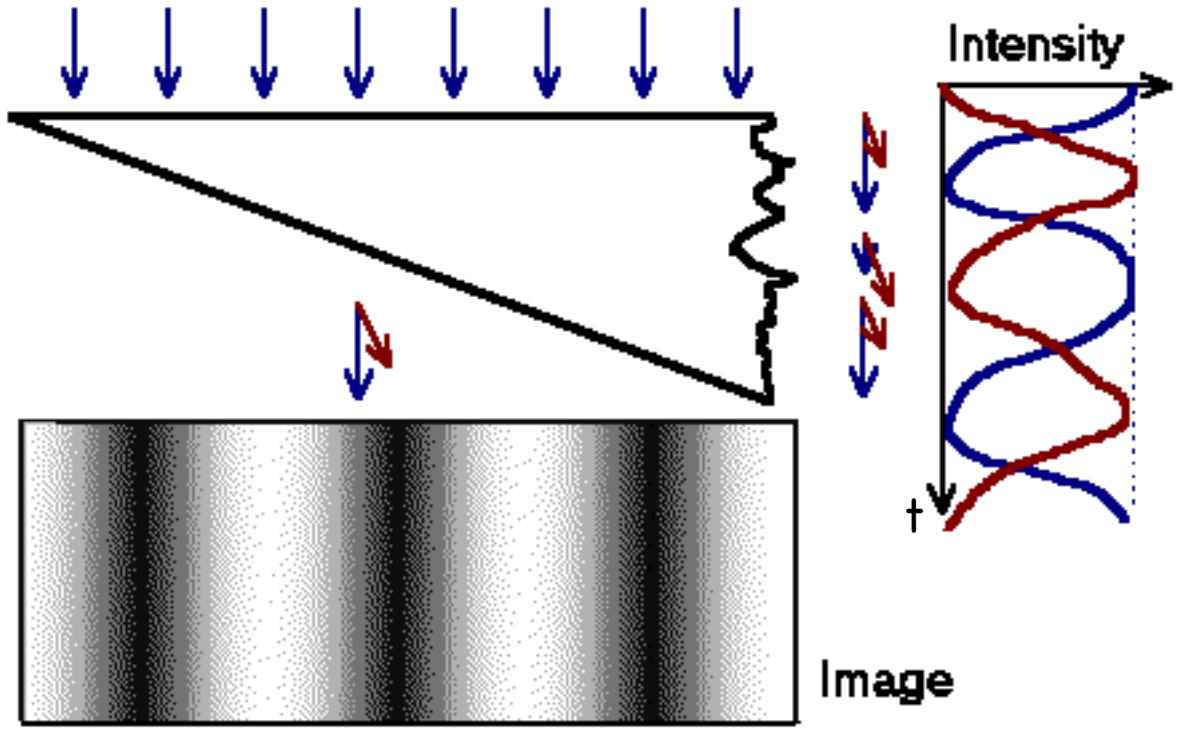

The images of wedged samples present series of so-called thickness fringes in **BF** or **DF** images (only one of the beams is selected).

http://www.tf.uni-kiel.de/

Remember: dynamical scattering for 2-beam conditions

The image intensity varies sinusoidally depending on the thickness and on the beam used for imaging.

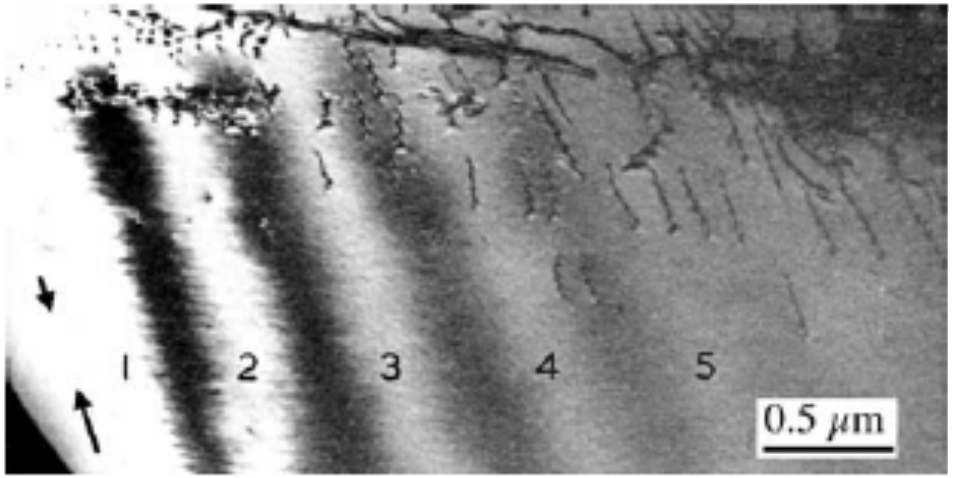

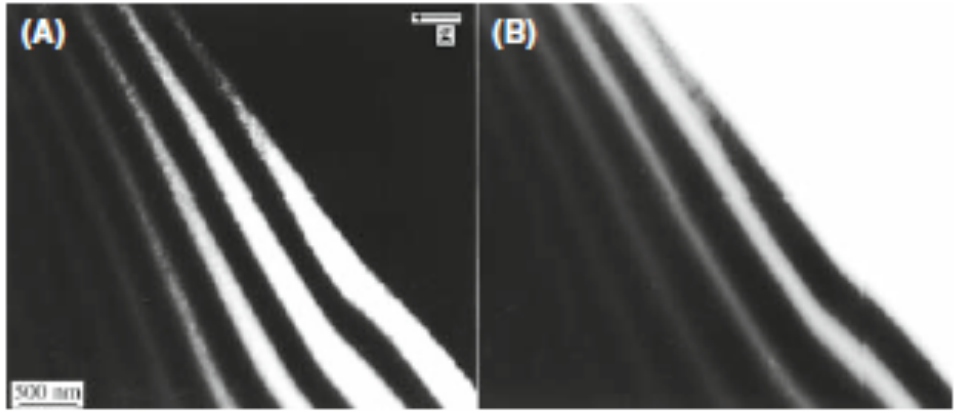

The contrast of thickness fringes in a two-beam BF image decreases when the effect of anomalous absorption is included. Note that the defects are still visible when the fringes have disappeared at a thickness of $\sim 5\,\xi_g$.

A) BF and (B) DF images from the same region of a wedge-shaped specimen of Si at 300 kV tilted so that g(220) is strong. The periodicity and contrast of the fringes are similar and complementary in each image.

Reduced contrast as thickness increases due to absorption

2-beam condition
A: image obtained with transmitted beam (Bright field)
B: image obtained with diffracted beam (Dark field)

Williams and Carter book

Planar defects under two-beam conditions

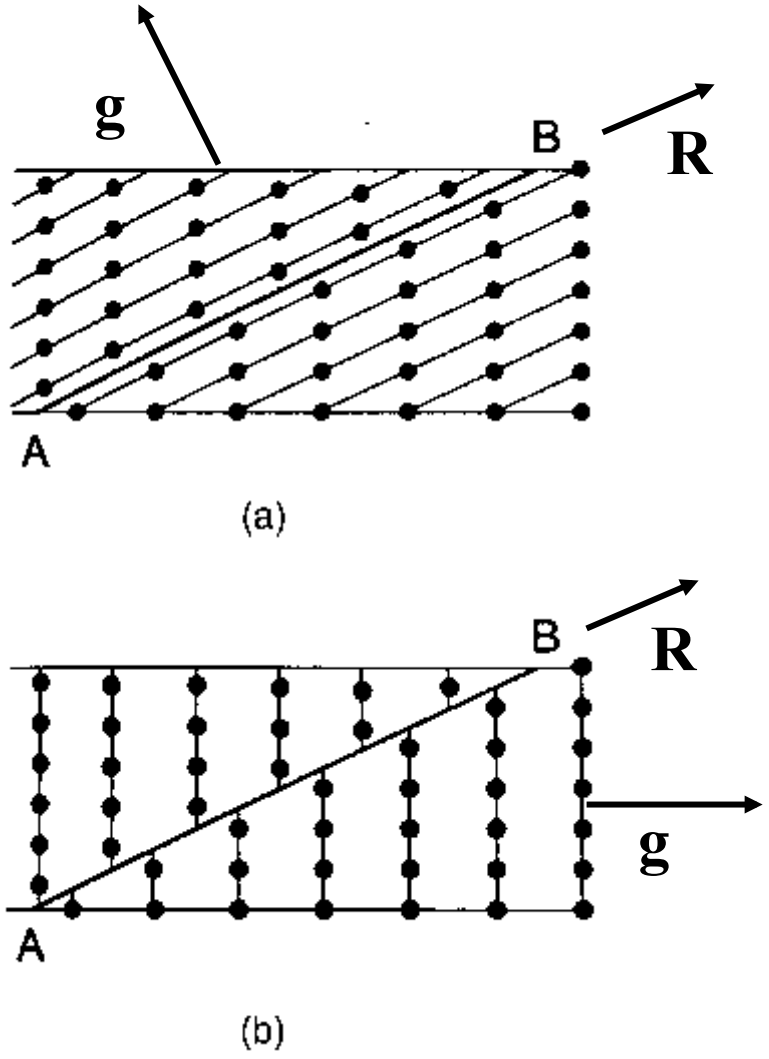

The upper crystal is considered fixed while the lower one is translated by a vector **R**(r) and/or rotated through some angle θ about any axis, v.

In (a) the stacking fault does not disrupt the periodicity of the planes (solid lines).

In (b) the stacking fault disrupts the periodicity of the planes (solid lines).

Planar defects under two-beam conditions

Two-beam condition and no thickness variation:

A phase shift proportional to **g.R** is introduced in the coupled beams

$$\frac{d\Psi_0}{dz} = \frac{i\pi}{\xi_0}\Psi_0 + \frac{i\pi}{\xi_g}\Psi_g \exp(2\pi i s z + 2\pi \mathbf{g}.\mathbf{R})$$

$$\frac{d\Psi_g}{dz} = \frac{i\pi}{\xi_0}\Psi_g + \frac{i\pi}{\xi_0}\Psi_0 \exp(-2\pi i s z + 2\pi \mathbf{g}.\mathbf{R})$$

Additional phase:

$$\boxed{\alpha = 2\pi\, \vec{g}\cdot\vec{R}}$$

Invisibility for: $\alpha = 0, 2\pi, 4\pi\ldots$

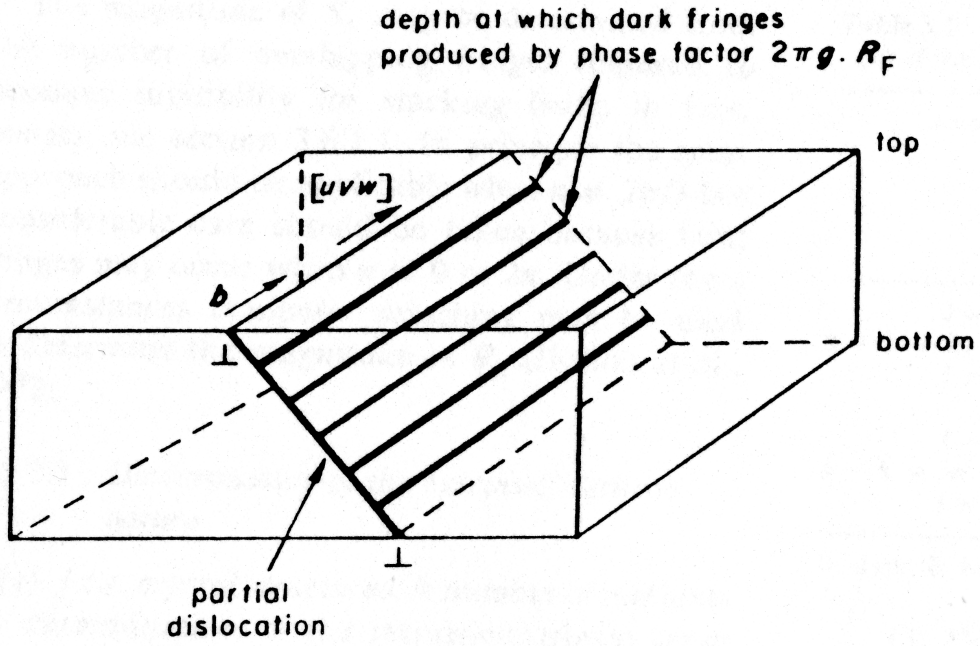

Planar defects under two-beam conditions

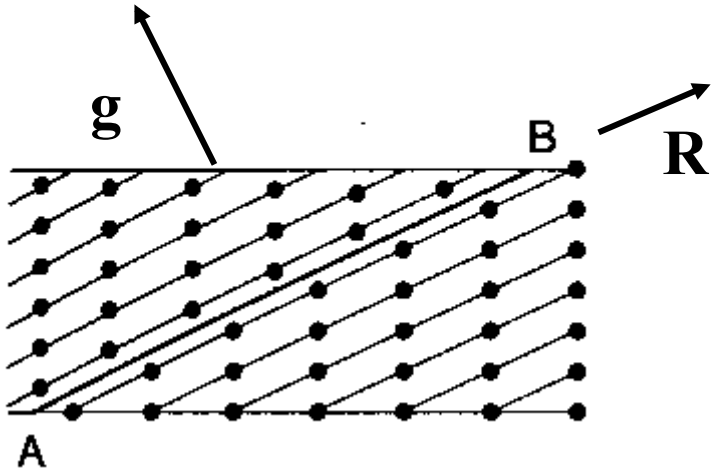

(a)

Invisible **g**.**R** = 0 or even integer

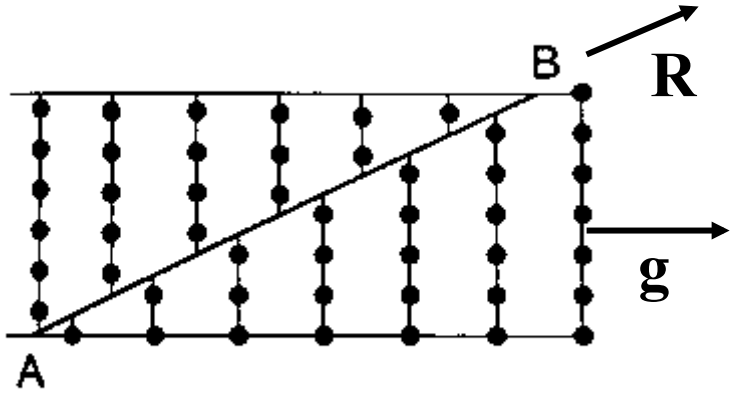

(b)

Visible **g**.**R** ≠ 0

(max contrast for 1 or odd integer)

from two invisibility conditions: $g_1 x g_2$: direction of R!

Planar defects under two-beam conditions

Example:

DO_{19} structure and close-pack preserving stacking faults

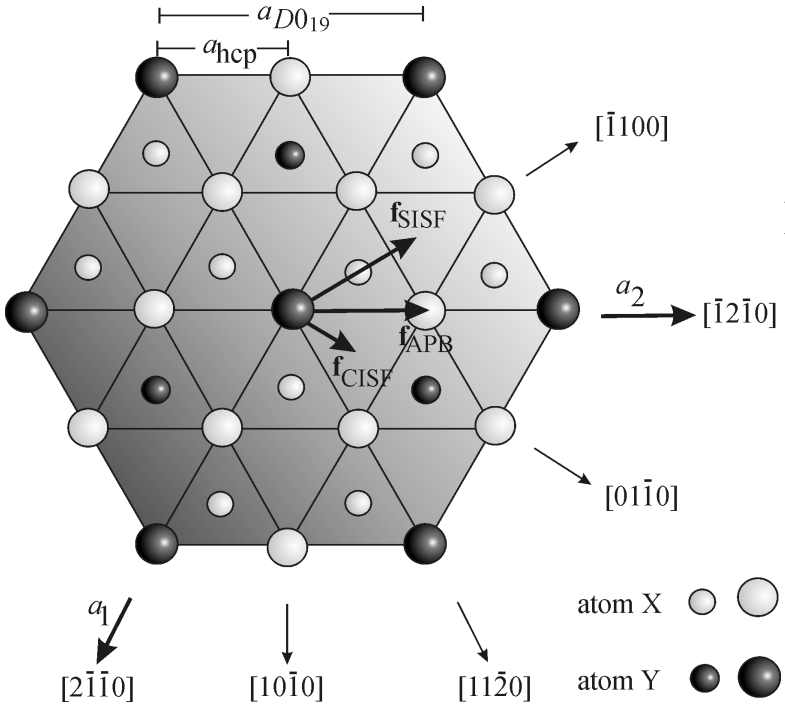

Types of faults

(0002) plane missing

Intrinsic

$$\mathbf{R}_{SISF} = \frac{1}{3}\langle \bar{1}100 \rangle$$

$$\mathbf{R}_{CISF} = \frac{1}{6}\langle 01\bar{1}0 \rangle$$

$$\mathbf{R}_{APB} = \frac{1}{6}\langle \bar{1}2\bar{1}0 \rangle \equiv \frac{1}{2}\langle \bar{1}010 \rangle$$

Intrinsic+Extrinsic

$$\mathbf{R}_{\pi RF} = \frac{1}{6}\langle \bar{2}203 \rangle \equiv \mathbf{R}_i + \mathbf{R}_e$$

$$\mathbf{R}_{CIESF} = \frac{1}{6}\langle 01\bar{1}3 \rangle$$

$$\mathbf{R}_{APB} = \frac{1}{6}\langle \bar{1}\bar{1}23 \rangle$$

I = Invisible
V = Visible

g	SISF	Complex			ESF	APB			
		1	2	3		1,4	2	3	5
$11\bar{2}0$	I	V	I	V	I	V	I	V	I
$22\bar{4}0$	I	I	I	I	I	I	I	I	I
$0\bar{2}22$	V	V	V	V	I	I	I	I	I
$01\bar{1}\bar{1}$	V	V	V	V	V	V	V	I	I
$2\bar{1}\bar{1}2$	I	I	V	V	I	V	V	I	V
$1\bar{2}12$	I	V	V	I	I	I	V	V	V

Planar defects under two-beam conditions

DO_{19} structure and close-pack preserving displacements

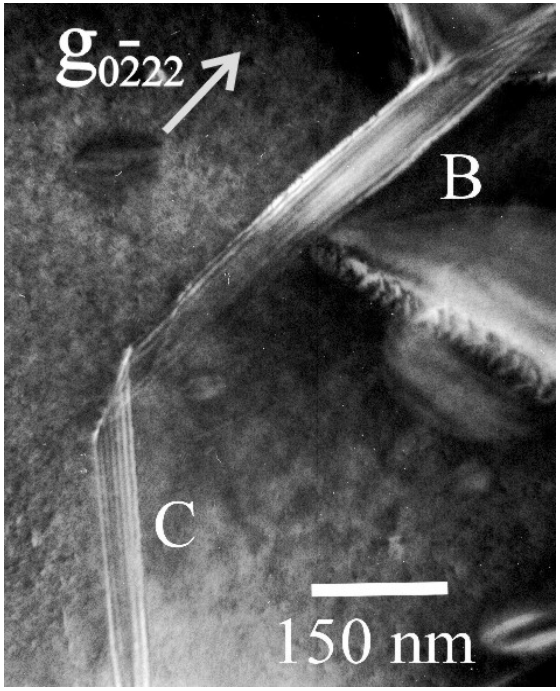

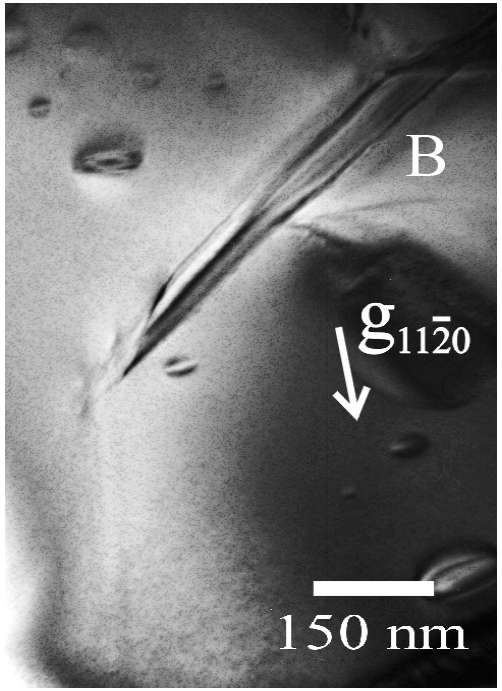

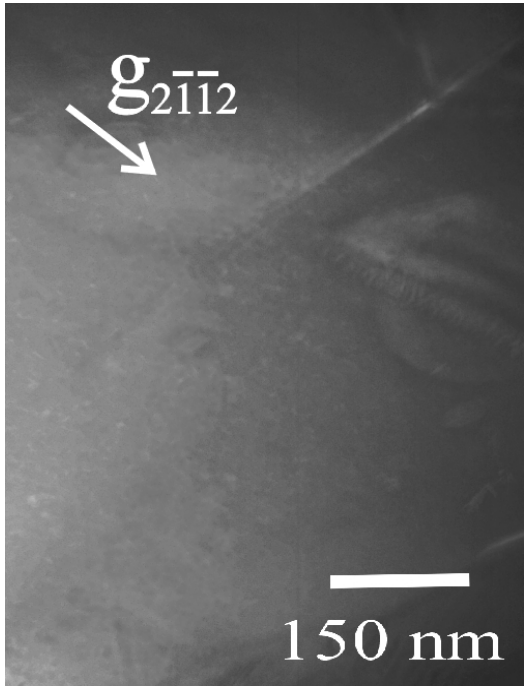

Determination of the fault vector

B: complex $\mathbf{R} = \frac{1}{6}\langle 01\bar{1}0 \rangle$

C: superlattice $\mathbf{R} = \frac{1}{3}\langle \bar{1}100 \rangle$

g	SISF	Complex			ESF	APB			
		1	2	3		1,4	2	3	5
$11\bar{2}0$	(I)	(V)	I	V	I	V	I	V	I
$22\bar{4}0$	I	I	I	I	I	I	I	I	I
$0\bar{2}22$	(V)	(V)	V	V	I	I	I	I	I
$01\bar{1}\bar{1}$	V	V	V	V	V	V	V	I	I
$2\bar{1}\bar{1}2$	(I)	(I)	V	V	I	V	V	I	V
$1\bar{2}12$	I	V	V	I	I	I	V	V	V

Imaging strain fields (typically dislocations)

(quantitative information from 2-beam conditions)

Imaging strain fields

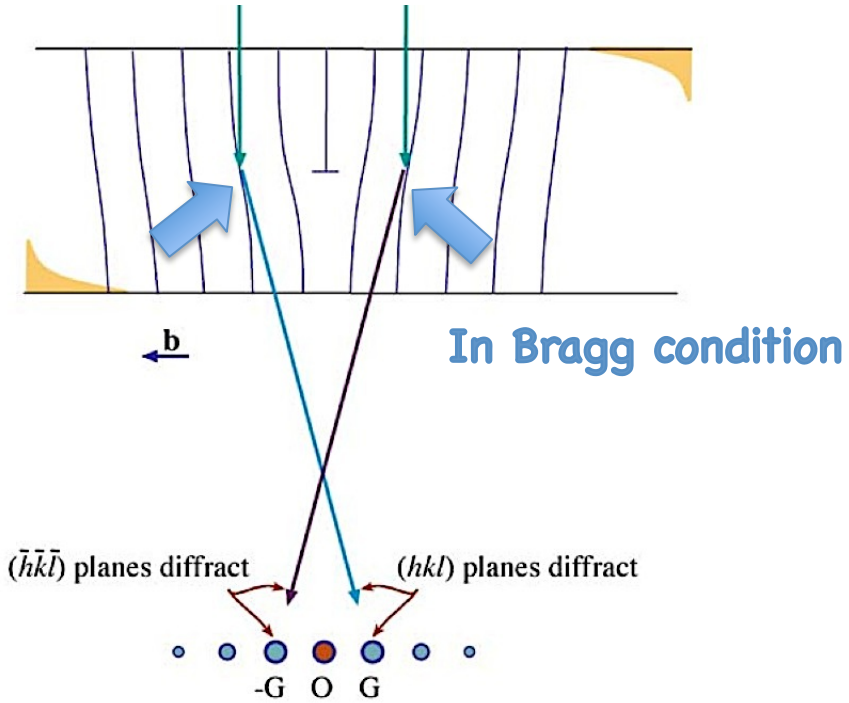

The specimen is tilted slightly away from the Bragg condition (**s** ≠ 0). The distorted planes close to the edge dislocation are bent back into the Bragg-diffracting condition (**s** = 0), diffracting into G and −G as shown.

Imaging strain fields

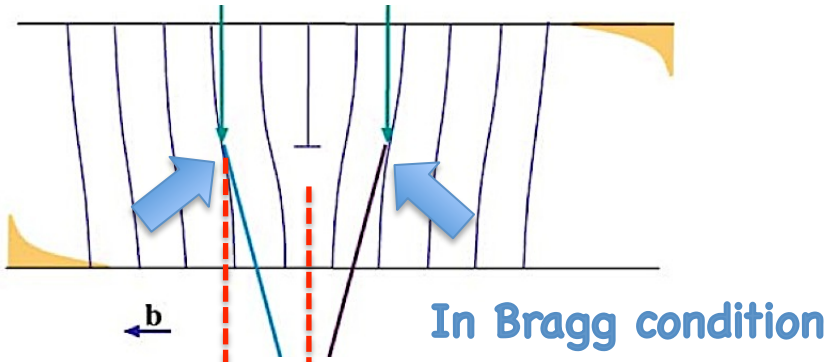

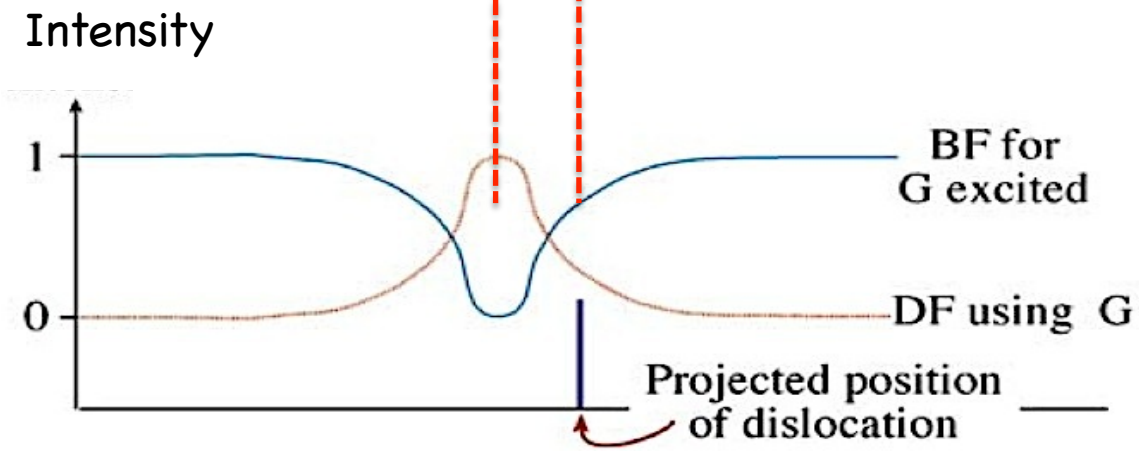

Schematic profiles across the dislocation image showing that the defect contrast is displaced from the projected position of the defect. (As usual for an edge dislocation, **u** points into the paper).

Imaging strain fields

The **g.b** rule

Only the planes belonging to $\mathbf{g}_1$ are affected by the presence of the dislocation.
Applying **g.b**:

$\mathbf{g}_1.\mathbf{b} \neq 0$
$\mathbf{g}_2.\mathbf{b} = 0$
$\mathbf{g}_3.\mathbf{b} = 0$

$\therefore \mathbf{g}_2 \otimes \mathbf{g}_3 = 0$

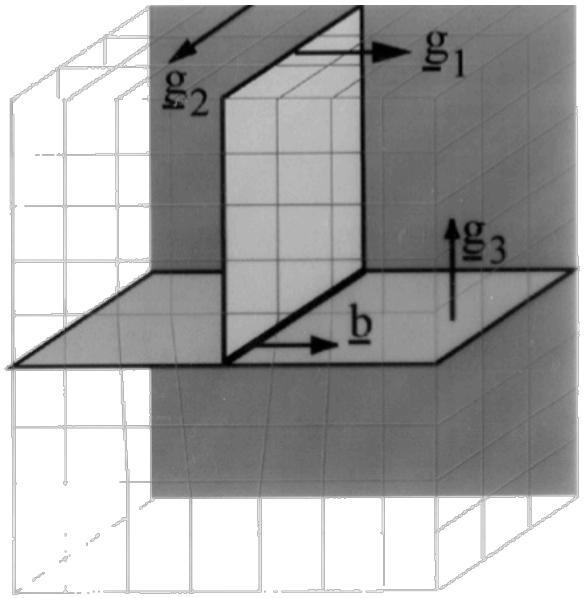

Invisibility criterion: **g.b** = 0

from two invisibility conditions: $\mathbf{g}_1 \times \mathbf{g}_2$: **b** direction

Imaging strain fields

Determination of **b** from the visibility conditions of the strain field associated with dislocations

Due to some stress relaxation complete invisibility is never achieved for edge dislocations, unlike screw dislocations

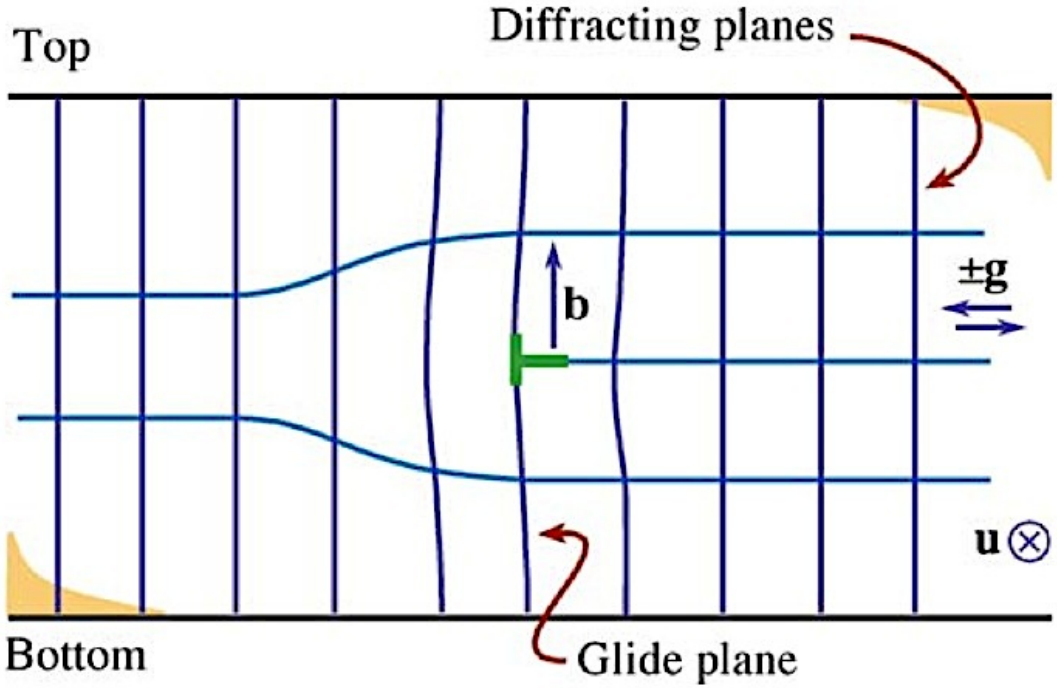

Invisibility criterion: $\mathbf{g}.\mathbf{b} = 0$

from two invisibility conditions: $\mathbf{g}_1 \times \mathbf{g}_2$: **b** directio

Imaging strain fields

Direction of g in the diffraction pattern gives an indication of the direction of displacement of the dislocation contrast

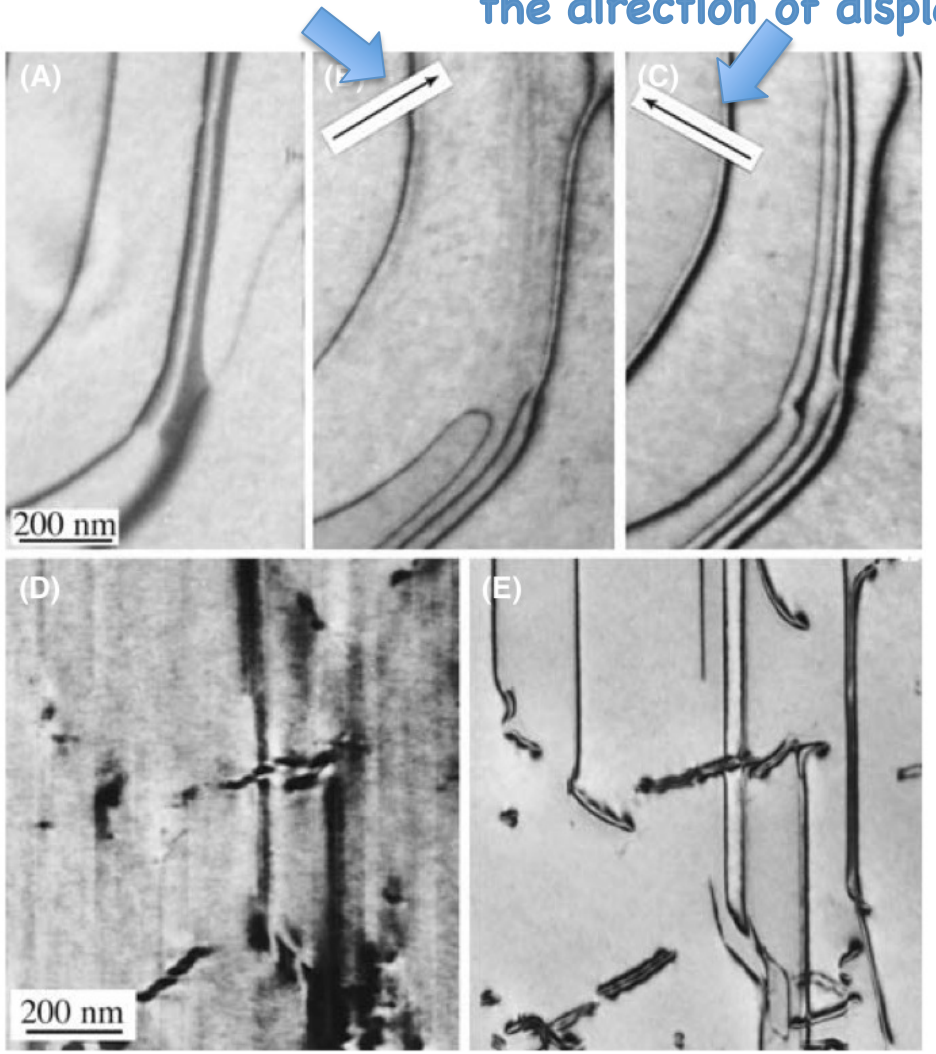

(A–C) Three strong-beam BF images from the same area using (A) {11-1 } and (B, C) {220} reflections to image dislocations which lie nearly parallel to the (111) foil surface in a Cu alloy which has a low stacking-fault energy.

(D, E) Dislocations in Ni_3Al in a (001) foil imaged in two orthogonal {220} reflections. Most of the dislocations are out of contrast in (D).

Williams and Carter book

Imaging strain fields

Nanoindentation generates pileups of dislocation loops in Ni (arrows).

Can we characterize them?

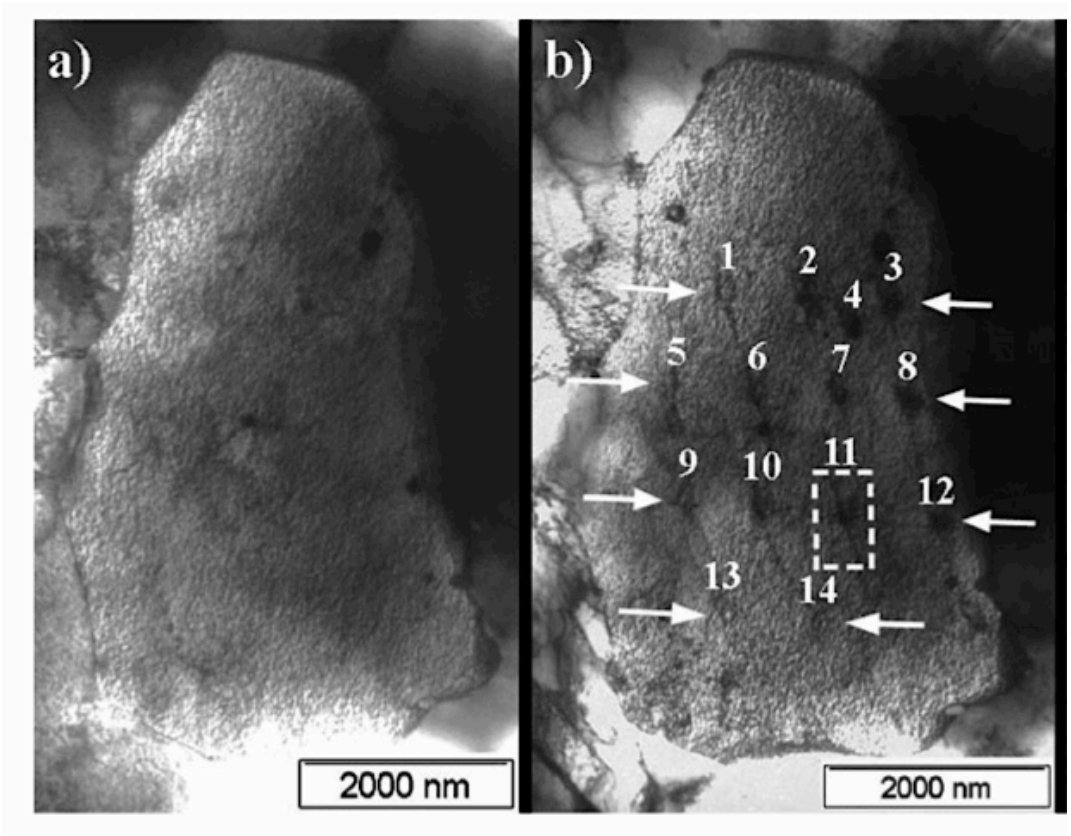

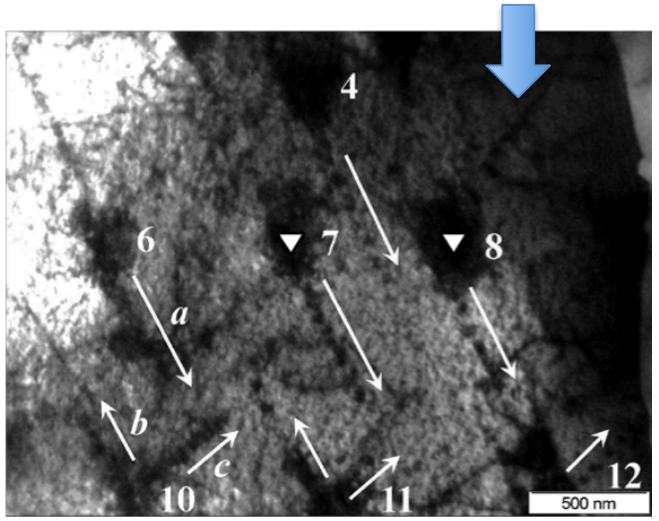

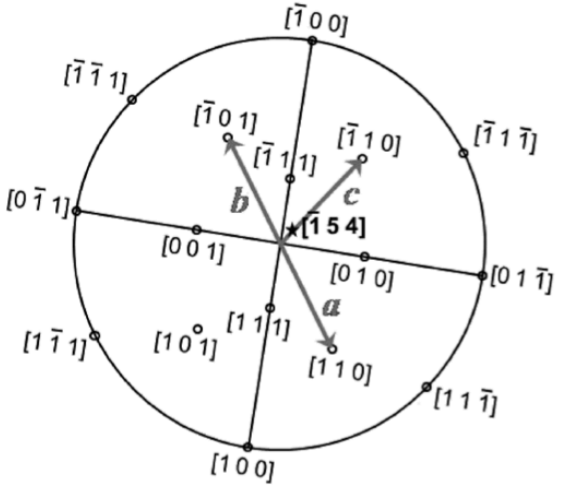

pileup directions: ⟨1 1 0⟩

Imaging strain fields

Magnified details

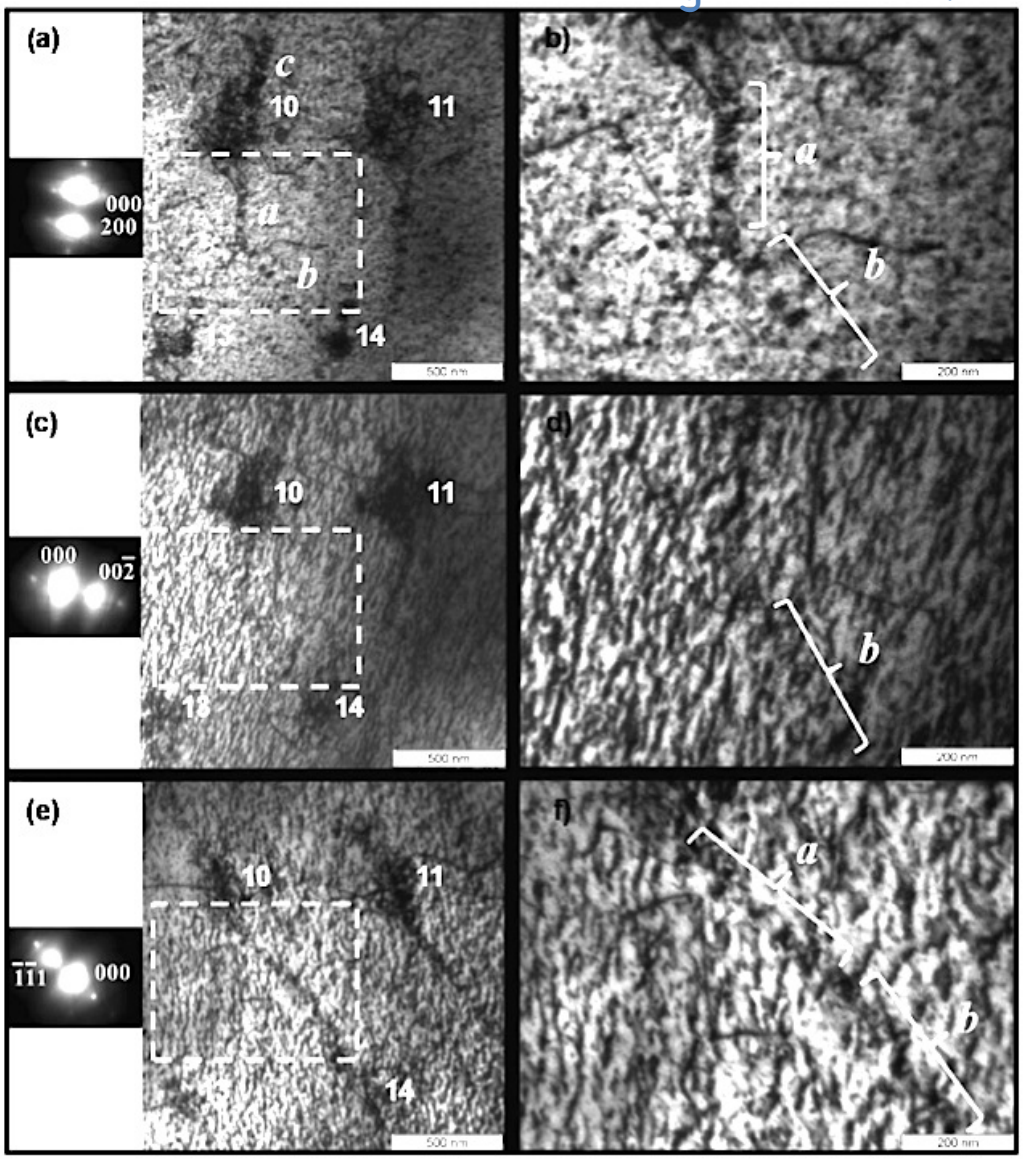

Values of g · b for perfect dislocations in FCC crystals. Dislocations become invisible when g · b = 0

b	200	$00\bar{2}$	$\bar{1}\,\bar{1}\,1$
$\pm 1/2[1\,1\,0]$	± 1	0	± 1
$\pm 1/2[\bar{1}\,0\,1]$	± 1	± 1	± 1
$\pm 1/2[\bar{1}\,1\,0]$	± 1	0	0
$\pm 1/2[1\,0\,1]$	± 1	± 1	0
$\pm 1/2[0\,1\,1]$	0	± 1	0
$\pm 1/2[0\,1\,\bar{1}]$	0	± 1	± 1

Pileups along a are visible in (a), (b) and (e), (f) but are invisible in (c), (d): $\mathbf{b} = \pm\frac{1}{2}[110]$

Pileups along b are visible in (a)–(f): $\mathbf{b} = \pm\frac{1}{2}[\bar{1}01]$

Pileups along c are visible in (a) and invisible with the other conditions: $\mathbf{b} = \pm\frac{1}{2}[\bar{1}10]$

Imaging strain fields

Weak beam = kinematical approximation

Before we saw for 2-beam condition:

$$I_{\mathbf{g}} = \left(\frac{\pi t}{\xi_{\mathbf{g}}}\right)^2 \frac{\sin^2(\pi t s_{eff})}{(\pi t s_{eff})^2} \qquad \text{where:} \qquad s_{eff} = \sqrt{s^2 + \frac{1}{\xi_{\mathbf{g}}{}^2}}$$

For **g**

Weak-beam imaging: make s large (~0.2 nm^{-1})

Now $I_{\mathbf{g}}$ is effectively independent of $\xi_{\mathbf{g}}$ - i.e. beam coupling "kinematical" conditions!

=> dark-field image intensity easier to interpret

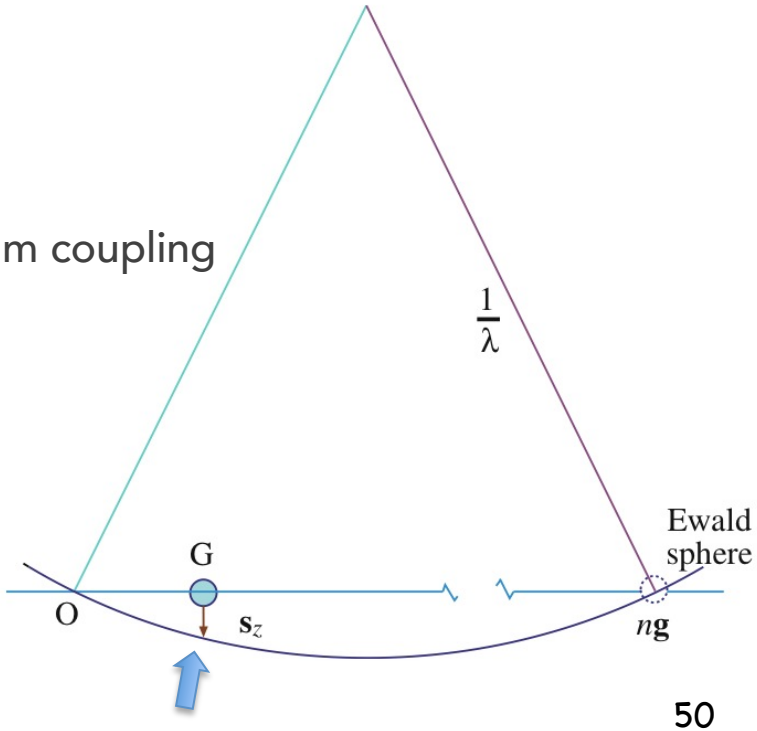

Imaging strain fields

In general we need to tilt both the specimen and the beam to achieve weak beam conditions

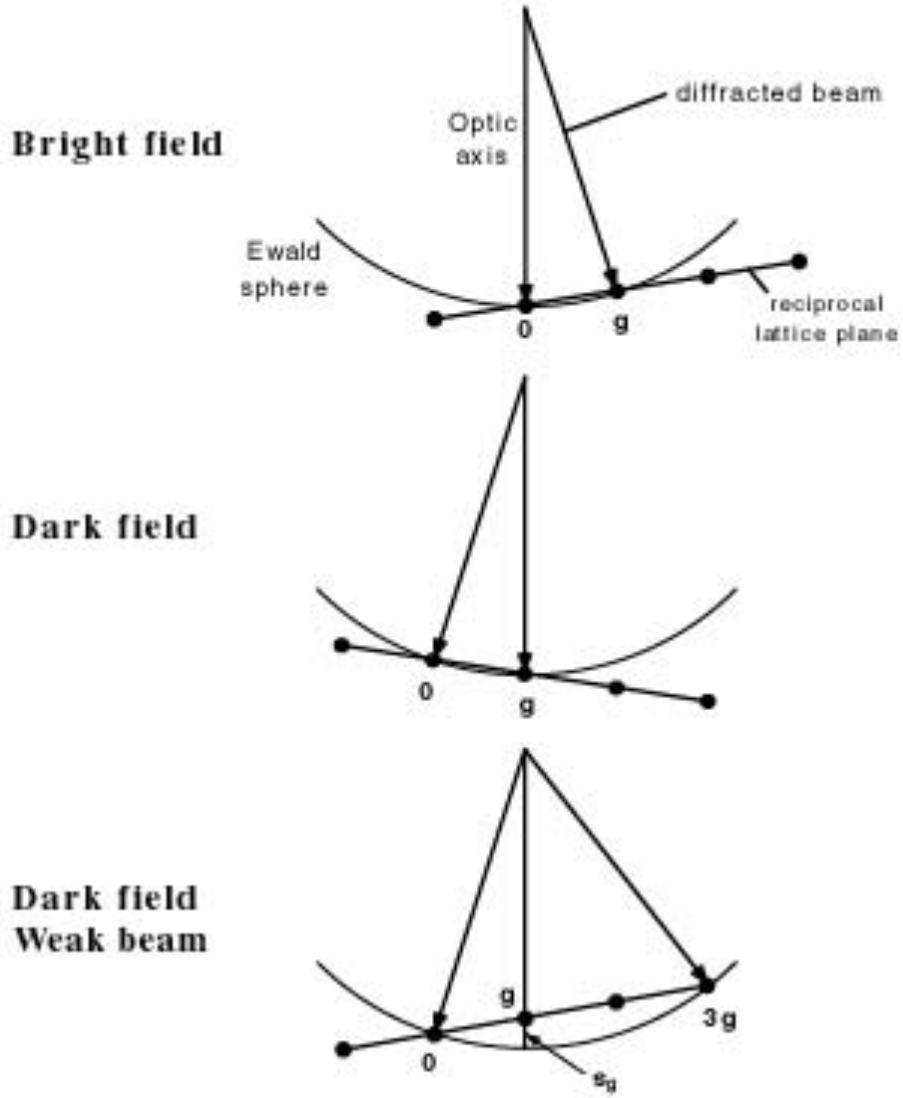

Imaging strain fields

Two beam BF WBDF

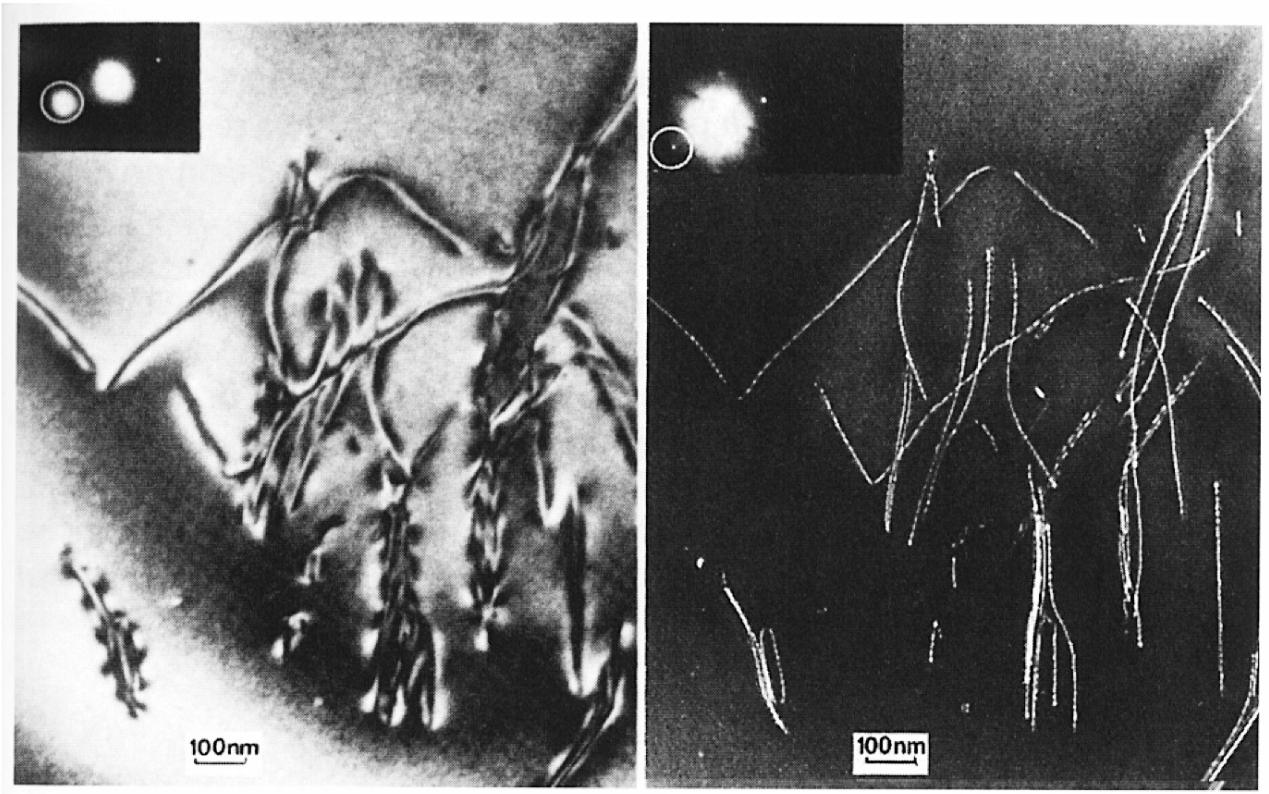

Fig. 7.41. Dislocations in Si. Left: BF image in two-beam condition with strong $(2\bar{2}0)$ diffraction. Right: g-$3g$ WBDF image with weak $(2\bar{2}0)$ diffraction. Compare the intensities of the active diffractions (circled in inserts). After [7.9].

Williams and Carter book

Weak beam: finer details easier to interpret!

Imaging strain fields
In summary:

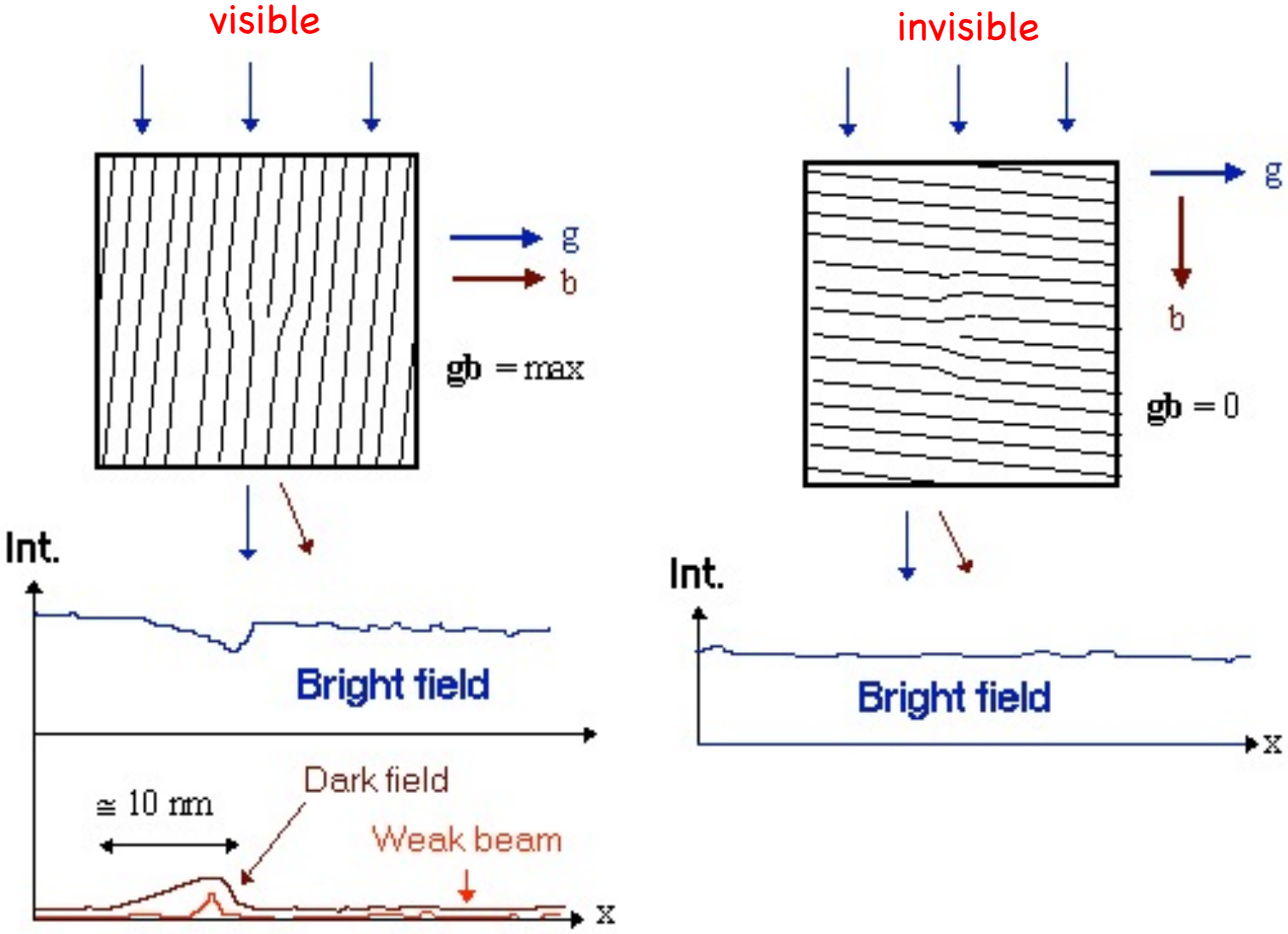

Resolution in HRTEM

Resolution of an optical system

Rayleigh criterion http://micro.magnet.fsu.edu/primer

- The resolving power of an optical system is limited by the diffraction occurring at the optical path every time there is an aperture/diaphragm/lens.
- The aperture causes interference of the radiation (the path difference between the green waves results in destructive interference while the path difference between the red waves results in constructive interference).
- An object such as point will be imaged as a disk surrounded by rings.
- The image of a point source is called the **Point Spread Function**

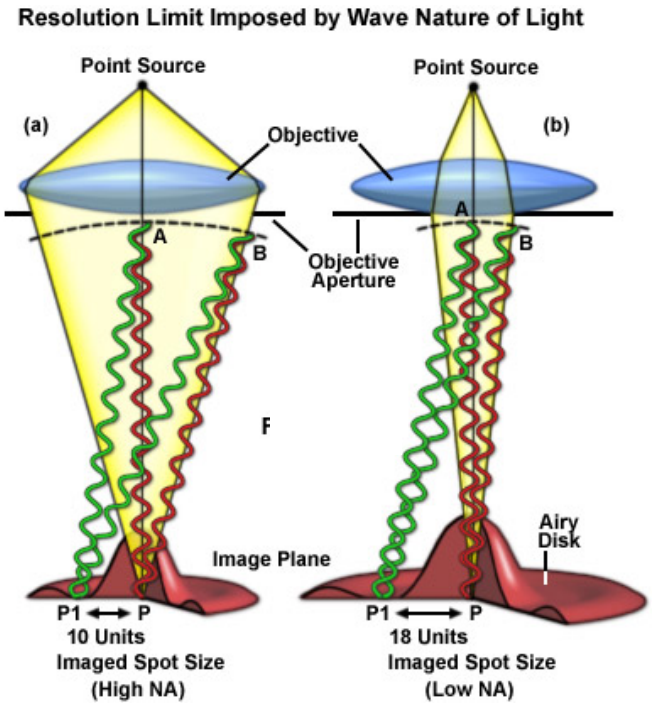

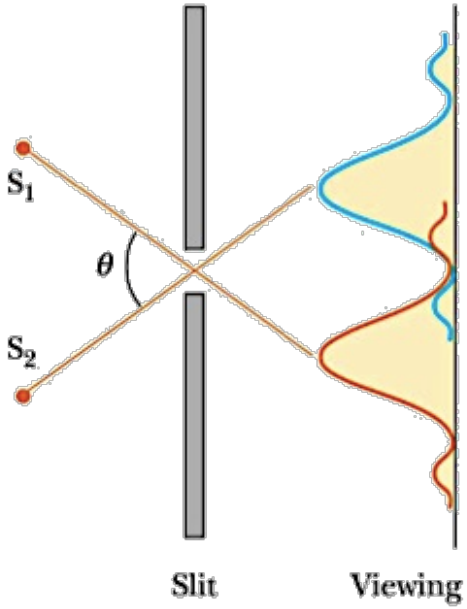

Point spread function (real space)

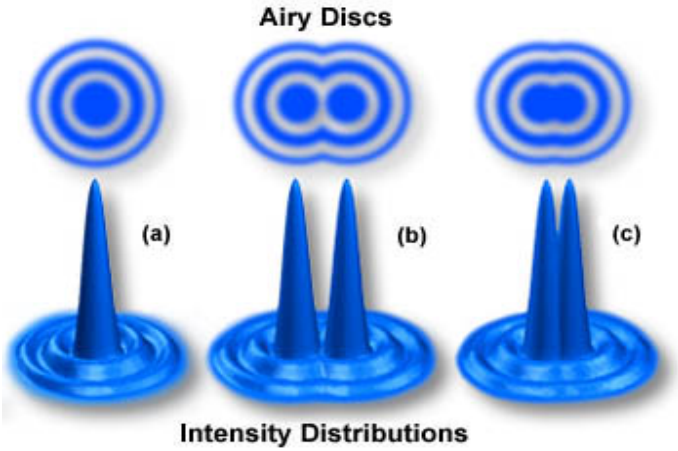

1 point

2 points resolved

2 points unresolved

Resolution of an optical system

http://micro.magnet.fsu.edu/primer

Diffraction at an aperture or lens - Rayleigh criterion

The Rayleigh criterion for the resolution of an optical system states that two points will be resolvable if the maximum of the intensity of the Airy ring from one of them coincides with the first minimum intensity of the Airy ring of the other. This implies that the resolution, d_0 (strictly speaking, the resolving power) is given by:

$$d_0 = 0.6\lambda/(n.\sin\mu) = 0.6\lambda/NA$$

where λ is the wavelength, n the refractive index and μ is the semi-angle at the specimen. NA is the numerical aperture.

This expression can be derived using a reasoning similar to what was described for diffraction gratings (path differences...).

When d_0 is small the resolution is high!

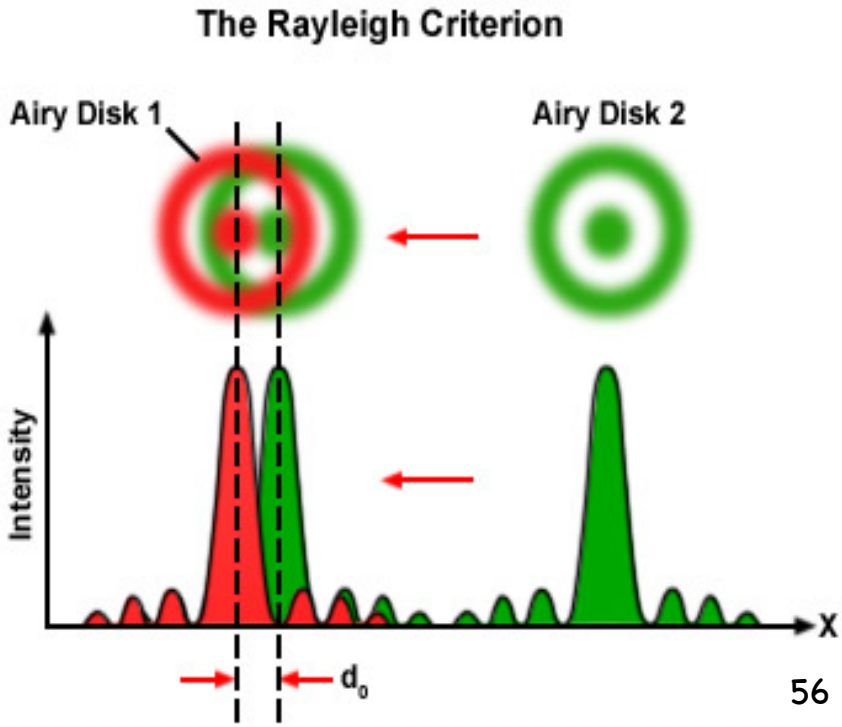

Resolution of an optical system

http://micro.magnet.fsu.edu/primer

Diffraction at an aperture or lens – Image resolution

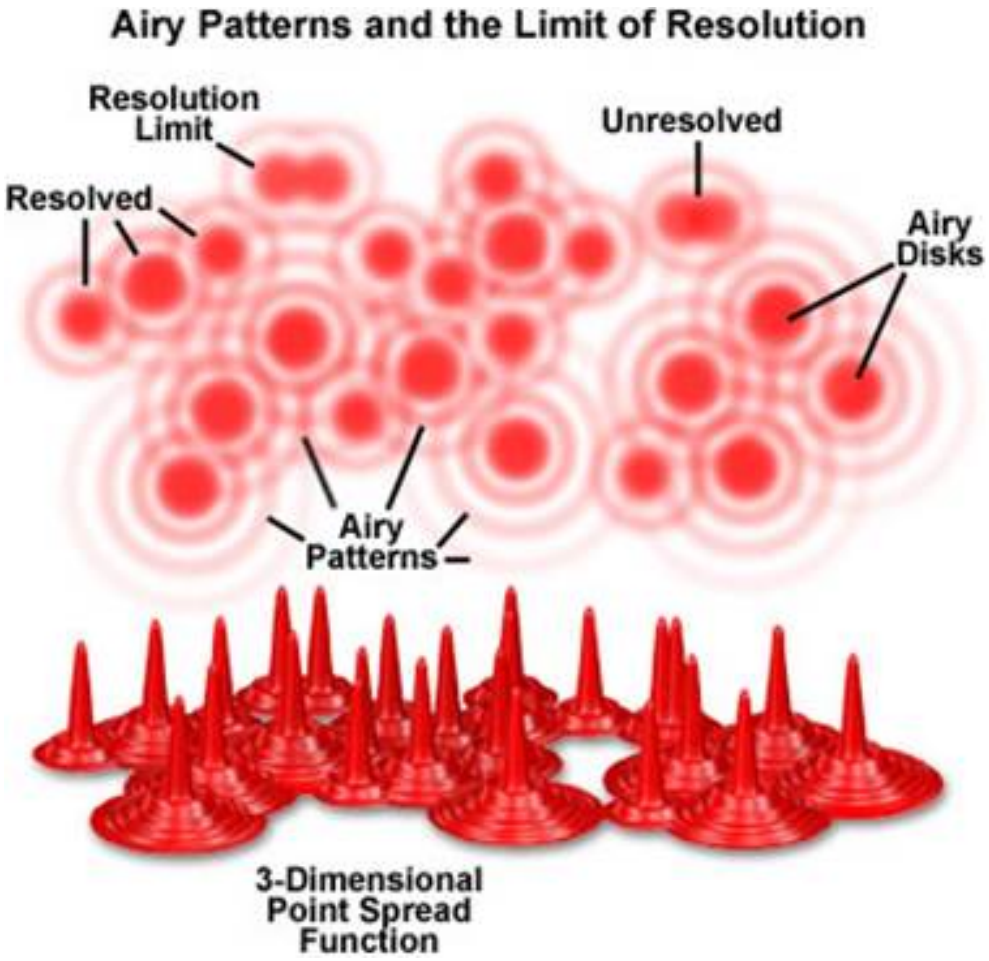

New concept:
Contrast Transfer Function (CTF)

Optical Transfer Function (OTF)

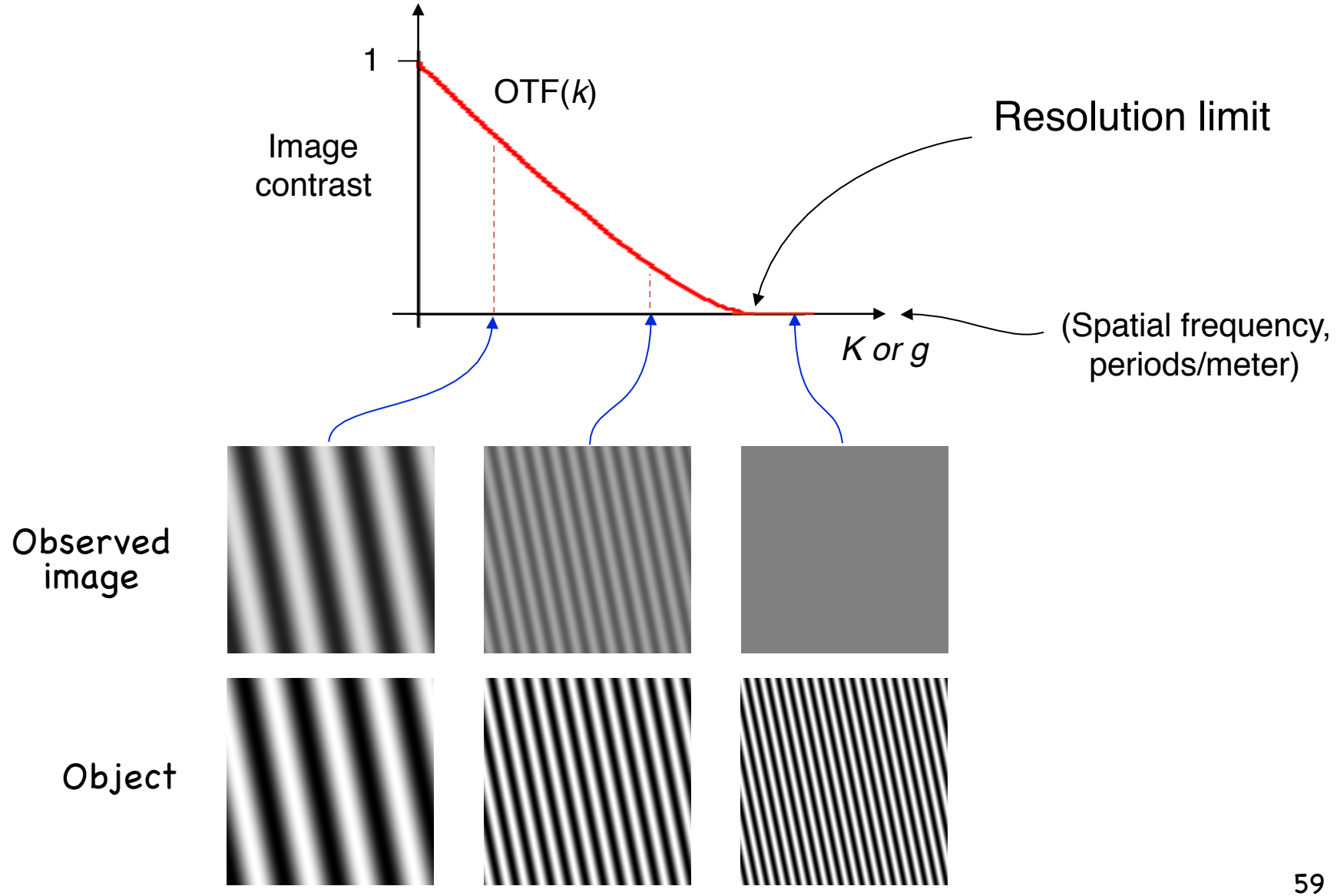

Definitions of Resolution

As the OTF cutoff frequency

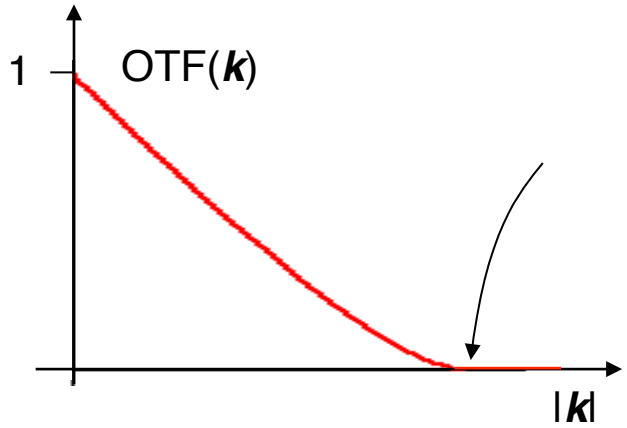

$1/k_{max}$
$= 0.5\ \lambda\ /NA$

As the Full Width at Half Max (FWHM) of the PSF

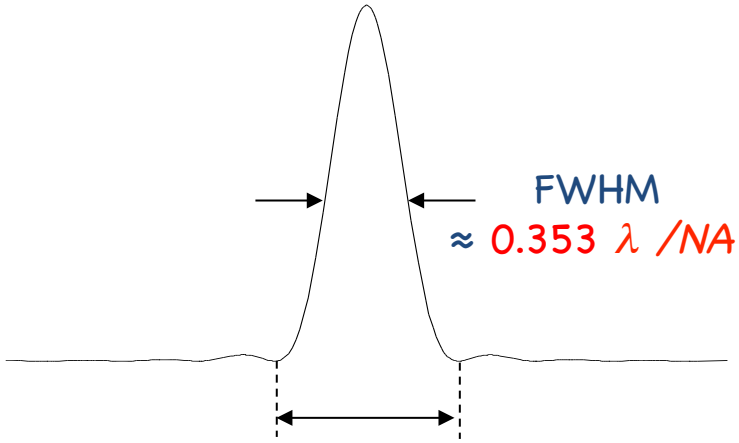

As the diameter of the Airy disk (first dark ring of the PSF)
= "Rayleigh criterion"

Airy disk diameter
$\approx 0.61\ \lambda\ /NA$

Remember: reciprocal/frequency space

To ***describe*** a wave, specify:

- Frequency (how many periods/meter?)
- Direction
- Amplitude (how strong is it?)
- Phase (where are the peaks & troughs?)

A wave can also be described by a complex number at a *point:*

- Distance from origin
- Direction from origin
- Magnitude of value at the point
- Phase of number

complex

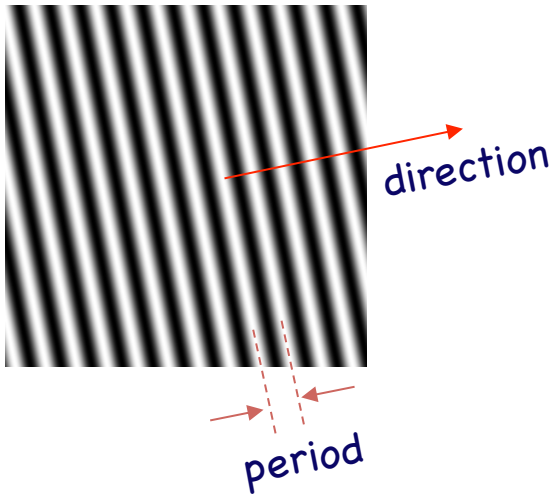

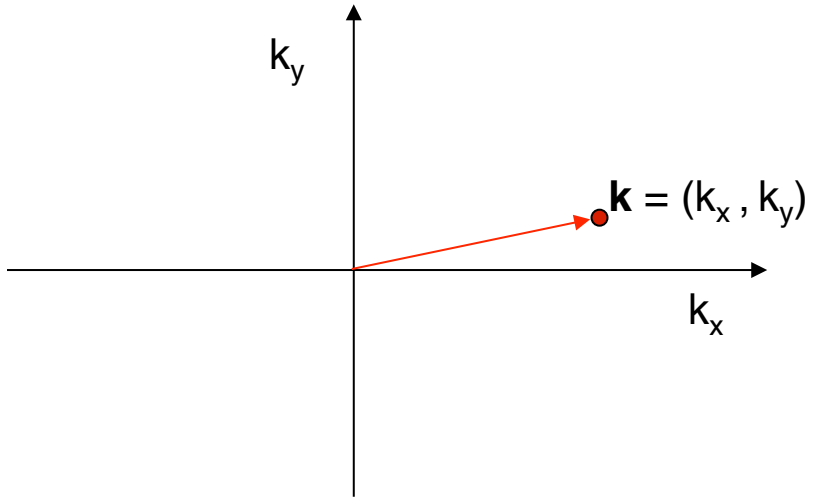

The Transfer Function Lives in Frequency Space

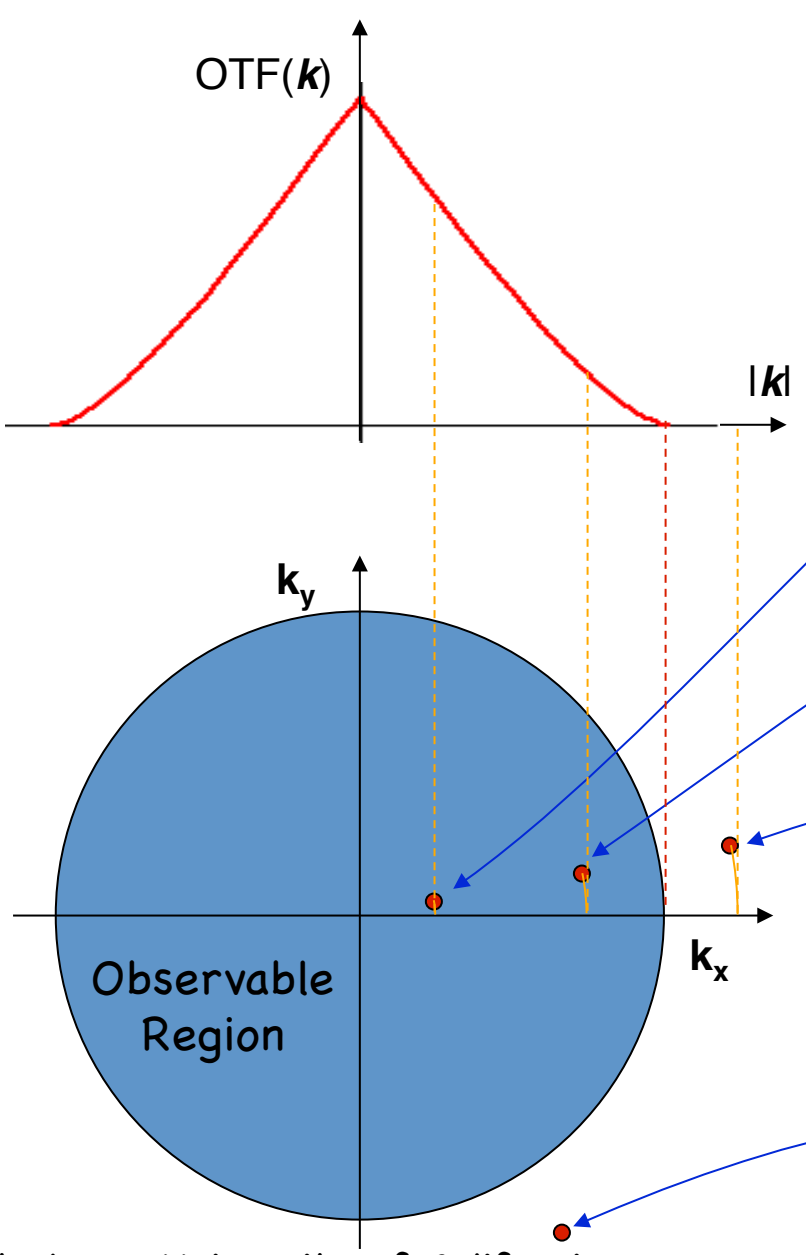

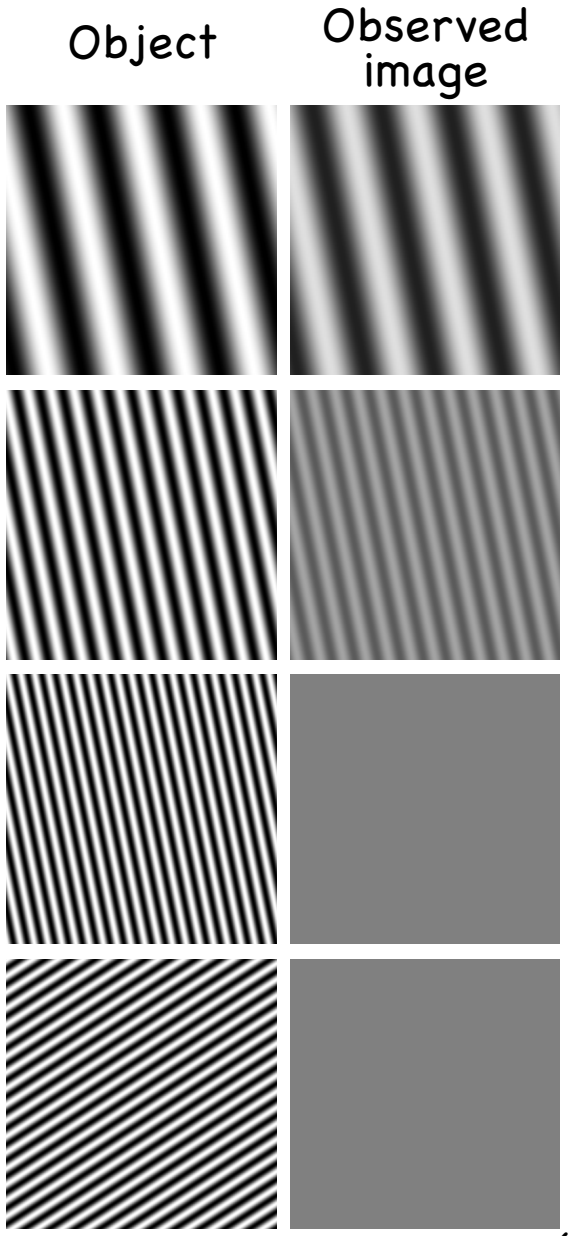

The OTF and Imaging

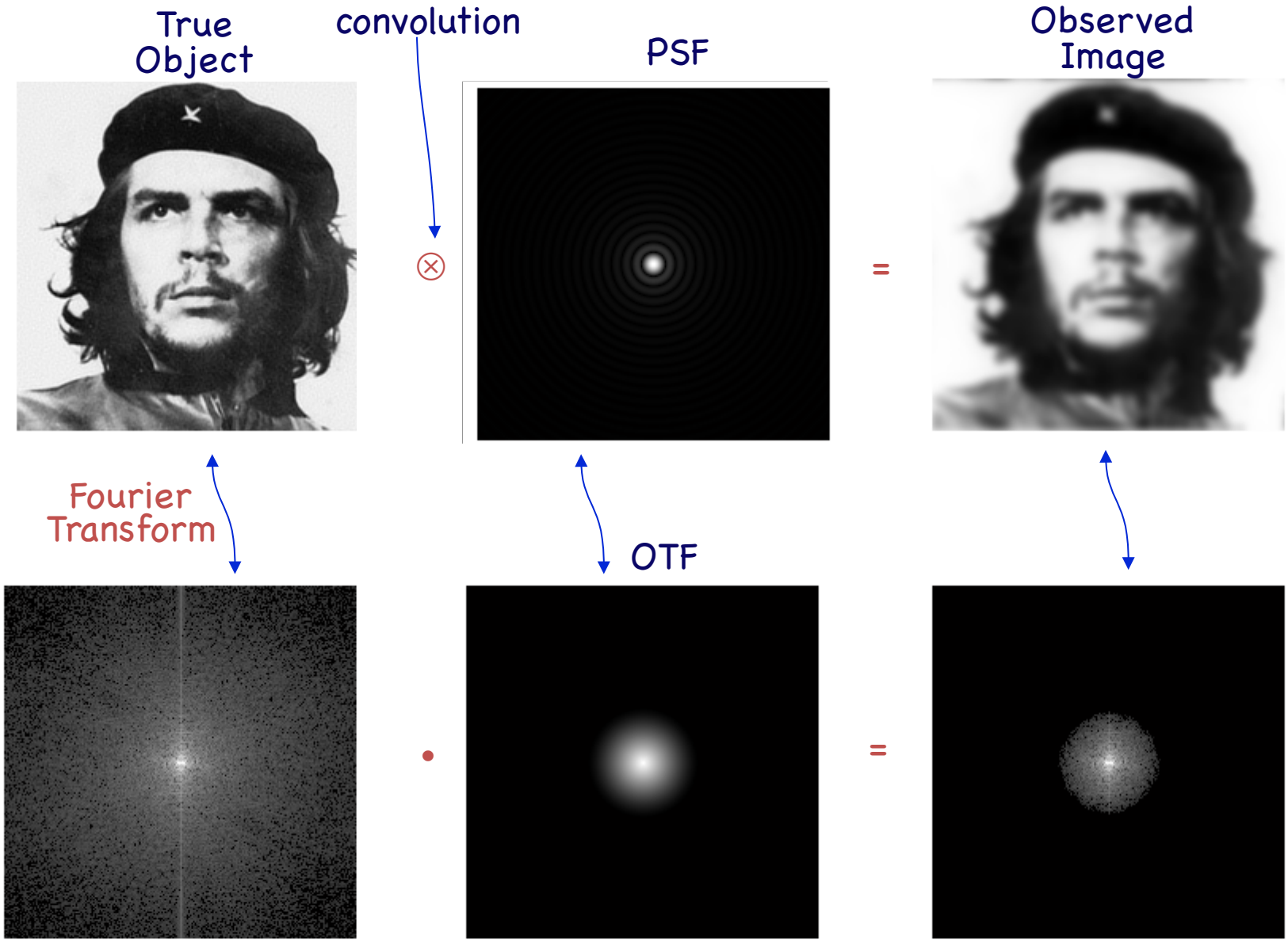

Nomenclature

Optical transfer function, OTF
Wave transfer function, WTF
Contrast transfer function, CTF

} Similar concepts:
Complex values (amplitude and phase)

Weak-phase object
very thin sample: no absorption (no change in amplitude) and only weak phase shifts induced in the scattered beams

Contrast Transfer Function in HRTEM, CTF
For weak-phase objects only the phase is considered

Resolution in HRTEM

In optical microscopy, it is possible to define point resolution as the ability to resolve individual point objects. This resolution can be expressed (using the criterion of Rayleigh) as a quantity independent of the nature of the object.

The resolution of an electron microscope is more complex. Image "resolution" is a measure of the spatial frequencies transferred from the image amplitude spectrum (exit-surface wave-function) into the image intensity spectrum (the Fourier transform of the image intensity). This transfer is affected by several factors:

- the phases of the diffracted beams exiting the sample surface,
- additional phase changes imposed by the objective lens defocus and spherical aberration,
- the physical objective aperture,
- coherence effects that can be characterized by the microscope spread-of-focus and incident beam convergence.

For thicker crystals, the frequency-damping action of the coherence effects is complex but for a thin crystal, i.e., one behaving as a weak-phase object (WPO), the damping action can best be described by quasi-coherent imaging theory in terms of envelope functions imposed on the usual phase-contrast transfer function.

The concept of HRTEM resolution is only meaningful for thin objects and, furthermore, one has to distinguish between point resolution and information limit.

O'Keefe, M.A., Ultramicroscopy, 47 (1992) 282-297

Contrast transfer function

In the Fraunhofer approximation to image formation, the intensity in the back focal plane of the objective lens is simply the Fourier transform of the wave function exiting the specimen. Inverse transformation in the back focal plane leads to the image in the image plane.

If the phase-object approximation holds (no absorption), the image of the specimen by a perfect lens shows no amplitude modulation. In reality, a combination with the extra phase shifts induced by defocus and the spherical aberration of the objective lens generates suitable contrast.

The influence of these extra phase shifts can be taken into account by multiplying the wavefunction at the back focal plane with functions describing each specific effect. The phase factor used to describe the shifts introduced by defocus and spherical aberration is:

$$\chi(k) = \pi \lambda \Delta f k^2 + 1/2\pi Cs \lambda^3 k^4$$

with Δf the defocus value and Cs the spherical aberration coefficient. The function that multiplies the exit wave is then:

$$B(k) = \exp(i\chi(k))$$

If the specimen behaves as a weak-phase object, only the imaginary part of this function contributes to the contrast in the image, and one can set:

$$B(k) = 2\sin(\chi(k))$$

The phase information from the specimen is converted into intensity information by the phase shift introduced by the objective lens and this equation determines the weight of each scattered beam transferred to the image intensity spectrum. **For this reason, $\sin(\chi)$ is known as the contrast transfer function (CTF) of the objective lens.**

Contrast transfer function

$$\sin \chi(k) = \sin(\pi\lambda\Delta f k^2 + 1/2\pi Cs\lambda^3 k^4)$$

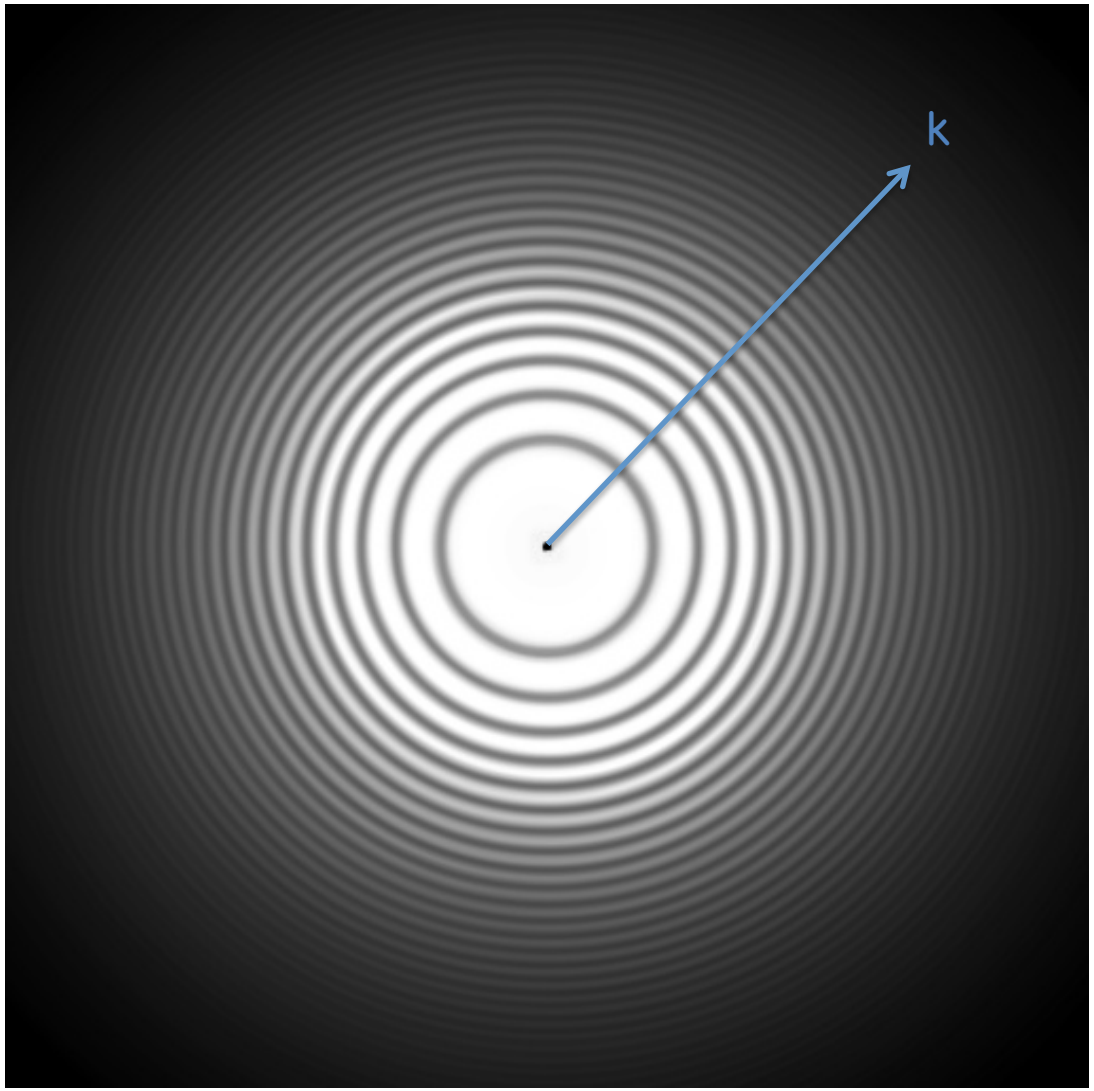

Contrast transfer function

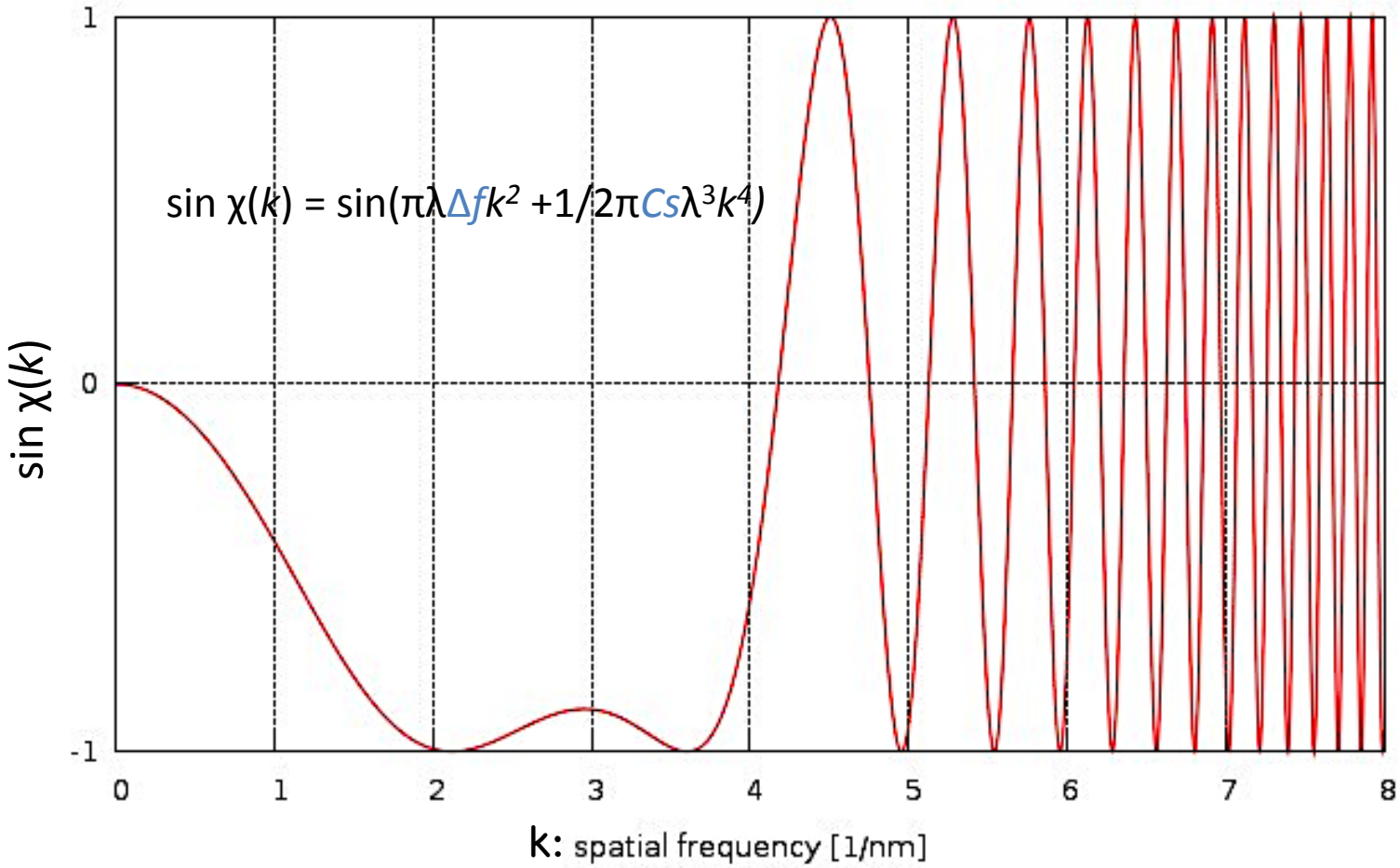

parameters: λ=0.0025 nm (200 kV), c_s =1.1 mm, Δf=60 nm

The CTF oscillates between -1 (negative contrast transfer) and +1 (positive contrast transfer). The exact locations of the zero crossings (where no contrast is transferred, and information is lost) depends on the defocus.

Point resolution

Point resolution: related to the finest detail that can be directly interpreted in terms of the specimen structure. Since the CTF depends very sensitively on defocus, and in general shows an oscillatory behavior as a function of *k*, the contribution of the different scattered beams to the amplitude modulation varies. However, for particular underfocus settings the instrument approaches a perfect phase contrast microscope for a range of *k* before the first crossover, where the CTF remains at values close to −1. It can then be considered that, to a first approximation, all the beams before the first crossover contribute to the contrast with the same weight, and cause image details that are directly interpretable in terms of the projected potential.

Optimisation of this behaviour through the balance of the effects of spherical aberration *vs.* defocus leads to the generally accepted *optimum defocus*1 −1.2($Cs\,\lambda$)$^{1/2}$. Designating an optimum resolution involves a certain degree of arbitrariness. However, the point where the CTF at optimum defocus reaches the value −0.7 for $k = 1.49C^{-1/4}\lambda^{-3/4}$ is usually taken to give the *optimum (point) resolution* ($0.67C^{1/4}\lambda^{3/4}$). This means that the considered passband extends over the spatial frequency region within which transfer is greater than 70%. Beams with k larger than the first crossover are still linearly imaged, but with reverse contrast. Images formed by beams transferred with opposite phases cannot be intuitively interpreted.

Scherzer defocus

Every zero-crossing of the graph corresponds to a contrast inversion in the image.

Up to the first zero-crossing k_0 the contrast does not change its sign.

The reciprocal value $1/k_0$ is called Point Resolution.

The defocus value which maximizes this point resolution is called the Scherzer defocus.

Optimum defocus: At Scherzer defocus, one aims to counter the term in u^4 with the parabolic term $\Delta f u^2$ of $\chi(u)$. Thus by choosing the right defocus value Δf one flattens $\chi(u)$ and creates a wide band where low spatial frequencies $\boldsymbol{k}$ are transferred into image intensity with a similar phase.

Working at Scherzer defocus ensures the transmission of a broad band of spatial frequencies with constant contrast and allows an unambiguous interpretation of the image.

Scherzer defocus

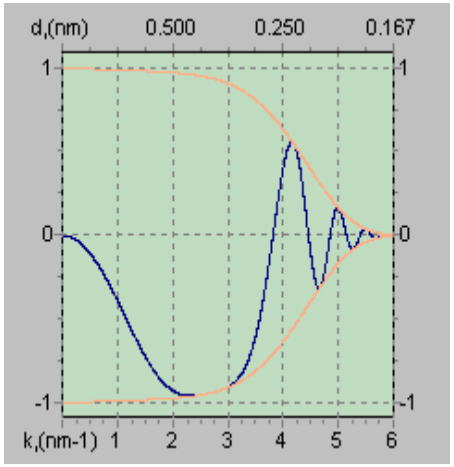

$\Delta f = -(C_s \lambda)^{1/2}$

Scherzer condition

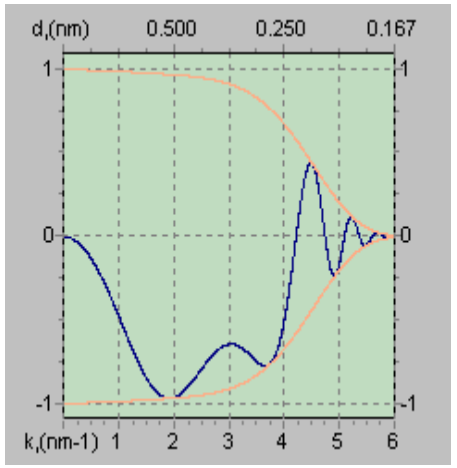

$\Delta f = -1.2(C_s \lambda)^{1/2}$

Extended Scherzer condition

http://www.maxsidorov.com/ctfexplorer/webhelp/effect_of_defocus.htm

The Envelope function

The resolution is also limited by the spatial coherence of the source and by chromatic effects (changes of electron energy in time):

$$T_{eff} = T(u)E_{sc}E_{tc}$$

(**u** = **k**)

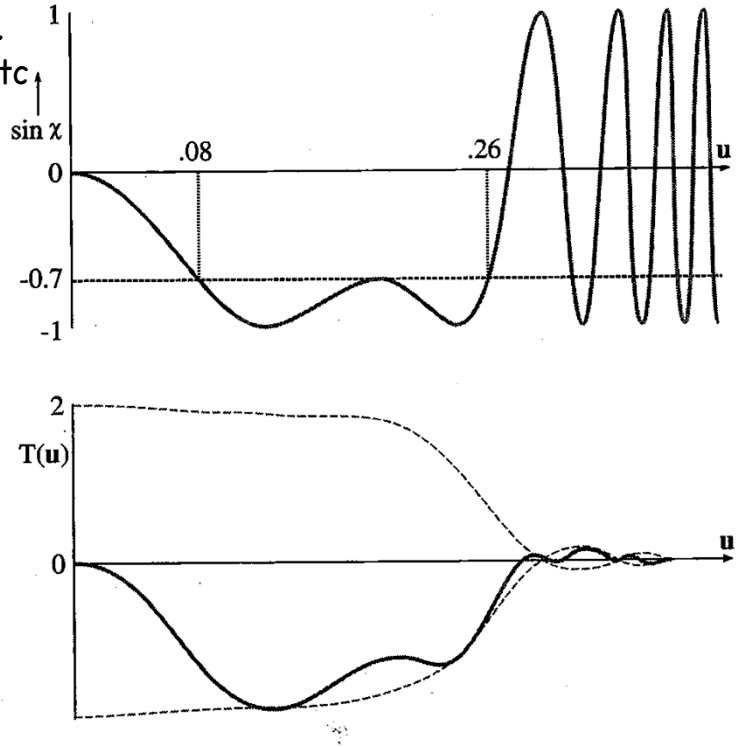

The envelope function imposes a "virtual aperture" in the back focal plane of the objective lens.

Information limit

Information limit: corresponds to the highest spatial frequency still appreciably transmitted to the intensity spectrum. This resolution is related to the finest detail that can actually be seen in the image (which however is only interpretable using image simulation). For a thin specimen, such limit is determined by the cut-off of the transfer function due to spread of focus and beam convergence (usually taken at $1/e^2$ or at zero).

These damping effects are represented by E_Δ or E_{tc} a *temporal coherency envelope* (caused by chromatic aberrations, focal and energy spread, instabilities in the high tension and objective lens current), and E_α or E_{sc} is the spatial coherency_*envelope* (caused by the finite incident beam convergence, i.e., the beam is not fully parallel).

The Information limit goes well beyond point resolution limit for FEG microscopes (due to high spatial and temporal coherency). For the microscopes with thermionic electron sources (LaB6 and W), the info limit usually coincides with the point resolution. \

The use of FEG sources minimises the loss of spatial coherence. This helps to increase the information limit resolution in the case of lower voltage (≤ 200 kV) instruments, because in these cases the temporal coherence does not usually play a critical role. However the point resolution is relatively poor due to the oscillatory behavior of the CTF. On the other hand, with higher voltage instruments, due to the increased brightness of the source, the damping effects are always dominated by the spread of focus and FEG sources do not contribute to an increased information limit resolution.

Phase-contrast transfer function at Scherzer's defocus

The point-spread function describes the effect of the aberrations of the objective lens in real space as $\mathrm{PSF}(r) = \mathrm{FT}^{-1}[\mathrm{WTF}(q)]$, i.e. the inverse Fourier transform of the wave-transfer function $\mathrm{WTF}(q) = E^{\mathrm{sc}}(q)E^{\mathrm{tc}}(q)\exp(-\mathrm{i}\chi(q))$, defined in Fourier space with coordinates q.

Damping of the Fourier components is described by the envelope functions $E_{\mathrm{sc}}(q)$ and $E_{\mathrm{tc}}(q)$ resulting from deficiencies of spatial and temporal coherence. They damp destroy information, in particular, of the high spatial frequencies. The arising limit is called the information limit.

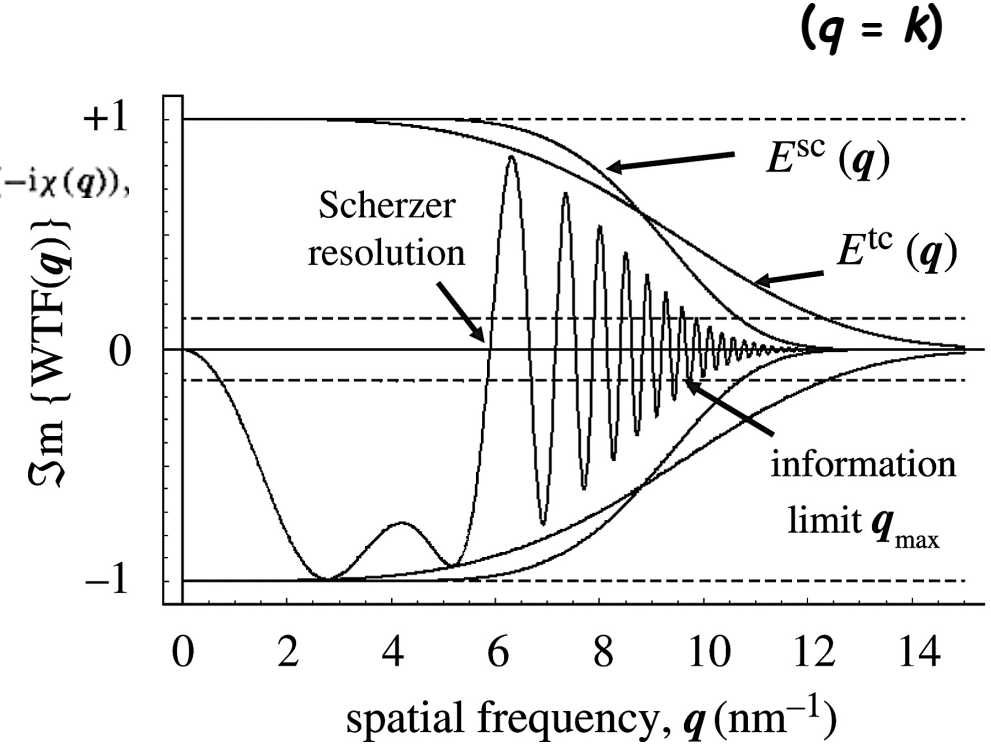

The imaginary part of the wave-transfer function (WTF) basically characterizes the contrast transfer from a phase-object to the image intensity. The oscillations restrict the interpretable resolution (Scherzer resolution) to below the highest spatial frequency transferred $\mathbf{q}_{max}$. $\mathbf{q}_{max}$ is called the information limit given by the envelope functions E_{sc} and E_{tc} of the restricted spatial and temporal coherence.

Lichte H et al. Phil. Trans. R. Soc. A 2009;367:3773-3793

Phase contrast and information limit

Point Resolution (or Point-to-Point, or Directly Interpretable Resolution) of a microscope corresponds to the to the point when the CTF first crosses the k-axis:

$$k = 0.67 C^{1/4} \lambda^{3/4}$$

Phase contrast images are directly interpretable only up to the point resolution (Scherzer resolution limit).

If the information limit is beyond the point resolution limit, one needs to use image simulation software to interpret any detail beyond point resolution limit.

Information limit goes well beyond point resolution limit for FEG microscopes (due to high spatial and temporal coherency).

For the microscopes with thermionic electron sources (LaB6 and W), the info limit usually coincides with the point resolution.

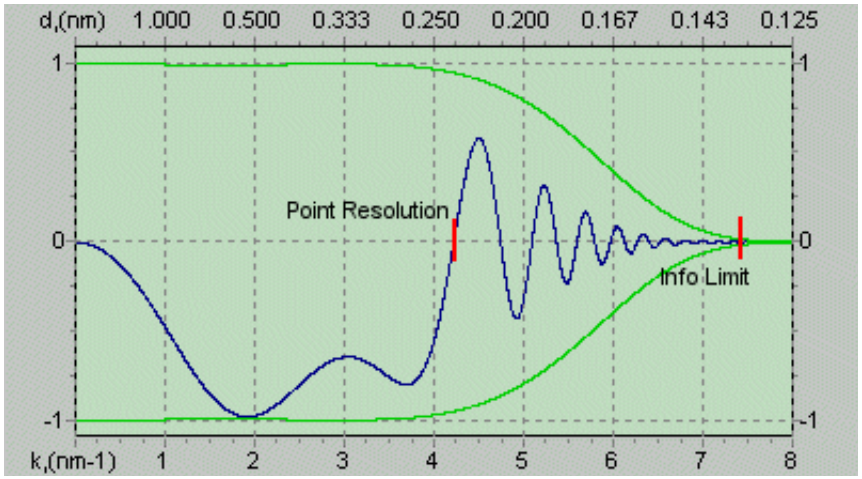

http://www.maxsidorov.com/ctfexplorer/webhelp/effect_of_defocus.htm

Damped contrast transfer function

Microscope examples

Configuration	JEOL 4000EX/II (Top-entry)	JEOL 2010F (Side-entry)
Emission	LaB_6 filament	Field emission gun
Operating voltage (kV)	400	200
Spherical aberration coefficient (mm)	0.97 ←	~1.00 ←
Spread of focus (nm)	7.8	4.0
Beam convergence angle (mrad)	0.8	0.1
Information limit resolution (nm)	0.14	0.11
Point Resolution (nm)	0.17	0.23
Optimum defocus (Scherzer) (nm)	-48.9	-61.0

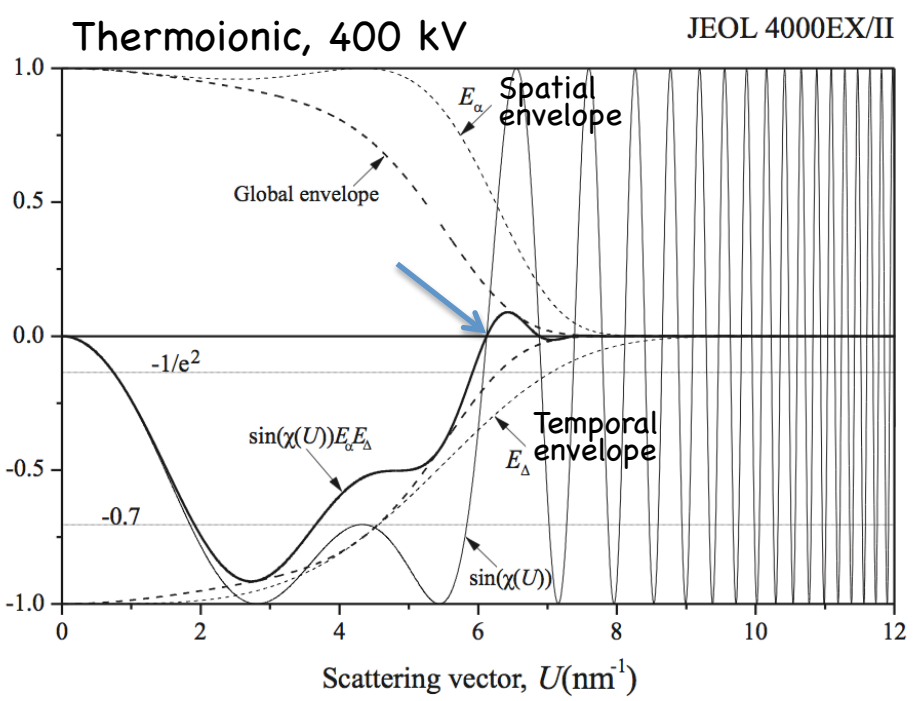

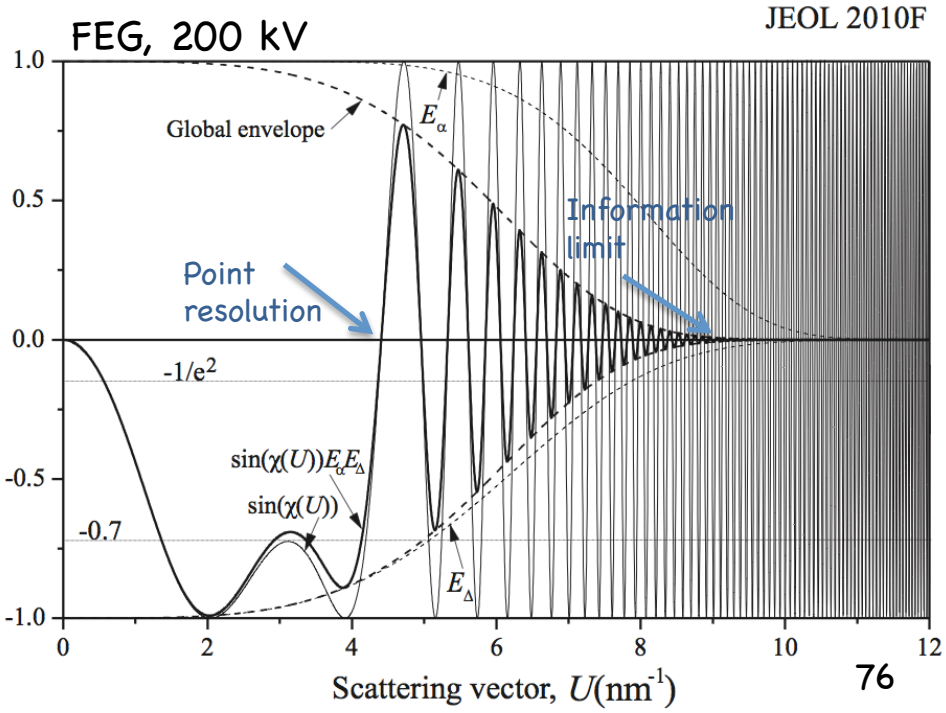

The effect of different C_s and Δ f on the damped CTF

$$\sin\chi = \sin(\pi\Delta f\lambda u^2 + \frac{1}{2}\pi C_s\lambda^3 u^4)$$

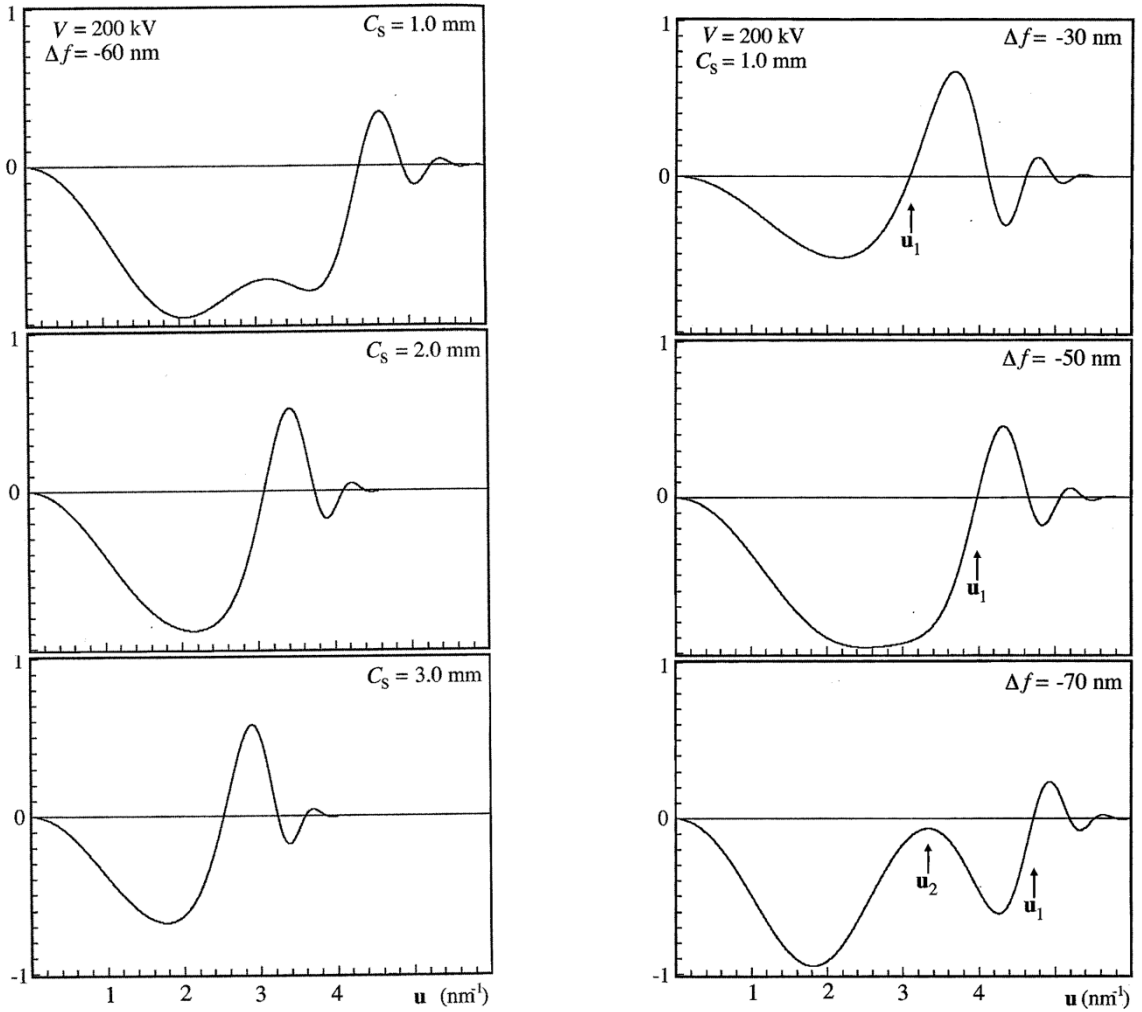

Important points to notice

- CTF is oscillatory: there are "passbands" where it is NOT equal to zero (good "transmittance") and there are "gaps" where it IS equal (or very close to) zero (no "transmittance").
- When it is negative, positive phase contrast occurs, meaning that atoms will appear dark on a bright background.
- When it is positive, negative phase contrast occurs, meaning that atoms will appear bright on a dark background.
- When it is equal to zero, there is no contrast (information transfer) for this spatial frequency.
- At Scherzer defocus CTF starts at 0 and decreases, then
- CTF stays almost constant and close to -1 (providing a broad band of good transmittance), then
- CTF starts to increase, and
- CTF crosses the *u*-axis, and then
- CTF repeatedly crosses the *u*-axis as *u* increases.
- CTF can continue forever but, in reality, it is modified by envelope functions and eventually dies off.

Spherical aberration correction

In every uncorrected electron microscope the reachable point resolution is much worse than the optimum information limit. **Using an electron microscope with spherical aberration correction allows for optimizing the spherical aberration coefficient and the defocus so that the point resolution equals the information limit.**

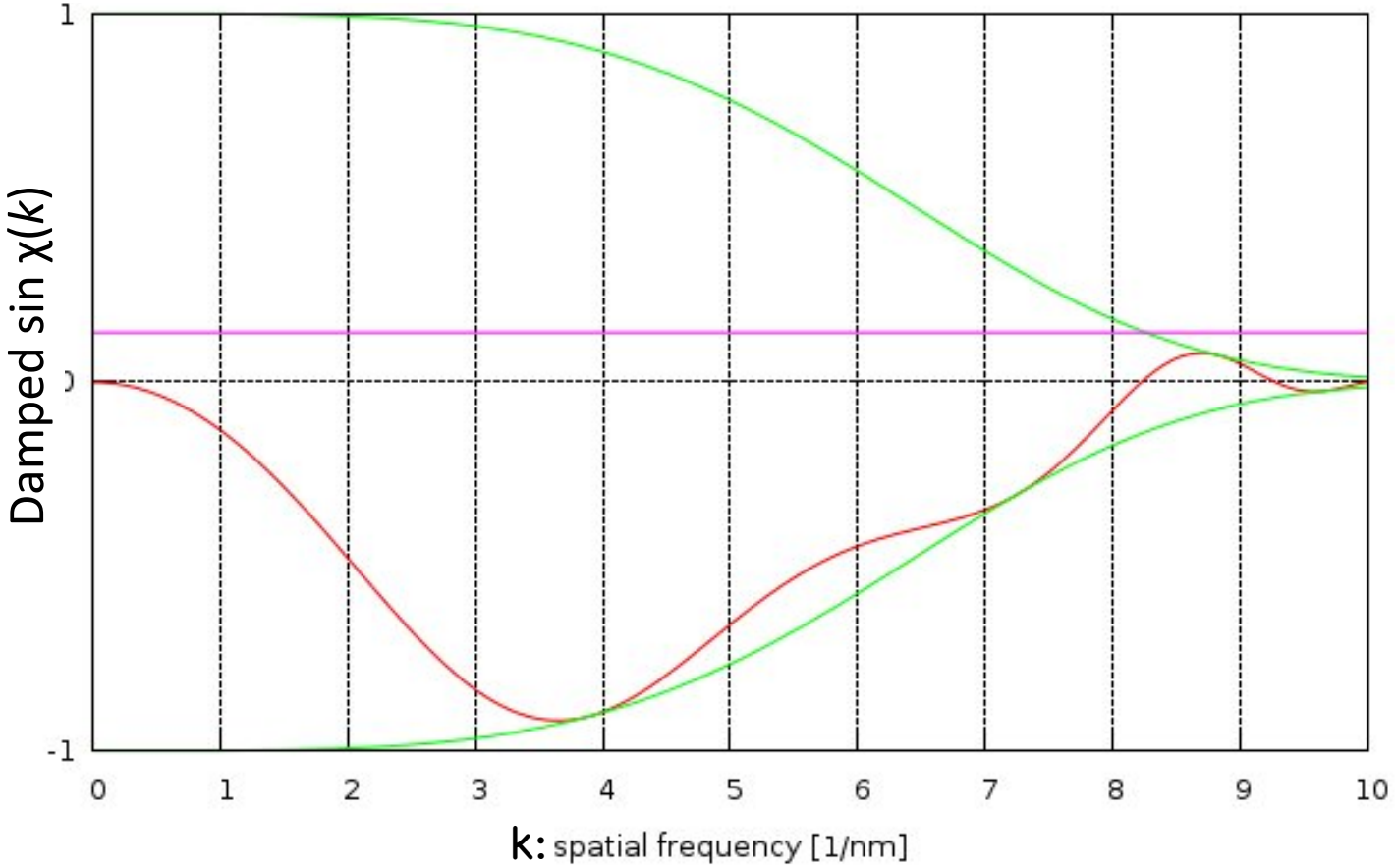

parameters: λ=0.0025 nm (200 kV), c_s =0.159 mm, c_c =1.6 mm, Δf=23.92 nm, ΔE=0.7 eV, E=300 kV

HRTEM image simulation

HRTEM image simulation

Simulation of HRTEM images is necessary due to the loss of phase information when obtaining an experimental image, which means the object structure can not be directly retrieved. Instead, one assumes a structure (perfect crystal or crystalline material containing defects), simulates the image, matches the simulated image with the experimental image, modifies the structure, and repeats the process. The difficulty is that the image is sensitive to several factors:

- Precise alignment of the beam with respect to both the specimen and the optic axis
- Thickness of the specimen
- Defocus of the objective lens
- Chromatic aberration which becomes more important as the thickness increases
- Coherence of the beam
- Other factors such as the intrinsic vibration in the material which we try to take account of through the Debye-Waller factor

Multislice method

The basic multislice approach used in most of the simulation packages is to section the specimen into many slices, which are normal to the incident beam.

The potential within a slice is projected onto the first projection plane; this is the phase grating. We calculate the amplitudes and phases for all the beams generated by interacting with this plane and then propagate all the diffracted beams through free space to the next projection plane, and repeat the process.

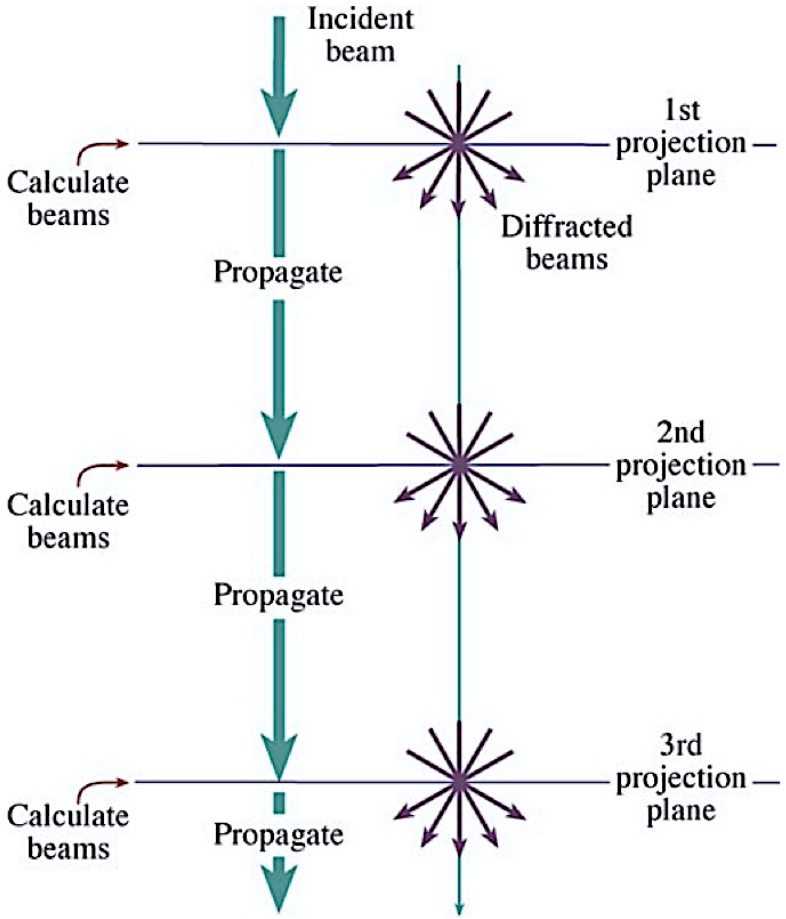

Williams and Carter

Other techniques

Cryo-TEM

(requires cooled stage)

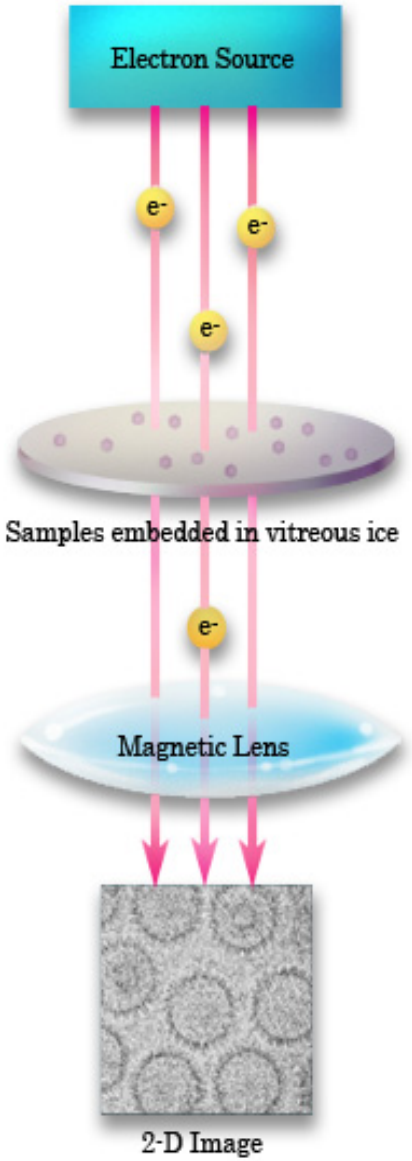

- Cryo-TEM permits macromolecules and molecular assemblies to be examined in as native a state as possible.
- Specimens are suspended in a thin film of water or buffer, and are then cooled by immersion into liquid ethane (-140°C) so rapidly that the surrounding water does not have the time to crystallize into ice and forms a glass.
- Specimens are examined using low-dose techniques.
- Contrast is low but image processing routines, such as image averaging is used to enhance the signal-to-noise ratio.

Electron tomography

(A) Two-dimensional transmission electron micrographs (projection images) are recorded at different tilt angles for individual 3D objects. The specimen holder is tilted incrementally around an axis perpendicular to the electron beam, and projection images of the same specimen area (field of view) are recorded on a CCD camera at each position. Tilt increments are typically 0.5° to 5° and the tilt range is about ±70°.

(B) Images projected by a specimen at successive tilt angles.

(C) After translationally and rotationally aligning all of these projection images, the imaged object is reconstructed into a 3D density map (often called the tomogram) by a weighted-backprojection procedure.

Analogous to confocal tomography but at much higher resolution and the beam does not scan the sample, instead the sample is tilted.

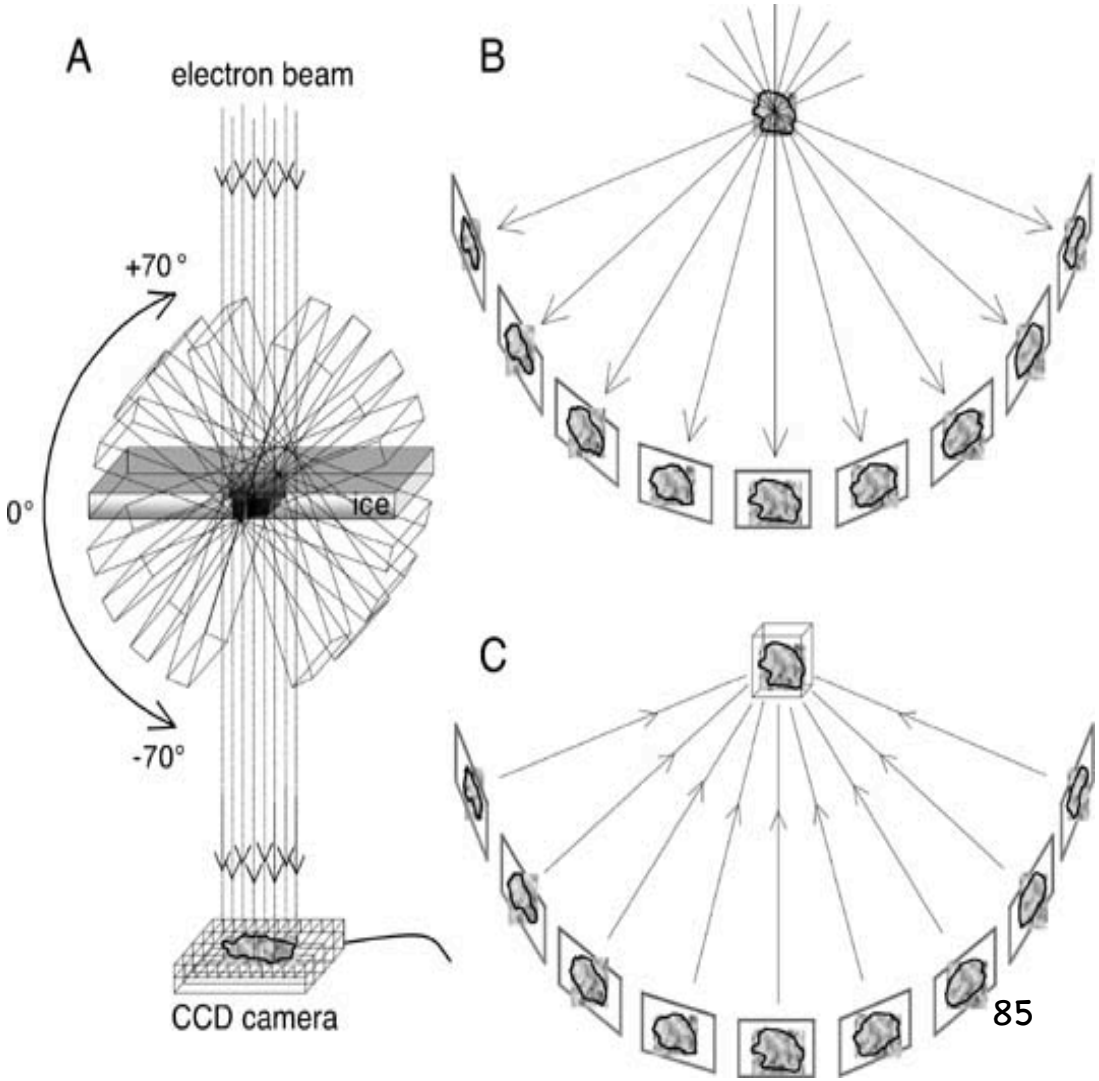

Cryo-TEM tomography

(requires cooled stage)

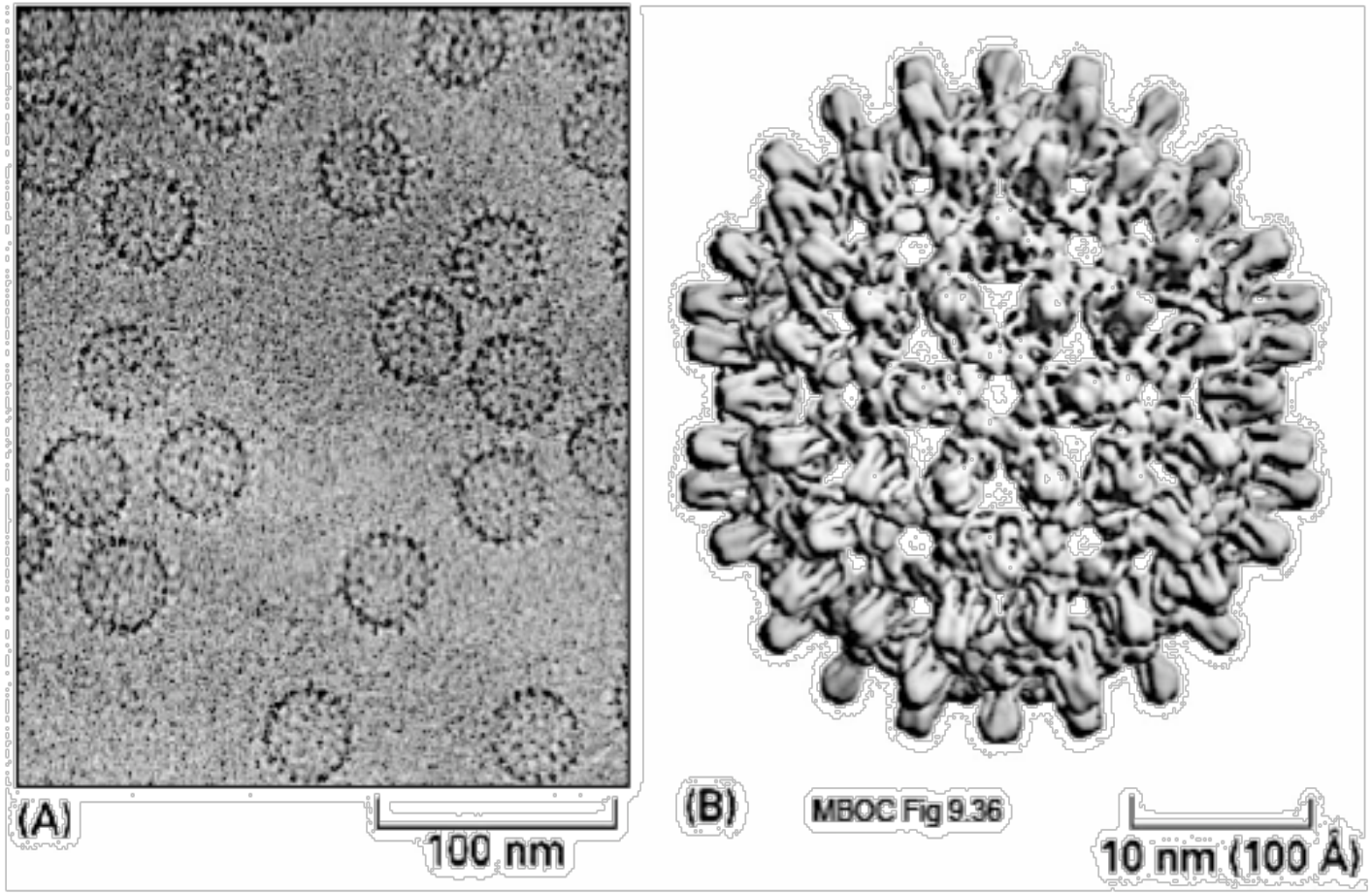

Structure of hepatitis B virus solved by cryo-EM

Crowther, Phil. Trans. R. Soc. B 27 July 2008 vol. 363 no. 1502 2441-2451

Cryo-electron tomography

The 3D ultrastructure of a human erythrocyte infected with P. Falciparum (malaria)

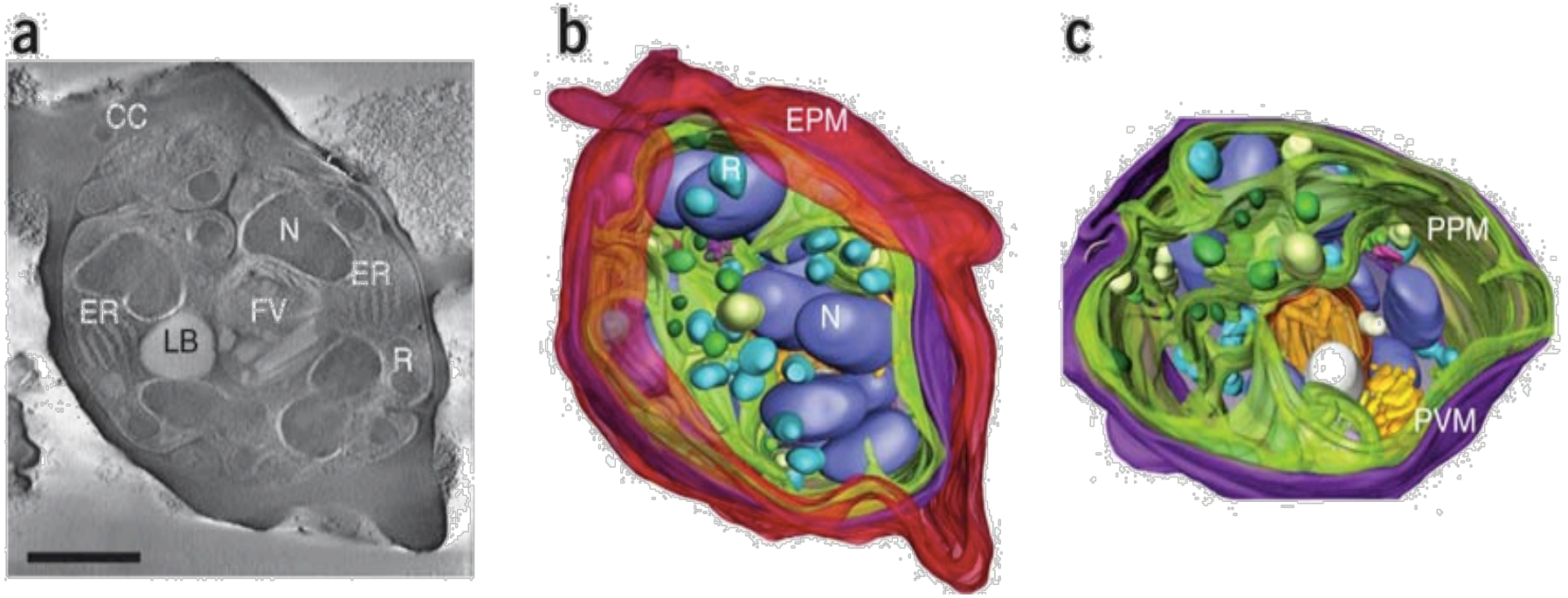

(a) Image of a 20-nm-thick slice across a bright-field STEM tomogram obtained from a 1 m-thick section. N, nucleus; FV, food vacuole; LB, lipid body; and CC, circular cleft. (**b**,**c**) Rendered 3D model of an infected erythrocyte.

Nature Methods 6, 729 - 731 (2009))

Cryo-electron tomography

Cryo-electron tomography

Resolving the structure and morphology of single molecules in the context of living ce

X-ray crystallography, NMR

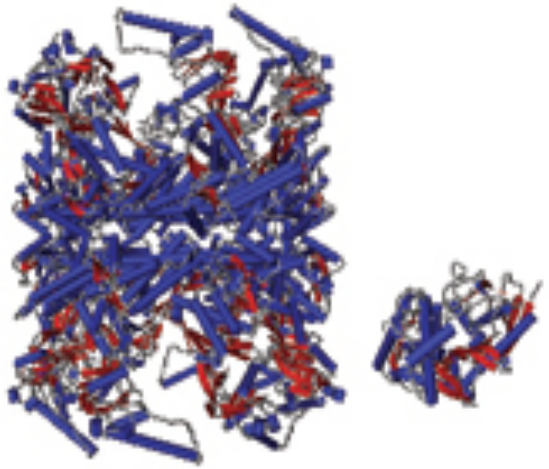

Single particle EM

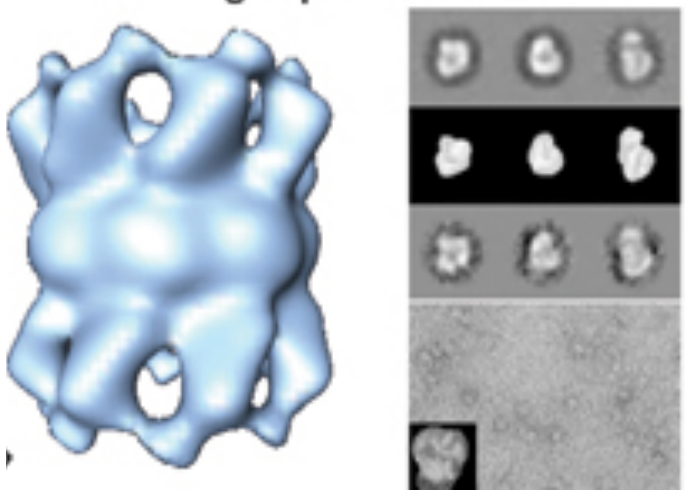

Integrating the information from X-ray crystallography and structural genomics with three-dimensional cryo-electron tomograms.

http://www.embl.de/frangakis/

Remember: magnetic domains

Magnetic domain walls (the coercivity of permanent magnets depends on the walls mobility)

Types of walls

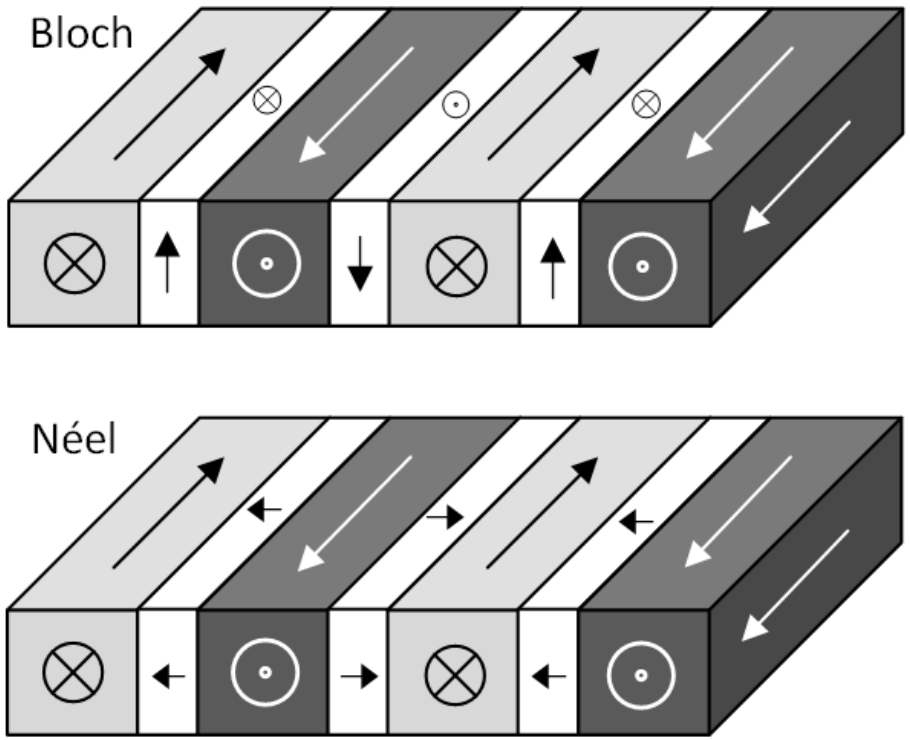

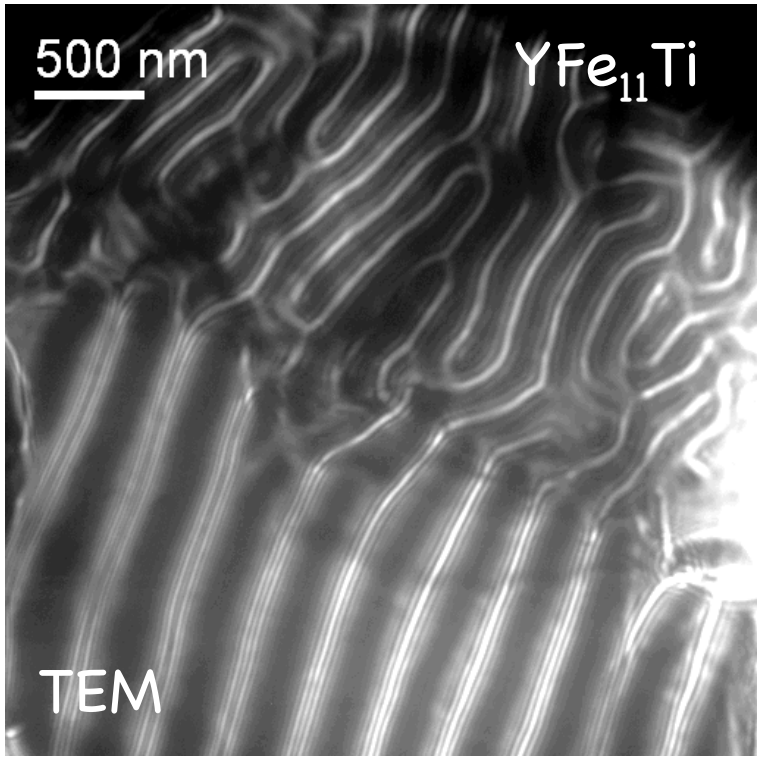

Lorentz microscopy (in Fresnel mode)

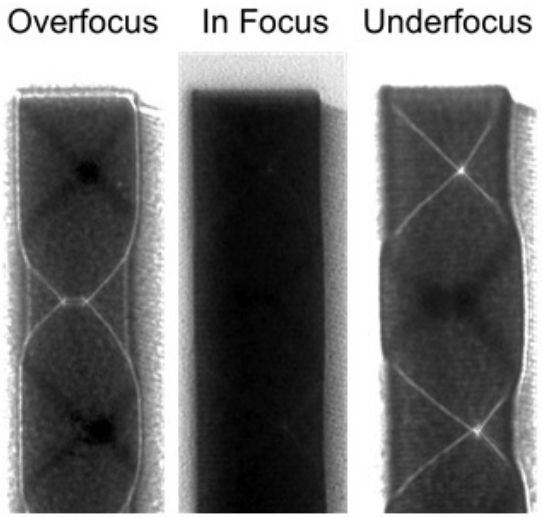

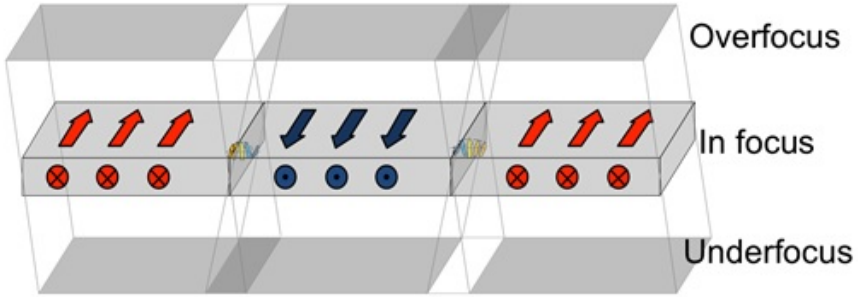

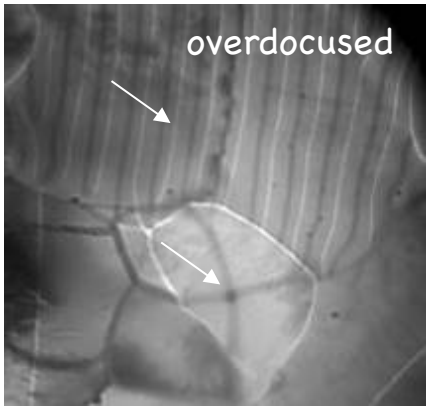

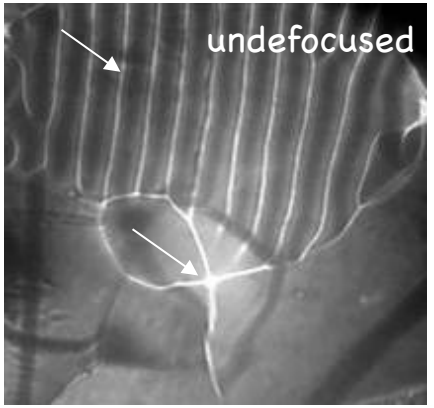

The magnetic field of each domains exerts a Lorentz force on the moving electrons deflecting their trajectory:

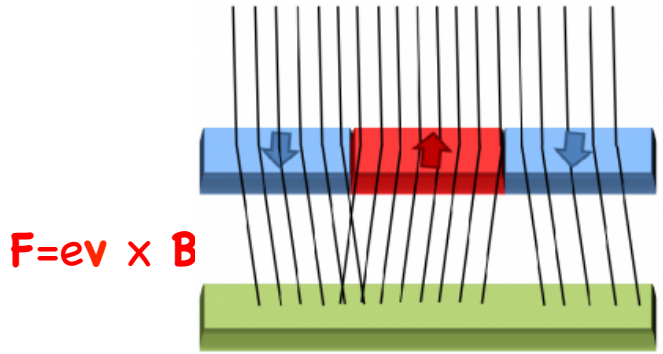

Lorentz microscopy

Example:

$YFe_{11}Ti$ + α-Fe

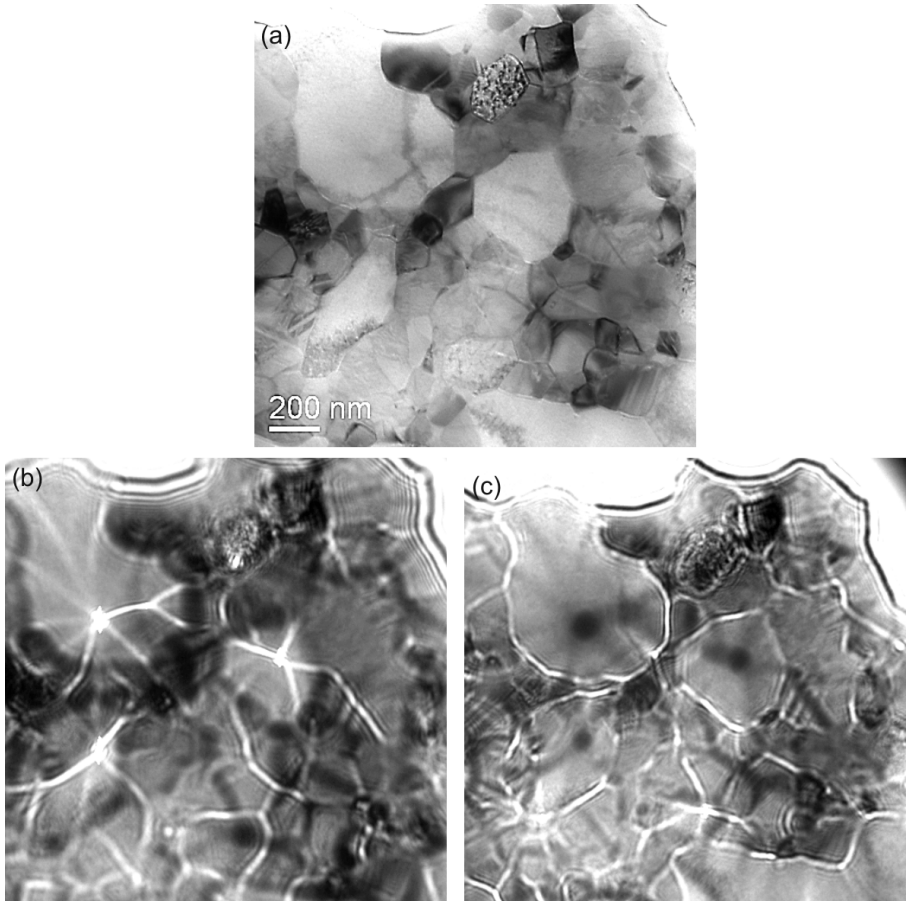

Polycrystalline microstructure and underlying domain configuration of the Y-Fe-Ti splat-quenched and annealed material.

(a) Overfocused: Δf = +213 nm,

(b) in focus: Δf = 0 nm,

(c) underfocused: Δf = -144 nm.

Lorentz microscopy

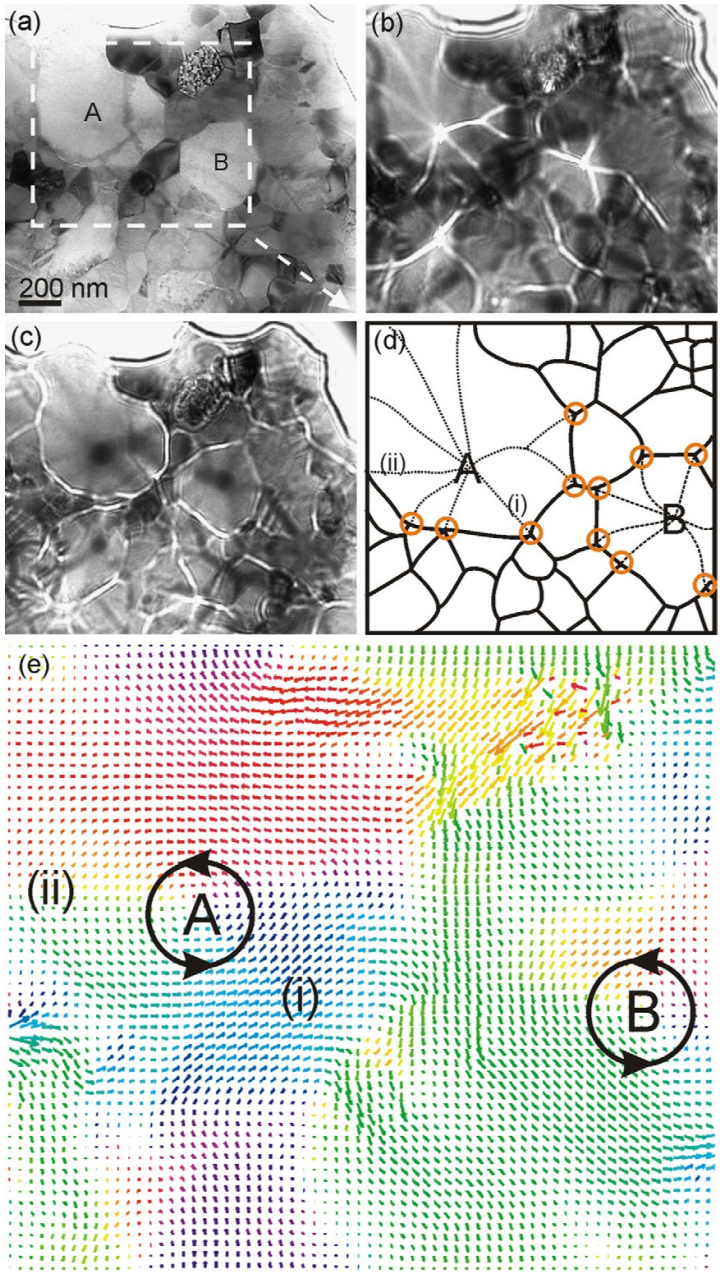

(a) In-focus: Df = 0 mm, (b) overfocused: Δf = +213 mm, and (c) underfocused: Δf = −144 mm. (d) Scheme showing the correspondence between domain wall position in grains A and B and the presence of neighbouring triple joints (circles). (e) Calculated projected local induction distribution for Δf = ±100 mm (obtained from the dashed rectangle area indicated in (a)), where the circles indicate the magnetization curling around vortices in a-Fe(Ti) grains.

A and B correspond to soft grains of alfa-Fe surrounded by smaller hard magnetic ThMn12 grains. The domain walls are largely associated with grain boundaries for the ThMn12-type grains, whereas vortex configurations were found at the soft phase. The scheme shows that the vortex configurations in the soft phase result from accommodation to the demagnetizing fields of neighboring magnetically harder YFe11Ti grains. The Lorentz images were used to determine a magnetic induction map, which clearly shows the vortex configuration of the magnetic induction and enables to establish that both Neel (i) and Bloch (ii) type walls are present.